
BIOANALYSIS AND METABOLIC INVESTIGATION OF PSYCHOACTIVE SUBSTANCES

Inauguraldissertation

zur

Erlangung der Würde eines Doktors der Philosophie

vorgelegt der

Philosophisch-Naturwissenschaftlichen Fakultät

der Universität Basel

von

Jan Thomann

2025

Originaldokument gespeichert auf dem Dokumentenserver der Universität Basel

edoc.unibas.ch



Dieses Werk ist lizenziert unter einer Creative Commons Namensnennung-Nicht kommerziell-Weitergabe unter gleichen Bedingungen 4.0 International Lizenz.

Genehmigt von der Philosophisch-Naturwissenschaftlichen Fakultät
auf Antrag von

Erstbetreuer: Prof. Dr. Matthias E. Liechi und PD Dr. Urs Duthaler

Zweitbetreuer: Prof. Dr. Jörg Huwiler

Externe Expertin: Prof. Dr. Andrea E. Steuer

Basel, den 19. November 2024

Dekan

Prof. Dr. Marcel Mayor

„Im Wald herrschte hoher Wellengang. Woge um Woge kam der Waldboden auf Blank zu. [...] Eine neongrüne Welle folgte einer phosphorgelben, einer saphirblauen, einer karminroten. Und die Bäume tanzten dazu, wie Bojen im aufgewühlten Meer.“

— Martin Suter, *Die dunkle Seite des Mondes*, 2000

PREFACE

This thesis is divided into three major parts. Part I describes the development and validation of liquid chromatography–tandem mass spectrometry (LC–MS/MS) methods for psychoactive substances and their metabolites. Part I is accompanied by three publications. Part II addresses the investigation of psilocybin’s metabolism and is accompanied by one publication. Finally, Part III contains a discussion of the content presented in Parts I and II.

The majority of research and data collection was conducted at the Psychopharmacology Research Laboratory of the Division of Clinical Pharmacology and Toxicology at the University Hospital Basel. A minor proportion of the research was conducted at the Preclinical Laboratory for Translational Research into Affective Disorders at the University of Zurich and the Pharma Research and Early Development (pRED) Roche Innovation Center at F. Hoffmann-La Roche in Basel. All projects were carried out between July 2021 and May 2024 and were published in peer-reviewed journals.

ACKNOWLEDGEMENTS

The research presented in this thesis would not have been possible without the generous support, guidance, and contributions of many individuals. First of all, I would like to thank my first supervisor and research group leader, Prof. Dr. Matthias Liechti, for giving me the opportunity to do my PhD in the Psychopharmacology Research Laboratory as well as for his support and generosity over the past few years. I also wish to express my gratitude to my other first supervisor, PD Dr. Urs Duthaler. As the head of the laboratory, Urs warmly welcomed me to the lab when I first arrived, introduced me to the fascinating field of bioanalytics, shared his invaluable expertise, and brightened the lab with his cheerful personality. I would like to thank Prof. Dr. Jörg Huwyler for acting as my second supervisor and Prof. Dr. Andrea Steuer for serving as the external expert on my PhD committee.

My sincere appreciation goes to all the members of the Psychopharmacology Laboratory. A big thank you to Dr. Dino Lüthi and Dr. Deborah Rudin for all their help, for being my “surrogate” supervisors, and for sharing their cozy office with me. Dino’s dad jokes and Deborah’s witty remarks brought a lot of joy to the lab. Special thanks go to Beatrice Vetter for her wonderful support, diligent assistance, and all her work behind the scenes. I want to thank Oliver Stöckmann for being a great master’s student and later a great fellow PhD student. Dr. Karolina Kolaczynska also deserves a special mention for supervising me during my master's thesis, introducing me to the world of PhD students, and being a great mentor. Further, I would like to thank all the interns and master’s students for the great time we spent together. They are Charlotte Kern, Robin Hanimann, Elisabeth Schreiner, Helene Rolli, Dr. Paola Forero Cortés, and Jan Valenta.

Moreover, I would like to thank all my colleagues in the Clinical Pharmacology and Toxicology Research Group for the great lunches, collaborations, wonderful team events, and conferences. Special thanks to Aaron Klaiber, Anna Becker, Caroline Mayer, Denis Arikci, Laura Ley, Livio Erne, Mélusine Humbert-Droz, Joyce dos Santos Jesus, Dr. Isabelle Straumann, Dr. Lorenz Müller, Dr. Severin Vogt, Dr. Patrick Vizeli, and Dr. Yasmin Schmid.

A huge thank you also goes to my family — Katrin, Reto, Marco, and Nadja — for their invaluable support over these years.

Last but not least, I am immensely thankful to Catherine for being by my side, for her endless care and encouragement, and for patiently listening to me talk about bioanalytics, even when it was probably hard to follow at times.

Merci à tous!

SUMMARY

In Part I, four liquid chromatography–tandem mass spectrometry (LC–MS/MS) methods for the bioanalysis of psychoactive substances and their metabolites were developed and validated according to United States Food and Drug Administration (FDA) guidelines.

The first method was validated for the quantification of mescaline and its metabolites 3,4,5-trimethoxyphenylacetic acid (TMPAA), *N*-acetyl mescaline (NAM), and 3,5-dimethoxy-4-hydroxyphenethylamine (4-desmethyl mescaline). A linear range of 12.5 to 5,000 ng/mL for mescaline and TMPAA, and 1.25 to 500 ng/mL for NAM and 4-desmethyl mescaline was achieved. For optimal chromatographic separation, an Acquity Premier HSS T3 C₁₈ column was employed. A single-step extraction procedure was implemented, enabling a non-laborious analysis of plasma samples with a runtime of 4.25 minutes per sample. The method satisfied all FDA validation criteria, including those on accuracy (85–106%), precision (coefficient of variation [CV] ≤ 7%), sensitivity and selectivity, matrix effect (92–100%), and extraction recovery (≥ 98%). Ultimately, the method was successfully employed for the analysis of mescaline, TMPAA, and NAM in pharmacokinetic samples from participants enrolled in a clinical phase I study. 4-desmethyl mescaline could not be selectively analyzed in pharmacokinetic samples due to interference and incomplete chromatographical separation with another metabolite, presumably 3,4-dimethoxy-5-hydroxyphenethylamine (3-desmethyl mescaline).

The second method was developed for the analysis of pharmacokinetic parameters in plasma samples from a clinical study involving diamorphine-dependent patients. The objective of the study was to investigate the feasibility of intranasal diamorphine administration as a component of diamorphine-assisted treatment. Analytes were separated using a Kinetex EVO C₁₈ analytical column. The method is capable of quantifying the concentrations of diamorphine, 6-monoacetylmorphine (6-MAM), morphine, morphine-3-glucuronide (M3G), and morphine-6-glucuronide (M6G) in human plasma, spanning a linear range of 1 to 1,000 ng/mL. The total runtime for a single sample was four minutes. The method was demonstrated to be accurate (91–106%) and precise (CV ≤ 9%) while exhibiting a high extraction recovery (> 87%) and a negligible matrix effect (99–125%) for all analytes. No interferences with endogenous plasma compounds were observed and the method was successfully applied for the analysis of numerous clinical study samples.

In the third project, two methods for the quantification of racemic and chiral 3,4-methylenedioxymethamphetamine (MDMA) and its metabolite 3,4-methylenedioxyamphetamine (MDA) in human plasma were developed and validated. A

linear range of 0.5–500 ng/mL was achieved for racemic MDMA and MDA analysis, while linear ranges of 0.5–1,000 ng/mL and 1–1,000 ng/mL were achieved for chiral MDMA and MDA, respectively. The achiral chromatographic separation of the compounds was performed using a Luna PFP(2) column and the chiral analysis was conducted with a Lux AMP column. The total run times were 4.25 and 6 minutes for achiral and chiral sample analysis, respectively. Both methods met the FDA validation guidelines criteria for accuracy, precision, selectivity, sensitivity, matrix effect, and extraction recovery. Finally, a subset of clinical plasma samples from a study involving *R*-, *S*-, and racemic MDMA was analyzed to demonstrate the method's functionality.

In conclusion, four sensitive, non-laborious, highly reliable, and robust LC–MS/MS methods for the bioanalysis of mescaline, diamorphine, racemic MDMA, and chiral MDMA plus their respective metabolites were developed and validated. These methods are applicable in pharmacokinetic investigations in a clinical setting as well as for forensic studies.

Part II of this thesis presents an investigation of the metabolic pathways of psilocybin's active metabolite psilocin. The primary focus was on the phase I metabolism of psilocin through the cytochrome P450 (CYP) system, as well as the influence of monoamine oxidases (MAOs). Phase II metabolism, with a particular focus on UDP-glucuronosyltransferases (UGTs), was also examined. To conduct a comprehensive analysis of psilocin's metabolism, enzymatic *in vitro* assays were performed using human liver microsomes (HLM) and recombinant CYP, MAO, and UGT enzymes. Moreover, plasma samples from C57BL/6J mice and humans were analyzed following psilocybin administration to obtain *in vivo* data.

After a 4-hour incubation period, approximately 29% of psilocin was metabolized by HLM. Recombinant CYP2D6 and CYP3A4 enzymes demonstrated even higher metabolic activity, with nearly 100% and 40% of psilocin being metabolized, respectively. The metabolites 4-hydroxyindole-3-acetic acid (4-HIAA) and 4-hydroxytryptophol (4-HTP) were identified in the presence of HLM, but not after incubation of psilocin with recombinant CYP enzymes. Nevertheless, trace amounts of 4-HIAA and 4-HTP were generated by MAO-A from psilocin, thereby substantiating its involvement in this metabolic pathway. In contrast to the *in vivo* data, where conjugated psilocin is one of the main metabolites, UGT1A10 did not extensively conjugate psilocin *in vitro*.

Furthermore, two potential metabolites were identified. *In vitro* and *in vivo* analyses identified *N*-methyl-4-hydroxytryptamine (norpsilocin) and an oxidized metabolite of psilocin. The former was detected following incubation with CYP2D6 and in the plasma of mice, while

the latter was identified in CYP2D6 incubations, in mice, and in humans. However, the investigation into the influence of the CYP2D6 genotype on psilocin degradation yielded no significant results. While norpsilocin has never been described as a psilocin metabolite in mice before, the exact structure of the oxidized metabolite remains to be elucidated.

In conclusion, the phase I enzymes CYP2D6, CYP3A4, and MAO-A are implicated in psilocin's metabolism. The identification of putative norpsilocin in mice and oxidized psilocin in humans offers further insight into the metabolic pathway of psilocybin and could contribute to the safety and efficacy of psilocybin application.

PROJECT RATIONALE

Psychedelics are a class of psychoactive substances that interact with the central nervous system. Classic serotonergic psychedelics like lysergic acid diethylamide (LSD), psilocybin, *N,N*-dimethyltryptamine (DMT), or mescaline mainly affect serotonin (5-hydroxytryptamine, 5-HT) receptors in the brain, which leads to the mind-altering effects associated with psychedelics. In particular, their interaction with the 5-HT_{2A} receptor is what is believed to produce psychedelic experiences (Nichols 2016, Nichols et al. 2008). Research on psychedelics but also entactogens like 3,4-methylenedioxymethamphetamine (MDMA) for the treatment of severe mental health disorders has gained increasing attention over the last few years. This resurgence in psychedelic research is driven by a growing recognition of the limitations of conventional treatments and renewed scientific interest in psychedelics (Lowe et al. 2021, National Academies of Sciences 2022). Historically stigmatized psychoactive and psychedelic substances are now the subject of numerous clinical studies, reflecting a paradigm shift in mental health treatment. They show promising potential in treating disorders like anxiety, treatment-resistant major depression, post-traumatic stress disorder (PTSD), or substance use disorder. Psilocybin-assisted therapy, for example, has shown significant efficacy in reducing symptoms of treatment-resistant major depression, while MDMA-assisted therapy has demonstrated remarkable results in alleviating PTSD symptoms (Carhart-Harris et al. 2021, Davis et al. 2021, Gasser et al. 2014, Griffiths et al. 2016, Kupferschmidt 2017, Lowe et al. 2021, Mithoefer et al. 2011, National Academies of Sciences 2022). When used in a controlled therapeutic setting, these substances appear to enhance emotional processing and neuroplasticity, leading to long-lasting positive outcomes while being well tolerated and generally safe (Becker et al. 2022, de Vos et al. 2021, Gasser et al. 2014, Holze et al. 2022b, Klaiber et al. 2024a, National Academies of Sciences 2022, Straumann et al. 2024b, Vizeli et al. 2017).

To analyze the acute subjective effects of psychoactive and psychedelic substances, their pharmacokinetic properties, including the concentrations of the substances and their metabolites, must be studied in human matrices such as blood and urine. Appropriate bioanalytical methods to analyze human samples often do not exist or are too work-intensive to be used for numerous clinical study samples. This requires the development and validation of new non-laborious and state-of-the-art methods. The gold standard for analyzing clinical study samples reliably and in a reasonable time is liquid chromatography–tandem mass spectrometry (LC–MS/MS). This technique promises fast and reliable analysis of multiple analytes while offering high selectivity and sensitivity (Ho et al. 2003).

Therefore, Part I of this thesis focuses first on psychoactive substances in general and then on the development and validation of LC–MS/MS methods to analyze these compounds in clinical study samples. The manuscripts accompanying this chapter focus on bioanalytical methods for three substances with distinct pharmacological and therapeutic profiles: mescaline, a psychedelic investigated for depression and anxiety; MDMA, considered for the treatment of PTSD; and diamorphine (also known as heroin), used in diamorphine-assisted treatment for opioid-dependent patients.

Part II addresses the metabolic degradation of psychedelics. Their metabolic pathways are frequently under-investigated or entirely unclear, and the impact of their metabolites on intrinsic targets remains unknown (Madrid-Gambin et al. 2023). The project included here investigated the metabolism of psilocybin’s active metabolite psilocin. Unraveling the metabolism of psilocybin provides important information on potential drug-drug interactions in clinical settings and could be beneficial in forensic research. The investigation employed three distinct approaches: the use of human liver microsomes (HLM) and recombinant enzymes *in vitro*, investigations in mice, and the analysis of human plasma samples. The primary focus was laid on cytochrome P450 (CYP) enzymes and unknown metabolites. The affinity of detected metabolites for 5-HT receptor subtypes was assessed and the influence of specific CYP2D6 genotypes on psilocin degradation was investigated.

CONTRIBUTIONS

I contributed as the first author to all the publications presented here, except for the bioanalytical method development for MDMA, for which I contributed as a co-author. In addition to myself, master's students, PhD students, postdoctoral fellows, and senior researchers contributed to the experiments and analyses. All contributors and their affiliations are listed in the respective publications.

Furthermore, in the writing progress of this thesis, artificial intelligence (AI) has been employed for translation as well as for the correction of grammatical and stylistic elements. If not otherwise referenced, the contents and thoughts of this thesis are entirely my work and have not been generated by AI.

TABLE OF CONTENTS

TABLE OF FIGURES.....	XIV
LIST OF ABBREVIATIONS	XV
PART I: BIOANALYSIS OF PSYCHOACTIVE SUBSTANCES.....	1
1 PSYCHOACTIVE SUBSTANCES	3
1.1 Psychedelics	3
1.1.1 Psilocybin	4
1.1.2 Mescaline.....	5
1.2 Entactogens	6
1.2.1 MDMA	7
1.3 Opioids	8
1.3.1 Diamorphine	9
2 BIOANALYSIS.....	11
2.1 High-performance liquid chromatography (HPLC).....	11
2.2 Tandem mass spectrometer (MS/MS).....	12
2.3 Bioanalytical method development and validation	14
2.3.1 Sample preparation and chromatographic method development	14
2.3.2 Mass spectrometric method development	16
2.3.3 Method validation.....	16
3 PUBLICATIONS	17
3.1 Manuscript 1.....	17
3.2 Manuscript 2.....	29
3.3 Manuscript 3.....	41
PART II: METABOLIC INVESTIGATIONS.....	51
4 METABOLISM OF PSYCHEDELICS	53
4.1 Drug metabolism.....	53
4.2 Current research on the metabolism of psychedelics	53
5 PUBLICATIONS	55
5.1 Manuscript 4.....	55
PART III: DISCUSSION, CONCLUSION, AND OUTLOOK.....	71
6 DISCUSSION.....	73
7 CONCLUSION AND OUTLOOK	77
8 REFERENCES	79
APPENDIX	93
9 CURRICULUM VITAE.....	95
10 PUBLICATION LIST	97

TABLE OF FIGURES

FIGURE 1 Chemical structures of psychoactive substances.....10
FIGURE 2 Working principle of a triple quadrupole tandem mass spectrometer.....14

LIST OF ABBREVIATIONS

2C-B	4-bromo-2,5-dimethoxyphenethylamine
4-HIA	4-hydroxindole-3-acetaldehyde
4-HIAA	4-hydroxindole-3-acetic acid
4-HTP	4-hydroxytryptophol
5-APB	5-(2-aminopropyl)benzofuran
5-HT	5-hydroxytryptamine, serotonin
5-MeO-DMT	5-methoxy- <i>N,N</i> -dimethyltryptamine
6-APB	6-(2-aminopropyl)benzofuran
6-MAM	6-monoacetylmorphine
ADH	Alcohol dehydrogenase
ALDH	Aldehyde dehydrogenase
AI	Artificial intelligence
APCI	Atmospheric pressure chemical ionization
CID	Collision-induced dissociation
COMT	Catechol-O-methyltransferase
CV	Coefficient of variation
CYP	Cytochrome P450
DMT	<i>N,N</i> -dimethyltryptamine
DOI	2,5-dimethoxy-4-iodoamphetamine
EM	Electron multiplier
EMA	European Medicines Agency
ESI	Electrospray ionization
EU	European Union
FDA	United States Food and Drug Administration
FMO	Flavin-containing monooxygenase
GPCR	G-protein coupled receptor
GST	Glutathion <i>S</i> -transferase
hCE	Human carboxylesterase
HLM	Human liver microsomes
HHA	3,4-dihydroxyamphetamine
HHMA	3,4-dihydroxymethamphetamine
HMA	4-hydroxy-3-methoxyamphetamine
HMMA	4-hydroxy-3-methoxymethamphetamine
HPLC	High-performance liquid chromatography
HRMS	High-resolution mass spectrometry
IAA	Indole-3-acetic acid
LC-MS/MS	Liquid chromatography-tandem mass spectrometry

LIST OF ABBREVIATIONS

LLE	Liquid-liquid extraction
LSD	Lysergic acid diethylamide
m/z	Mass-to-charge ratio
M3G	Morphine-3-glucuronide
M6G	Morphine-6-glucuronide
MALDI	Matrix-assisted laser desorption/ionization
MAO	Monoamine oxidase
MAOI	Monoamine oxidase inhibitor
MAPS	Multidisciplinary Association for Psychedelic Studies
MDA	3,4-methylenedioxyamphetamine
MDEA	3,4-methylenedioxy- <i>N</i> -ethylamphetamine
MDMA	3,4-methylenedioxymethamphetamine
MRM	Multiple reaction monitoring
NAM	<i>N</i> -acetyl mescaline
NAT	N-acetyltransferase
NMR	Nuclear magnetic resonance
Nor-LSD	6-norlysergic acid diethylamide
OCD	Obsessive compulsive disorder
OH-LSD	2-oxo-3-hydroxy-lysergic acid diethylamide
PPT	Protein precipitation
pRED	Pharma Research and Early Development
PTSD	Post-traumatic stress disorder
Q0	Quadrupole 0
Q1	Quadrupole 1
q2	Quadrupole 2, collision cell
Q3	Quadrupole 3
sMRM	Scheduled multiple reaction monitoring
SPE	Solid phase extraction
SRM	Selected reaction monitoring
SULT	Sulfotransferase
TMPA	3,4,5-trimethoxyphenylacetaldehyde
TMCAA	3,4,5-trimethoxyphenylacetic acid
TMPE	3,4,5-trimethoxyphenylethanol
TPMT	Thiopurine S-methyltransferase
UGT	UDP-glucuronosyltransferase
UV	Ultraviolet

**PART I:
BIOANALYSIS OF PSYCHOACTIVE
SUBSTANCES**

1 PSYCHOACTIVE SUBSTANCES

Psychoactive substances affect the central nervous system and can alter feelings, mood, perception, cognition, or behavior. Most psychoactive substances can readily cross the blood-brain barrier due to their lipophilicity and access neurons in the brain. They affect synaptic transmission by interfering with neurotransmitter transport and release or affect receptor activity (Dietrich 2009, Luethi et al. 2020, Muller et al. 2015, Wadley 2016). Psychoactive substances that are consumed for their narcotic or stimulant effect are often scheduled and illegal. This classification is commonly associated with the substances' abuse and addictive potential. However, there are exceptions where the substance is illegal but does not pose an addiction risk (e.g., psychedelics such as psilocybin) or where the substance is legal but demonstrates a high addiction potential (e.g., alcohol or nicotine) (Wadley 2016). The scheduling of a drug is often subject to change throughout its history, depending on the circumstances of its social usage. Several psychoactive substances are used for recreational purposes or in religious and spiritual practices, such as traditional medicine and rituals. Frequently these substances are also studied and used for medical purposes, with both areas of application often closely intertwined (Luethi et al. 2020, Wadley 2016).

Different approaches have been taken to classify psychoactive substances. Generally, they are divided into several subclasses based e.g., on their mode of action or structural similarities. One approach is to classify them as stimulants (including entactogens), sedatives (including opioids and benzodiazepines), dissociatives, cannabinoids, and psychedelics (Dietrich 2009, Luethi et al. 2020). However, these classes are not static and can vary depending on the approach. The three subclasses of psychoactive substances most relevant to this thesis are psychedelics, entactogens, and opioids.

1.1 Psychedelics

Psychedelics are a class of psychoactive compounds that interact primarily with serotonin (5-hydroxytryptamine, 5-HT) receptors. They induce alterations in perception, thought, emotion, mood, consciousness, and cognition. These alterations are often characterized by visual and auditory hallucinations, profound emotional experiences, and an altered sense of time (Dinis-Oliveira et al. 2019, Geyer 2024, Holze et al. 2024a, Luethi et al. 2020, Nichols 2016, Nichols et al. 2008). Specifically, agonism at the 5-HT_{2A} receptor is responsible for the psychedelic effect of classic serotonergic psychedelics (Liechti 2017, Nichols 2016, Nichols et al. 2008). A variety of psychedelic substances can be found in nature e.g., in plants and animals. Natural substances include psilocybin, mescaline,

N,N-dimethyltryptamine (DMT), and 5-methoxy-*N,N*-dimethyltryptamine (5-MeO-DMT) while lysergic acid diethylamide (LSD), 4-bromo-2,5-dimethoxyphenethylamine (2C-B), or 2,5-dimethoxy-4-iodoamphetamine (DOI) are examples of synthetic psychedelics (Madrid-Gambin et al. 2023, Nichols 2016).

Psychedelics are generally considered to be non-addictive and to have a low risk of physical harm (Holze et al. 2024a, Johnson et al. 2008, Klaiber et al. 2024a, Nichols 2004, Straumann et al. 2024b). However, they can also lead to challenging psychological experiences, often referred to as ‘bad trips’. These can involve intense anxiety, panic attacks, flashbacks, and negative feelings. Set (mindset) and setting (environment) play a crucial role in the nature of the psychedelic experience and are therefore important in avoiding ‘bad trips’ (Barrett et al. 2016, Holze et al. 2022b, Klaiber et al. 2024a, Straumann et al. 2024b). Additionally, psychedelics can induce changes in vital parameters such as an increase in blood pressure or heart rate, and can also lead to nausea and headache. However, most adverse effects are tolerable in clinical and controlled settings, and serious adverse events are rare (Holze et al. 2024a, Holze et al. 2024b).

The psychedelics investigated in the projects included in this thesis are psilocybin and mescaline. Thus, they will be discussed in more detail in the following sections.

1.1.1 Psilocybin

The psychedelic compound psilocybin (*O*-phosphoryl-4-hydroxy-*N,N*-dimethyltryptamine) is a naturally occurring tryptamine structurally similar to 5-HT or DMT (Figure 1). It is found mainly in mushrooms e.g., from the *Psilocybe* or *Conocybe* genus, which are colloquially known as ‘magic mushrooms’ (Dinis-Oliveira 2017, Lowe et al. 2021, Tyls et al. 2014). Psilocybin acts as a prodrug and is in vivo rapidly dephosphorylated to form the psychoactive metabolite psilocin (4-hydroxy-*N,N*-dimethyltryptamine). Psilocin is predominantly conjugated to psilocin-*O*-glucuronide by UDP-glucuronosyltransferases (UGTs). Another major pathway is the oxidative deamination and oxidation to 4-hydroxyindole-3-acetic acid (4-HIAA) via the intermediate 4-hydroxyindole-3-aldehyde (4-HIA). The formation of 4-hydroxytryptophol (4-HTP) from 4-HIA represents a minor metabolic route (Dinis-Oliveira 2017, Hasler et al. 1997, Holze et al. 2022a, Kolaczynska et al. 2021).

Psilocin exerts its effects primarily by interacting with 5-HT receptors located in the brain but also in the central and peripheral nervous system (Lowe et al. 2021). Psilocin’s activation of the 5-HT_{2A} receptor subtype is responsible for the subjective psychedelic effects,

while its affinity for the 5-HT_{1A} receptor is linked to the anxiolytic and antidepressant effects. Additional interactions have been identified with the 5-HT_{2B} and 5-HT_{2C} receptors while it also moderately inhibits serotonin transporters (Lowe et al. 2021, Nichols et al. 2008, Rickli et al. 2016).

Psilocybin exhibits a favorable safety profile with minimal adverse effects when administered under controlled clinical or research conditions. However, mild cardiovascular stimulation, transient anxiety, and other unpleasant adverse effects may occur (Holze et al. 2024b, Straumann et al. 2024b, Studerus et al. 2011). Currently, it is probably the most widely investigated psychedelic compound (Nichols 2020). Due to its activity at the 5-HT receptors and its promising safety profile, psilocybin-assisted therapy is proposed for depression, anxiety, substance use disorder, mental health in life-threatening illnesses, cluster headaches, and migraine (Becker et al. 2022, Bogenschutz et al. 2018, Carhart-Harris et al. 2017, Davenport 2016, Dos Santos et al. 2016, Griffiths et al. 2016, Johnson et al. 2017, Madden et al. 2024, Moreno et al. 2006, Ross et al. 2016, Schindler et al. 2021, Straumann et al. 2024b, von Rotz et al. 2023).

Psilocybin is the main focus of the project presented in Chapter 5.1.

1.1.2 Mescaline

Mescaline (3,4,5-trimethoxyphenethylamine) is an alkaloid found mainly in the peyote cactus (*Lophophora williamsii*) but also in other species of cacti (e.g., *Echinopsis pachanoi*) (Cassels et al. 2018, Dinis-Oliveira et al. 2019, Vamvakopoulou et al. 2023). Chemically mescaline (Figure 1) is a phenethylamine and has structural similarities with dopamine, amphetamines, or the phenethylamine-based psychedelics 2C-B and DOI. Although structurally related to stimulants, mescaline interacts with the 5-HT receptors and exerts psychedelic effects. Primarily, it exhibits affinity for the 5-HT_{1A} and 5-HT_{2A} receptors but it is also an agonist at the 5-HT_{2B} and 5-HT_{2C} receptors. However, in comparison to other classic psychedelics, mescaline displays a relatively low affinity for the 5-HT₁ and 5-HT₂ receptor subfamilies (Dinis-Oliveira et al. 2019, Olejnikova-Ladislavova et al. 2024, Rickli et al. 2015c). The low affinities for the 5-HT receptors are in line with the high doses that are required to experience a psychedelic effect. However, at equally strong doses, mescaline produces a subjective experience comparable to that of LSD or psilocybin (Ley et al. 2023, Olejnikova-Ladislavova et al. 2024, Rickli et al. 2016).

The primary metabolic pathway of mescaline is oxidative deamination to the unstable intermediate 3,4,5-trimethoxyphenylacetaldehyde (TMPA). This intermediate can undergo

transformation to 3,4,5-trimethoxyphenylacetic acid (TMPAA), a major mescaline metabolite (Dinis-Oliveira et al. 2019, Klaiber et al. 2024b, Ley et al. 2023). An alternative metabolic pathway involves the conversion of the aldehyde to 3,4,5-trimethoxyphenylethanol (TMPE) (Dinis-Oliveira et al. 2019). Another significant pathway appears to be the N-acetylation of mescaline to *N*-acetyl mescaline (Dinis-Oliveira et al. 2019, Klaiber et al. 2024b, Ley et al. 2023). Minor pathways include the demethylation of one of the methoxy moieties to either 3,5-dimethoxy-4-hydroxyphenethylamine (4-desmethyl mescaline) or 3,4-dimethoxy-5-hydroxyphenethylamine (3-desmethyl mescaline). However, further minor metabolites have been reported (Dinis-Oliveira et al. 2019).

Mescaline is one of the oldest psychedelics used by humans, having been part of the indigenous cultures throughout the Americas for several thousand years (Cassels et al. 2018, Dinis-Oliveira et al. 2019). In the 20th century, mescaline was already the subject of clinical research and recently it has been proposed as a potential treatment for depression, anxiety, headaches, obsessive-compulsive disorder (OCD), and alcohol addiction (Dinis-Oliveira et al. 2019, Guttman 1936, Guttman et al. 1936, Hermle et al. 1992, Unger 1963). However, the amount of contemporary research conducted is relatively limited (Vamvakopoulou et al. 2023). In a recent clinical study, the dose-equivalence of mescaline, LSD, and psilocybin was investigated while another study investigated the pharmacokinetics and acute subjective effects of several doses of mescaline (Klaiber et al. 2024b, Ley et al. 2023).

Mescaline is the main focus of the project presented in Chapter 3.1.

1.2 Entactogens

Entactogens are a class of psychoactive substances that promote emotional openness, empathy, acute anxiolysis, and feelings of connectedness. The term ‘entactogen’ has its etymological roots in Greek and Latin, and means ‘touching within’. It was first proposed by David E. Nichols in the late 1980s. Entactogens mainly release the monoamines serotonin and norepinephrine, and to a lesser extent dopamine (de la Torre et al. 2004, Nash et al. 1994, Nichols 2022). The best-known entactogen is 3,4-methylenedioxymethamphetamine (MDMA) (Figure 1), the active ingredient of so-called ‘ecstasy’ tablets, which is widely used as a recreational drug (Liechti et al. 2000, Nichols 2022). Other entactogens include MDMA’s metabolite 3,4-methylenedioxyamphetamine (MDA) or several designer drugs such as 3,4-methylenedioxy-*N*-ethylamphetamine (MDEA), 5-(2-aminopropyl)benzofuran (5-APB), and 6-(2-aminopropyl)benzofuran (6-APB) (Holka-Pokorska 2023, Luethi et al. 2020, Rickli et al. 2015a, Rickli et al. 2015b, Rudin et al. 2022, Simmler et al. 2014).

1.2.1 MDMA

MDMA is a substituted amphetamine that causes the release of stored neurotransmitters from neurons into the synaptic cleft by reversing the monoamine transporters, thereby increasing the interaction of these monoamines with postsynaptic receptors. In particular, it strongly promotes the efflux of serotonin and norepinephrine, but also dopamine (de la Torre et al. 2004, Liechti et al. 2000, Nichols 2022, Verrico et al. 2007). While serotonin release is associated with an elevated mood, norepinephrine release is linked to increased energy levels (Smith et al. 2022). Furthermore, it induces a release of oxytocin leading to prosocial effects such as trust, closeness to others, or fear extinction (Atila et al. 2023, Smith et al. 2022). In addition to monoamine release, MDMA also acts as a mild monoamine reuptake inhibitor (de la Torre et al. 2004, Nash et al. 1994, Rickli et al. 2015b).

The MDMA products used recreationally and in clinical studies are usually a racemic mixture of the two enantiomers *R*- and *S*-MDMA (Figure 1). However, the two enantiomers differ in their pharmacological activity. While *S*-MDMA is more effectively releasing monoamines and oxytocin, *R*-MDMA more potently activates the 5-HT_{2A} receptor and is a stronger inhibitor of cytochrome P450 (CYP) 2D6 (Luethi et al. 2019b, Pitts et al. 2018, Rickli et al. 2015b, Straumann et al. 2024a).

MDMA is metabolized via two distinct metabolic pathways. The N-demethylation of MDMA results in the production of MDA. MDA also releases monoamines and has affinity for the 5-HT_{2A} receptor which may contribute to the psychedelic effects observed following the ingestion of MDMA (Baggott et al. 2019, de la Torre et al. 2004, Luethi et al. 2019b, Nash et al. 1994, Nichols 2022, Papaseit et al. 2020, Rickli et al. 2015b). Both MDMA and MDA can undergo O-demethylation to 3,4-dihydroxymethamphetamine (HHMA) and 3,4-dihydroxyamphetamine (HHA), respectively. HHMA and HHA then undergo O-methylation again to yield 4-hydroxy-3-methoxymethamphetamine (HMMA) and 4-hydroxy-3-methoxyamphetamine (HMA), respectively (de la Torre et al. 2004, Papaseit et al. 2020). The methyl group transfer is mainly mediated by catechol-O-methyltransferase (COMT) while demethylation is mediated mainly by CYP2D6 but also CYP1A2, CYP2B6, and CYP3A4 (de la Torre et al. 2004, Papaseit et al. 2020). Additionally, HHMA can be conjugated by sulfotransferases (SULTs) and HMMA by SULTs or UGTs (Steuer et al. 2015).

Illicit and uncontrolled MDMA use poses the risk of hyperthermia and hyponatremia which can lead to rhabdomyolysis and renal damage. Cardiovascular stimulation including elevated blood pressure, tachycardia, and arrhythmias can occur. Additionally, bruxism (jaw clenching) and anhedonia due to 5-HT depletion have been reported (Smith et al. 2022, Vizeli

et al. 2017). However, a single-dose administration in healthy subjects in a controlled setting did not raise safety concerns in previous investigations (Straumann et al. 2024a, Vizeli et al. 2017).

Moreover, MDMA shows potential therapeutic benefits, particularly using MDMA-assisted psychotherapy for the treatment of post-traumatic stress disorder (PTSD), anxiety, and depression by enabling patients to process emotions more openly (Smith et al. 2022). Lykos Therapeutics, a company of the Multidisciplinary Association for Psychedelic Studies (MAPS), conducted several clinical trials on MDMA with considerable success. In 2023, a phase III trial of MAPS was published, demonstrating that MDMA could effectively reduce PTSD symptoms and functional impairment (Mitchell et al. 2023). However, in August 2024 the United States Food and Drug Administration (FDA) rejected the approval of MDMA as a therapeutic agent for PTSD, following a recommendation by their advisory committee (Reardon 2024a, Reardon 2024b). Despite this, the FDA has not ruled out the possibility of approving MDMA in the future. However, additional research is necessary to support the approval of MDMA-assisted psychotherapy for PTSD. The impact of this decision on the approval of other psychedelic therapies is currently unclear (Knopf 2024, Reardon 2024a).

MDMA and MDA are the subject of the project presented in Chapter 3.3.

1.3 Opioids

Opioids are a group of compounds that include natural, semi-synthetic, and synthetic substances that exert their effects via opioid receptors. Naturally occurring opioids, such as morphine (Figure 1) and codeine, are alkaloids from the poppy plant (*Papaver somniferum*) while oxycodone and diamorphine (Figure 1) are semi-synthetic opioids derived from morphine. Fentanyl or methadone are examples of synthetic opioids (Trescot et al. 2008). Opioid receptors belong to the G-protein coupled receptors (GPCRs) and are distributed in the central nervous system and throughout the peripheral tissue. Normally, these receptors are activated by endogenous alkaloids (e.g., endorphins) (Dhaliwal et al. 2023, Trescot et al. 2008). While there are several subclasses of opioid receptors (μ , μ ; kappa, κ ; delta, δ), the μ -opioid receptor is the primary receptor target for substances such as morphine, codeine, and fentanyl (Dhaliwal et al. 2023, Trescot et al. 2008).

Opioids have been used traditionally for the treatment of pain for several thousands of years. Nowadays, analgesics like morphine and especially fentanyl are still in use in pain management (Boysen et al. 2023). Moreover, opioids such as codeine are commonly prescribed as an antitussive and are regarded as the gold standard in this context. However, codeine's

efficacy is debated since it might only be effective in specific situations (Bolser et al. 2007, Freestone et al. 1997, Takahama et al. 2007). On the other hand, opioids are frequently consumed recreationally for their induction of euphoria, anxiolysis, and relaxation. Conversely, they can also cause emesis, sedation, urinary retention, pruritus, constipation, and respiratory depression (Luethi et al. 2020, Trescot et al. 2008). Chronic opioid use results in the development of tolerance, withdrawal symptoms, and dependence. However, the emergence of an opioid use disorder is influenced by a complex interplay of genetic, environmental, and psychosocial factors (Pergolizzi et al. 2020). Due to the high potency, variable purity, and products stretched with potent substances such as fentanyl, overdoses are common with opioids. These result in respiratory depression, coma, and death (Britch et al. 2022, Darke et al. 1999).

1.3.1 Diamorphine

Diamorphine was first marketed under the brand name ‘heroin’ for use as an antitussive and analgesic (Häbel et al. 2018). Although still employed for medical purposes, particularly in palliative care and the treatment of chronic diamorphine dependence, the addictive potential and high risk of overdose associated with this substance have resulted in its control and prohibition in the majority of countries (Martins et al. 2021, Morris 2022, Rook et al. 2006, Schmitt-Koopmann et al. 2022, Trescot et al. 2008). In comparison to morphine, diamorphine possesses two additional acetyl groups, which renders it more lipophilic. It is capable of crossing the blood-brain barrier more efficiently than morphine, which is responsible for the rapid onset and more intense effect associated with diamorphine (Maurer et al. 2006, Rook et al. 2006).

Metabolically, diamorphine undergoes extensive first-pass metabolism in the liver and has poor bioavailability. It is first degraded to 6-monoacetylmorphine (6-MAM) and then morphine by human carboxylesterase-1 and 2 (hCE-1 and hCE-2), or pseudo-cholinesterase (Maurer et al. 2006, Rook et al. 2006). Both 6-MAM and morphine have higher opioid receptor affinities than diamorphine itself (Rook et al. 2006). Morphine is mainly glucuronidated to the morphine-3-glucuronide (M3G) and morphine-6-glucuronide (M6G) by different UGTs. M3G is inactive but M6G exerts equivalent analgesic effects as morphine with fewer side effects. Lastly, morphine can be metabolized into normorphine by CYP3A4 and CYP2C8 (Maurer et al. 2006, Rook et al. 2006).

The development of a bioanalytical method for the analysis of diamorphine and its metabolites is the subject of the project presented in Chapter 3.2.

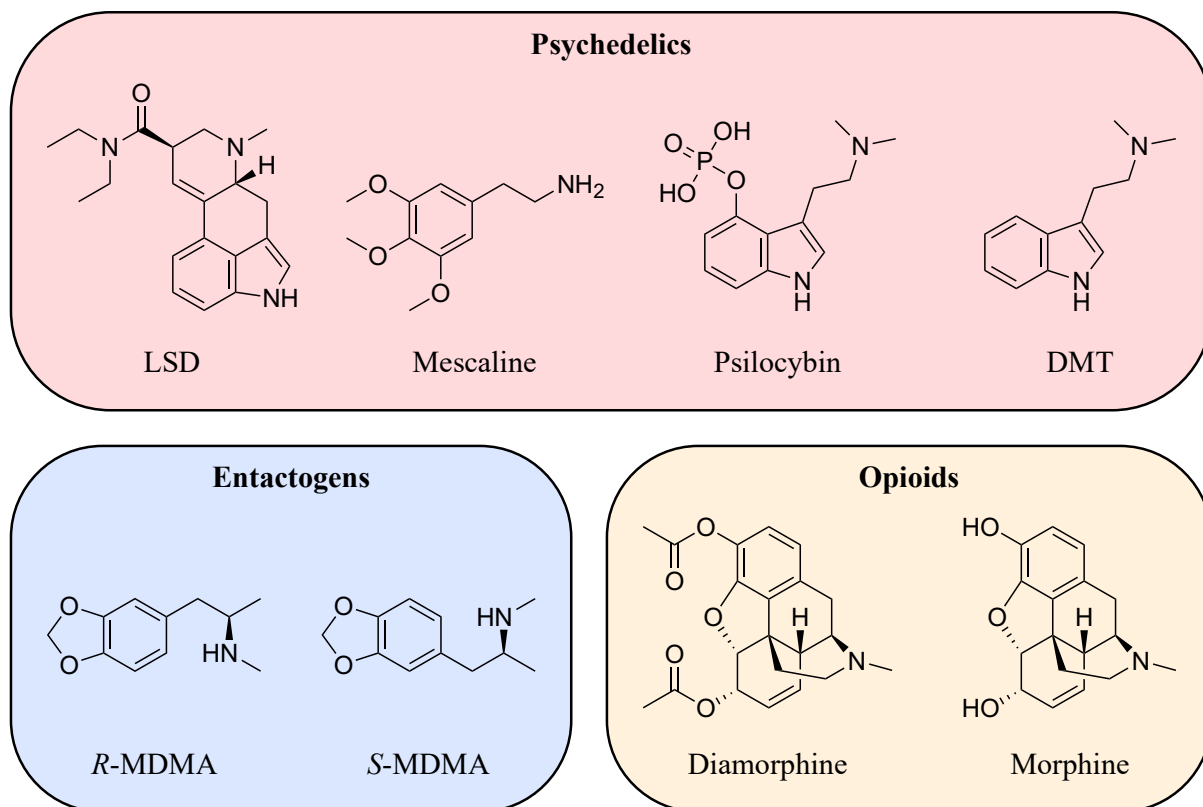


Figure 1 Chemical structures of psychoactive substances relevant to this thesis, including psychedelics, entactogens, and opioids.

2 BIOANALYSIS

High-performance liquid chromatography–tandem mass spectrometry (HPLC–MS/MS) is the current benchmark method for analyzing analytes in clinical samples, offering excellent accuracy, selectivity, sensitivity, reproducibility, and high-throughput sample analysis (Ho et al. 2003). HPLC is the analytical technique used to separate, identify, quantify, or purify components within a biological sample. The coupled tandem mass spectrometer acts as a highly sensitive detector in this process (Blum 2014, Nagy et al. 2008, Snyder et al. 2011). In the projects discussed in this thesis, LC–MS/MS was the primary technique used for sample analysis and will thus be explained in more detail in Chapters 2.1–2.3.

2.1 High-performance liquid chromatography (HPLC)

An HPLC system generally consists of an analytical column (stationary phase), mobile phases with different polarities transported by two or more pumps, and a detector (e.g., an ultraviolet [UV] detector or a mass spectrometer for enhanced analysis) (Blum 2014). Two principal modes of liquid chromatography exist, differing primarily in the nature of the stationary and mobile phases. Normal-phase chromatography is utilized in specialized applications, such as the separation of highly polar compounds whereas reversed-phase chromatography is a more versatile approach and is the preferred method in most cases (Boyes et al. 2018, Nagy et al. 2008).

In normal-phase chromatography, the stationary phase is polar, typically consisting of unmodified silica or silica modified with polar functional groups (e.g., cyano, nitro, diol, or amino groups). Organic solvents such as hexane, chloroform, and ethyl acetate are employed as mobile phases and the gradient moves from non-polar to polar solvent. Polar compounds in the sample interact more strongly with the polar stationary phase (e.g., through hydrogen bonding or dipole-dipole interactions) and are retained longer, whereas non-polar compounds elute faster (Akash et al. 2020, Blum 2014, Boyes et al. 2018, Ganesh et al. 2023, Nagy et al. 2008, Snyder et al. 2011).

On the other hand, in reversed-phase chromatography, the analytical column is packed with silica particles of a specific diameter that have been chemically modified with hydrophobic alkyl chains (e.g., C₁₈ or C₈). The mobile phase gradient moves from polar to non-polar solvent and often comprises an aqueous solution mixed with organic solvents such as methanol or acetonitrile. Non-polar or hydrophobic analytes exhibit a stronger interaction with the hydrophobic stationary phase and are therefore adsorbed more strongly, resulting in a prolonged retention. In contrast, more polar compounds elute at a faster rate. This makes it an

efficacious method for the separation of a wide range of compounds including small proteins, peptides, and organic molecules (Akash et al. 2020, Blum 2014, Boyes et al. 2018, Ganesh et al. 2023, Schlüter 1999, Snyder et al. 2011).

Besides these two principal modes, several other parameters influence the separation and retention time of compounds such as the pH of the mobile phase, the flow rate of the solution, or the analysis temperature (Akash et al. 2020, Ganesh et al. 2023). Mobile phases can be supplemented with additives to control the pH and enhance the ionization of the analytes (e.g., formic acid or acetic acid), act as a buffering agent, or improve chromatographic resolution (e.g., ammonium salts) (Boyes et al. 2018).

2.2 Tandem mass spectrometer (MS/MS)

Mass spectrometry is an analytical technique employed for the qualitative and quantitative analysis of ionized molecules. Following the prior separation of a sample by HPLC, the eluent is introduced into the ionization chamber (ionization source) of the mass spectrometer, where the molecules are positively or negatively ionized (Figure 2) (Ho et al. 2003). Different modes of sample ionization exist. Besides atmospheric pressure chemical ionization (APCI) or matrix-assisted laser desorption/ionization (MALDI), electrospray ionization (ESI) is the main ionization technique used today when analyzing liquid samples. ESI is a soft ionization technique that transfers analytes to the gas phase with minimal fragmentation, preserving the molecular integrity of the analytes. The sample moves through a charged capillary and is sprayed into the ionization source as fine ionized droplets. The liquid is then evaporated by high temperatures and gas streams, leaving behind the charged molecules (Akash et al. 2020, De Hoffmann et al. 2007, Domon et al. 2006, Ho et al. 2003).

Subsequently, the ions enter the mass spectrometer through an opening called orifice. Behind the orifice, there is a sequence of quadrupoles that guide the ions (Figure 2) (AB Sciex 2010). A quadrupole consists of four metal rods at equal distances, with an electrical field in between them. By using the amplitude of oscillation, specific mass-to-charge ratios (m/z) can be guided, allowing them to travel through the quadrupole without colliding with the metal rods. Undesired ions will be eliminated. This purification step makes laborious purification processes before the measurement redundant (De Hoffmann et al. 2007, Haag 2016, Ho et al. 2003). In some mass spectrometer systems, such as those employed in the projects presented in this thesis (e.g., API 4000 QTRAP or API 5000, AB Sciex, Ontario, Canada), the first quadrupole that the ions encounter is a so-called QJet. The QJet does not act as a mass filter but guides and prefocuses the ions at high pressure. This focusing reduces ion loss, thus

increasing selectivity and lowering the noise level of the analysis. The ions are then focused again at low pressure in another quadrupole called Q0 before entering quadrupole Q1 (Figure 2). The Q0 also acts as an ion guide rather than a mass filter. The two ion guides in combination provide maximum ion transmission, focusing, and sensitivity. However, other systems with just one ion guide are also available (AB Sciex 2008, AB Sciex 2010, De Hoffmann et al. 2007, Gross 2006).

In a triple quadrupole mass spectrometer, there are three main quadrupoles (Figure 2). In the first quadrupole (Q1), the analyte ion of interest (precursor ion) is filtered as described above. In the second quadrupole, called the collision cell or q2, the previously selected precursor ion collides with a collision gas (e.g., argon or nitrogen) and is fragmented. The product ions generated through this collision-induced dissociation (CID) are directly linked to the parent compound and its molecular structure. These fragments are then monitored by the third quadrupole (Q3) (Figure 2) (Gross 2006, Haag 2016, Ho et al. 2003). Following Q3, the ions reach an electron multiplier (EM), which enhances detection efficiency by amplifying the ion signal. The resulting electrical signal is recorded by a metal anode acting as the detector and is then transformed into a graphical representation known as a mass spectrum. In the mass spectrum, the m/z of the ions are plotted against their relative abundance or signal intensity (Figure 2) (De Hoffmann et al. 2007, Ho et al. 2003).

Several data acquisition modes can be used to detect analyte ions. The most common mode with ESI is selected reaction monitoring (SRM). In SRM, Q1 and Q3 are static and scan only for an exact and fixed m/z of the parent compound and its fragment. This results in high specificity and sensitivity. SRM can be extended to multiple reaction monitoring (MRM), which monitors several transitions simultaneously. Scheduled MRM (sMRM), in contrast, is an optimized version of MRM, monitoring transitions only during specific time windows. This can be employed to further optimize sensitivity and accuracy while managing complex analyses. Other scan modes include product ion scan, precursor ion scan, and neutral loss scan (De Hoffmann et al. 2007, Gross 2006, Haag 2016, Ho et al. 2003).

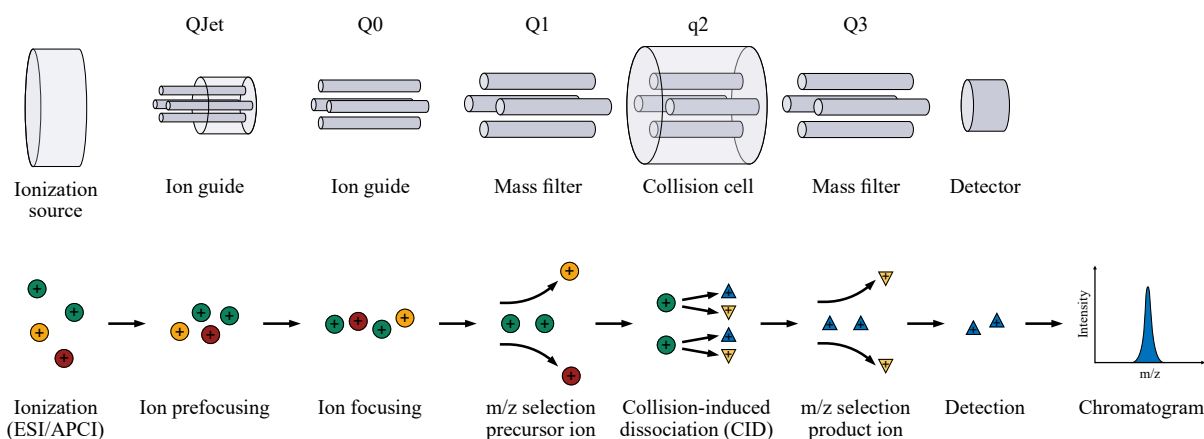


Figure 2 Working principle of a triple quadrupole tandem mass spectrometer, as used for the analyses in this thesis. The most important components of a mass spectrometer are illustrated above, while the fundamental principles on a molecular basis are elucidated below. The illustration was adapted from Jaiswal et al. (2020) and modified to include additional elements.

2.3 Bioanalytical method development and validation

When developing a bioanalytical method, the definition of the overall operation conditions, the design, and the suitability of the method are essential, as they provide the foundation for a successful validation. Regulatory agencies such as the FDA and its European counterpart, the European Medicines Agency (EMA), have published guidance documents. The two guidelines are largely similar, but there are some differences, such as the suggested validation parameters and the structure (Kaza et al. 2019). Although these are only non-binding recommendations, they are widely regarded as industry standards and are often rigorously followed to ensure compliance, credibility, and overall success. Adherence to these guidelines not only increases the reliability of the data generated, but also facilitates the regulatory approval process by demonstrating that the analytical method is scientifically sound and capable of producing accurate, precise, and reproducible results (European Medicines Agency 2022, United States Food and Drug Administration 2018).

2.3.1 Sample preparation and chromatographic method development

In method development, the conditions for the optimal sample extraction and detection of the analytes are defined (European Medicines Agency 2022, United States Food and Drug Administration 2018). Prior to injection into the HPLC, the sample must undergo preparation during which the analytes are extracted from the matrix. Sample preparation aims to eliminate

ion suppression through interfering substances, pre-concentrate the samples to enhance sensitivity, and transform the sample into a suitable form for injection, separation, or detection (Ashri et al. 2011). There are three main methods for sample preparation. A widely used technique for purifying and concentrating samples is solid phase extraction (SPE). In SPE, the analytes are separated from the matrix using a sorbent in a cartridge. The sorbent selectively retains specific analytes, thereby facilitating their separation or concentration. SPE is convenient for concentrating or purifying trace analytes in biological samples (Ashri et al. 2011, Moein et al. 2017). Another main technique is liquid-liquid extraction (LLE) where an aqueous sample is combined with a non-miscible organic solvent to extract the analyte from the aqueous phase into the organic phase. Although laborious and requiring significant quantities of organic solvents, this technique has been demonstrated to yield high recovery rates (Ashri et al. 2011, Moein et al. 2017). The extraction method of choice for all projects included in this thesis is protein precipitation (PPT). In this straightforward approach, a biological matrix (such as plasma, or urine) is combined with e.g., a miscible organic solvent, metal ions, salts, or an acidic solution to precipitate undesired proteins (Ashri et al. 2011, Moein et al. 2017).

Besides sample extraction, different analytical columns need to be evaluated when developing a chromatographic method. Physicochemical properties and chemical structure influence the characteristics of an analytical column. These properties include the type of medium (monolithic, porous, or nonporous), the geometry (diameter, pore volume, particle size, and shape), the type of ligands, ligand density, and the type of stationary phase carrier (silica, polymer, or carbon) (Zuvela et al. 2019). As the column is the core of the chromatographic method, the selection of the most appropriate column is crucial.

Another major role in HPLC method development is the selection of the best mobile phase combination and the right solvent elution. Mobile phases dissolve the sample, transport it, affect system backpressure based on their viscosity, and influence analyte separation, retention time, and ionization capability. Often, mixtures of organic and aqueous mobile phases are used with different additives (Moldoveanu et al. 2022, Nagy et al. 2008). Organic solvents such as methanol or acetonitrile affect peak shape and resolution and determine the amount of interaction between the analyte and the stationary phase. Polarity and pH have a major impact on how well analytes are separated. Adjusting the pH affects the ionization state of the analytes, which can be particularly important when analyzing acidic or basic components. Choosing the right buffer ensures pH consistency and controls the ionization (Moldoveanu et al. 2022, Nagy et al. 2008). Finally, developing an appropriate mobile phase elution ensures optimal analyte

separation. Typically, isocratic or gradient elution is used. In isocratic elution, the mobile phase composition remains constant throughout the analysis, while in gradient elution the composition changes over time (Moldoveanu et al. 2022, Nagy et al. 2008). Gradient elution was utilized for all methods presented in this thesis.

2.3.2 Mass spectrometric method development

In mass spectrometric method development for targeted analysis, the process of introducing new compounds and optimizing parameters for their optimal detection is referred to as ‘tuning’ (Jia et al. 2023). Analytes are introduced to the mass spectrometer via a syringe infusion pump, enabling the finding and selection of mass transitions with the highest intensity and best signal-to-noise ratio (Kumar et al. 2023, Sargent 2013). In ‘auto-tuning’, which is the current standard for most devices, the mass spectrometer automatically adjusts parameters such as gas flow or ionization voltages (e.g., declustering potential, entrance potential, or collision energy). This guarantees ideal conditions for ionization and sensitive detection, thereby ensuring optimal and accurate quantification of the target compound (Jia et al. 2023, Kumar et al. 2023, Sargent 2013).

2.3.3 Method validation

A validated bioanalytical method is essential to reliably analyze a substance in biological samples from a clinical trial. Thorough validation ensures the robustness and quality of a method. A range of bioanalytical method validations may be conducted. While a full validation is recommended when analyzing analyte concentration in samples from clinical and non-clinical studies, partial validations may be employed to evaluate modifications to a validated method. Further, cross-validations can be executed when several bioanalytical processes or laboratories are involved (European Medicines Agency 2022, United States Food and Drug Administration 2018).

A full validation for chromatographic methods can include parameters such as accuracy, precision, calibration range, selectivity, specificity, sensitivity, carry-over, matrix effect, extraction recovery, dilution integrity, reinjection reproducibility, and stability depending on the guideline (European Medicines Agency 2022, United States Food and Drug Administration 2018). The detailed validation parameters that were executed to validate the LC–MS/MS methods included in this thesis are described in Chapters 3.1, 3.2, and 3.3.

3 PUBLICATIONS

3.1 Manuscript 1

Development and validation of an LC-MS/MS method for the quantification of mescaline and major metabolites in human plasma

Jan Thomann^{a,b}, Laura Ley^{a,b}, Aaron Klaiber^{a,b}, Matthias E. Liechti^{a,b,*}, Urs Duthaler^{a,b}

^a Division of Clinical Pharmacology and Toxicology, Department of Biomedicine, University Hospital Basel, Switzerland

^b Division of Clinical Pharmacology and Toxicology, Department of Pharmaceutical Sciences, University of Basel, Switzerland

* Corresponding author

J Pharm Biomed Anal. 2022 Oct 25;220:114980

DOI: 10.1016/j.jpba.2022.114980



Contents lists available at ScienceDirect

Journal of Pharmaceutical and Biomedical Analysis

journal homepage: www.journals.elsevier.com/journal-of-pharmaceutical-and-biomedical-analysis

Development and validation of an LC-MS/MS method for the quantification of mescaline and major metabolites in human plasma

Jan Thomann^{a,b}, Laura Ley^{a,b}, Aaron Klaiber^{a,b}, Matthias E. Liechti^{a,b,*}, Urs Duthaler^{a,b}^a Division of Clinical Pharmacology and Toxicology, Department of Biomedicine, University Hospital Basel, Switzerland^b Division of Clinical Pharmacology and Toxicology, Department of Pharmaceutical Sciences, University of Basel, Switzerland

ARTICLE INFO

Keywords:

Psychedelics
Drug metabolism
Pharmacokinetics
Liquid chromatography
Tandem Mass spectrometry
Forensics

ABSTRACT

Mescaline is a psychedelic phenethylamine found in different species of cacti. Currently, mescaline's acute subjective effects and pharmacokinetics are investigated in several modern clinical studies. Therefore, we developed a bioanalytical method for the rapid quantification of mescaline and its metabolites in human plasma. Mescaline and its metabolites 3,4,5-trimethoxyphenylacetic acid (TMPAA), N-acetyl mescaline (NAM), and 3,5-dimethoxy-4-hydroxyphenethylamine (4-desmethyl mescaline) were simultaneously analyzed by ultra-high performance liquid chromatography tandem mass spectrometry (LC-MS/MS). Optimal chromatographic separation was achieved with an Acquity Premier HSS T3 C₁₈ column. The analytes were detected in positive ionization mode using scheduled multiple reaction monitoring. A single step extraction method was implemented to enable fast and automatable plasma sample preparation. An intra-assay accuracy between 84.9% and 106% and a precision of $\leq 7.33\%$ was observed in three validation runs. Plasma was extracted by simple protein precipitation, resulting in a complete recovery ($\geq 98.3\%$) and minor matrix effects ($\leq 7.58\%$). No interference with endogenous matrix components could be detected in human plasma samples ($n = 7$). Importantly, method sensitivity sufficed for assessing pharmacokinetic parameters of mescaline in clinical study samples with lower limits of quantification of 12.5, 12.5, and 1.25 ng/mL for mescaline, TMPAA, and NAM, respectively. Nonetheless, 4-desmethyl mescaline could not be selectively quantified in pharmacokinetic samples due to interference with another mescaline metabolite. Overall, we developed and validated a reliable and very easy-to-use method for forensic applications as well as investigating the clinical pharmacokinetics of mescaline.

1. Introduction

Mescaline, also known as 3,4,5-trimethoxyphenethylamine, is a psychoactive alkaloid abundant in various species of cacti such as *Lophophora williamsii* (peyote), *Trichocereus pachanoi* (san pedro), or *Trichocereus peruvianus* (peruvian torch). The peyote cactus occurs in the southwest of the United States and the north of Mexico, while the two other species grow in South America [1–3]. The psychoactive properties of mescaline are known to the indigenous people of America for at least 5700 years, being used in religious and spiritual ceremonies but also for psychotherapeutic purposes [3,4]. Today, mescaline is utilized in religious and recreational settings and is a scheduled substance in most western countries. However, the frequency of mescaline use is rather low compared to other psychedelics [1,5,6]. Mescaline's acute subjective effects and pharmacokinetics (PK) are currently investigated in

several clinical studies, as it holds promise for the therapy of various psychiatric disorders such as depression, addiction, anxiety disorder, but also in palliative care similar to other classic psychedelics [7–9].

Mescaline's mind-altering effects resemble those of LSD and psilocybin and probably also occur primarily through an interaction with the human 5-HT_{2A-C} receptors. It shows agonistic properties at the 5-HT_{2A} receptor, the receptor thought to play a key role in exerting hallucinogenic effects in humans [10,11]. However, in comparison to LSD and psilocybin, mescaline has the lowest potency in activating 5-HT_{2A} and 5-HT_{2B} receptors [2,12–14]. Additionally, mescaline is a highly polar compound and accordingly possesses a low ability to cross the blood-brain-barrier. For these reasons, high doses of around 200 – 400 mg are necessary to exert psychoactive effects [2,14].

Mescaline is readily absorbed in the gastro-intestinal tract so that first pharmacological effects occur about 30 min after oral

* Correspondence to: Division of Clinical Pharmacology and Toxicology, Department of Biomedicine, University Hospital Basel and University of Basel, Switzerland.

E-mail address: matthias.liechti@usb.ch (M.E. Liechti).

<https://doi.org/10.1016/j.jpba.2022.114980>

Received 28 June 2022; Received in revised form 28 July 2022; Accepted 31 July 2022

Available online 1 August 2022

0731-7085/© 2022 The Authors. Published by Elsevier B.V. This is an open access article under the CC BY license (<http://creativecommons.org/licenses/by/4.0/>).

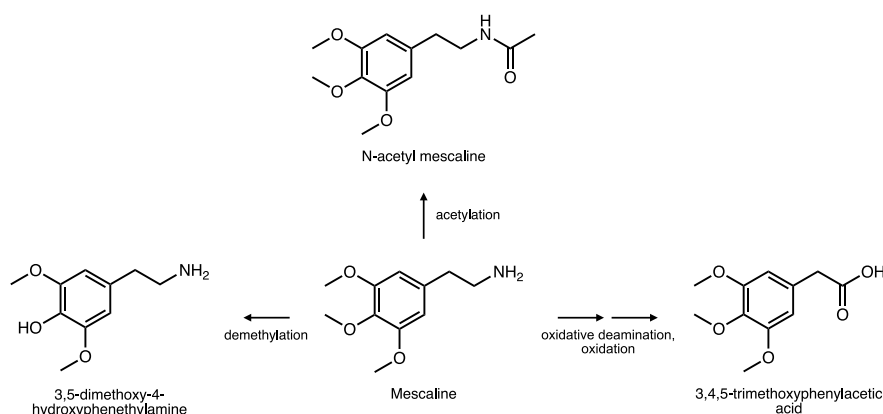


Fig. 1. Chemical structures of mescaline and metabolites detected in humans. Mescaline is *in vivo* mainly metabolized into 3,4,5-trimethoxyphenylacetic acid through oxidative deamination and subsequent oxidation. Further metabolic pathways involve N-acetylation of mescaline to N-acetyl mescaline and demethylation of the 4-methoxy group to 3,5-dimethoxy-4-hydroxyphenethylamine.

administration. The effects usually peak around 2 h post-ingestion and last for 8 – 12 h, which is generally longer compared to other hallucinogens [2,5,14,15]. PK studies have shown that mescaline is largely excreted unchanged via urine [2,16]. Nevertheless, mescaline undergoes oxidative deamination followed by immediate oxidation to the inactive 3,4,5-trimethoxyphenylacetic acid (TMPAA) metabolite (Fig. 1) [2,16,17]. Another major metabolic pathway seems to be the N-acetylation of mescaline to N-acetyl mescaline (NAM) [16]. Moreover, mescaline is to a minor extent demethylated either to 3,4-dimethoxy-5-hydroxyphenethylamine (3-desmethyl mescaline) or 3,5-dimethoxy-4-hydroxyphenethylamine (4-desmethyl mescaline) [2,5,18]. Further minor metabolites have been predicted by others, but their clinical relevance is unknown [2,3].

Several analytical methods have been published which focus on the quantification of mescaline, but so far rarely incorporate analysis of its metabolites (Table 1). Most methods used either gas chromatography (GC) or high performance liquid chromatography (HPLC) coupled to a diode array detector, a single, or tandem mass spectrometer. Methods were developed to determine mescaline in various matrices such as plant material, urine, hair, saliva, and plasma. However, these methods required mostly large amounts of sample. Work- and time-intensive extraction procedures were employed including multistep solid-phase or liquid-liquid extraction protocols. In addition, extensive gradient programs of 5 – 21 min were used to separate the analytes of interest [19–33].

Altogether, a bioanalytical method is required that enables rapid analysis of large amounts of samples collected within clinical trials. In the present study we developed and validated an LC-MS/MS method to investigate the clinical pharmacokinetics of mescaline and its two major metabolites TMPAA and NAM. The method requires only a small amount of plasma which is processed by a simple and automatable protocol and analyzed within few minutes.

2. Material and methods

2.1. Chemicals, reagents, and reference compounds

Mescaline (99.1% purity) was obtained from Lipomed (Arllesheim, Switzerland), 3,4,5-trimethoxyphenylacetic acid (99.8% purity) from Toronto Research Chemicals (TRC, Toronto, Canada), N-acetyl mescaline (> 99.0% purity) from Biosynth Carbosynth (Compton, United Kingdom), and 3,5-dimethoxy-4-hydroxyphenethylamine (non-specified purity) from Sigma Aldrich (St. Louis, USA). The deuterated internal standard mescaline- d_3 (3,5-dimethoxy-4-(methoxy- d_3)-phenylethylamine hydrochloride, 99.5% isotopic purity) was synthesized by

Reseachem (Burgdorf, Switzerland). LC-MS grade water, methanol, isopropanol, and acetic acid were products from Merck (Darmstadt, Germany). LC-MS grade acetonitrile was purchased from Thermo Fisher Scientific (Waltham, USA). LC-MS grade ammonium acetate as well as dimethyl sulfoxide (DMSO) were obtained from Sigma Aldrich.

Human blood was collected in lithium heparin coated S-Monovette tubes (Sarstedt, Nümbrecht, Germany) and obtained from the local blood donation center (Basel, Switzerland). The blood was centrifuged at $1811 \times g$ for 10 min (5810 R, Eppendorf, Hamburg, Germany) to produce plasma.

2.2. Stock solution preparation

A separate analyte stock solution was prepared for calibrator (CAL) and quality control (QC) samples. The analytes were weighed in on a XP 26 microbalance (Mettler Toledo, Columbus, USA) and dissolved in DMSO to receive a final concentration of 10 mg/mL for mescaline and TMPAA and 1 mg/mL for NAM and 4-desmethyl mescaline. Mescaline- d_3 was prepared in methanol to obtain a solution of 10 mg/mL. This stock solution was further diluted to 5 ng/mL in methanol to create the internal standard working solution (ISTD). All stocks were stored at -20°C .

2.3. Calibration and quality control sample preparation

CAL and QC working solutions were prepared in DMSO. Firstly, all four analytes were mixed to receive a solution of 1'000 $\mu\text{g/mL}$ mescaline and TMPAA and 100 $\mu\text{g/mL}$ NAM and 4-desmethyl mescaline. Secondly, the CAL and QC mixtures were serially diluted with DMSO. Finally, a pool of blank human plasma ($n = 7$ donors) was spiked with the CAL and QC working solutions at a ratio of 1:100 (v/v). The CAL line in plasma contained nine points and ranged from 12.5 ng/mL to 5'000 ng/mL for mescaline and TMPAA and from 1.25 ng/mL to 500 ng/mL for NAM and 4-desmethyl mescaline.

The same procedure was used to prepare five QC levels in plasma including a lower limit of quantification (LLOQ), low QC (LQC), medium QC (MQC), high QC (HQC), and the upper limit of quantification (ULOQ) sample. The QC levels corresponded to 12.5 ng/mL, 25 ng/mL, 250 ng/mL, 2'500 ng/mL, and 5'000 ng/mL for mescaline and TMPAA and 1.25 ng/mL, 2.5 ng/mL, 25 ng/mL, 250 ng/mL, and 500 ng/mL for NAM and 4-desmethyl mescaline.

2.4. LC-MS/MS instrumentation and setting

The bioanalysis was performed on an ultra-high performance liquid

Table 1
Overview of existing bioanalytical methods for the analysis of mescaline and metabolites in various matrices.

Publication	Analytical Method	Analyte (s)	Examined Matrix	Sample Volume / Sample Mass	Sample Processing	Quantification Range	Injection Volume	Run Time	Reference
Ma et al. 1986	TLC-MS/MS	Mescaline and 4-desmethyl mescaline	Plant material	5'000 mg	LE	NA	NA	NA	[32]
Helmlin et al. 1992	HPLC-DAD	Mescaline (i.a.)	Plant material	10 mg	LE	20'000 – 75'000 ng/mL	5 µL	12.0 min	[31]
Valentine et al. 2000	GC-MS	Mescaline (i.a.)	Human urine	100 µL	LLE	NA	1 µL	8.00 min	[25]
Habrdova et al. 2005	GC-MS	Mescaline (i.a.)	Human plasma	1'000 µL	LLE / SPE	5.00 – 500 ng/mL	1 µL	10.0 min	[26]
Beyer et al. 2007	LC-MS/MS	Mescaline (i.a.)	Human plasma	1'000 µL	SPE	10.0 – 1'000 ng/mL	5 µL	17.0 min	[27]
Kim et al. 2007	GC-MS	Mescaline (i.a.)	Human hair	20 mg	LE	0.05 – 25.0 ng/mg	1 µL	15.0 min	[28]
Björnstad et al. 2008	LC-MS/MS	Mescaline	Human urine	20 µL	LLE / SPE	5.00 – 10'000 ng/mL	10 µL	9.00 min	[19]
Casado et al. 2008	HPLC-DAD	Mescaline	Plant material	1'000 mg	LE	5'000 – 200'000 ng/mL	20 µL	8.00 min	[20]
Sergi et al. 2010	LC-MS/MS	Mescaline (i.a.)	Human saliva	90 µL	SPE	LOQ: 0.20 ng/mL	NA	21.0 min	[33]
Gambelunghe et al. 2013	GC-MS/MS	Mescaline	Human urine, hair	2'000 µg / 20 mg	LE	50.0 – 500 ng/mL / 100 – 1'200 pg/mg	1 µL	> 16.0 min	[21]
Pichini et al. 2014	LC-MS/MS	Mescaline (i.a.)	Human hair	25 mg	LE	LOQ: 0.05 ng/mg	10 µL	16.5 min	[29]
Battal et al. 2015	GC-MS	Mescaline	Human urine	1'000 µL	LLE / SPE	1.00 – 250 ng/mL	2 µL	9.50 min	[22]
Longo et al. 2020	DART-HRMS	Mescaline	Plant material	> 150 mg	LE	1'000 – 100'000 ng/mL	NA	> 18.0 min	[23]
Francisco da Cunha et al. 2020	LC-MS/MS	Mescaline (i.a.)	Human saliva	500 µL	LLE	NA	NA	13.5 min	[30]
Yang et al. 2022	LC-MS/MS	Mescaline	Human hair	20 mg	LE	0.01 – 1.00 ng/mL	5 µL	5.00 min	[24]
Current method	LC-MS/MS	Mescaline, TMPAA, NAM, and 4-desmethyl mescaline	Human plasma	50 µL	LLE	12.5 – 5'000 ng/mL / 1.25 – 500 ng/mL	5 µL	4.25 min	–

4-desmethyl mescaline, 3,5-dimethoxy-4-hydroxyphenethylamine; DART-HRMS, direct analysis in real time high-resolution mass spectrometry; GC-MS, gas chromatography mass spectrometry; LC-MS/MS, liquid chromatography tandem mass spectrometry; HPLC-DAD, high performance liquid chromatography with photodiode-array detection; i.a., among other analytes analyzed; LC-MS/MS, liquid chromatography tandem mass spectrometry; LE, liquid extraction; LLE, liquid-liquid extraction; LOQ, limit of quantification; NA, not assessed; NAM, N-acetyl mescaline; SPE, solid phase extraction; TLC-MS/MS, thin layer chromatography tandem mass spectrometry; TMPAA, 3,4,5-trimethoxyphenylacetic acid.

chromatography system (UHPLC, Shimadzu, Kyoto, Japan) coupled to an API 5000 triple quadrupole tandem mass spectrometer (MS, AB Sciex, Ontario, Canada).

The following analytical columns were tested during method development: Luna PFP(2) (3 µm, 50 × 2 mm, Phenomenex, Torrance, USA), Halo 90 Å Biphenyl (2.7 µm, 2.1 × 50 mm, Advanced Materials Technology, Wilmington, USA), Accucore Biphenyl (2.6 µm, 100 × 2.1 mm, Thermo Fisher Scientific), Hypersil GOLD aQ (1.9 µm, 50 × 2.1 mm, Thermo Fisher Scientific), Symmetry C₁₈ (3.5 µm, 4.6 × 75 mm, Waters, Milford, USA), Kinetex XB-C₁₈ (2.6 µm, 50 × 2.1 mm, Phenomenex), Kinetex EVO C₁₈ (1.7 µm, 50 × 2.1 mm, Phenomenex), Acquity Premier HSS T3 C₁₈ (1.8 µm, 2.1 × 100 mm, Waters), Atlantis Premier BEH C₁₈ AX (2.5 µm, 2.1 × 150 mm, Waters), and Atlantis dC₁₈ (3 µm, 2.1 × 50 mm, Waters). After the screening, the validation was executed with the Acquity Premier HSS T3 C₁₈ analytical column (1.8 µm, 2.1 × 100 mm, Waters) which provided most promising results.

The modular UHPLC system included an autosampler (set to 10 °C), a system controller, four pumps (A, B, C, and D), two degassing units, and a column oven (set to 45 °C). Mobile phase A and C was an aqueous solution of ammonium acetate (10 mM) supplemented with 0.1% acetic acid (pH 4.4). Mobile phase B was methanol containing 0.1% acetic acid. Before and after sample injection (5 µL), the autosampler port was rinsed with 500 µL washing solution consisting of equal amounts of water, methanol, acetonitrile, and isopropanol (1:1:1:1, v/v). The injected sample was transported by pump A and B onto the analytical column. A T-union was installed in front of the column to mix the injected sample with mobile phase C (0.20 mL/min, 0 – 0.50 min). The initial total flow of pump A (2%) and B (98%) was set to 0.20 mL/min and raised to 0.40 mL/min after 0.50 min. Mobile phase B concentration was linearly increased from 2% to 50% between 0.50 min and 0.75 min and from 50% to 70% between 0.75 and 2.75 min. Afterwards, the column was washed with 95% mobile phase B for 1.00 min and reconditioned at 2% mobile phase B for another 0.50 min. The UHPLC was connected to the mass spectrometer from 1.40 min to 3.00 min of each run, otherwise the eluate was directed into the waste bottle. The gradient program lasted 4.25 min and resulted in retention times of 1.89 min for 4-desmethyl mescaline, 2.04 min for mescaline, 2.40 min for TMPAA, and 2.53 min for NAM (Table 2).

The analytes were charged by positive electron spray ionization (ESI) and detected using scheduled multiple reaction monitoring (sMRM). The general MS parameters were set as follows: ion spray voltage (IS), 5500 V; temperature (TEM), 500 °C; curtain gas (CUR), 10 psi; nebulizer gas (ion source gas 1, GS1), 60 psi; heater gas (ion source gas 2, GS2) 50 psi; collision gas (CAD), 4 psi. Elemental nitrogen (N₂) was used as gas supply. The analyte specific settings and mass transitions (Q1 → Q3) are listed in Table 2. To quantify mescaline, transition m/z 215.1 → m/z 165.2 of mescaline-d₃ was used while transition m/z 215.1 → m/z 198.2 of mescaline-d₃ was used for the quantification of TMPAA, NAM, and 4-desmethyl mescaline.

Analyst Instrumental Control and Data Processing Software (Version 1.7.2, AB Sciex) and MultiQuant Software (Version 3.0.3, AB Sciex) were used for LC-MS/MS operation and data analysis, respectively.

2.5. Sample extraction

Human plasma samples of 50 µL were aliquoted into matrix tubes (0.7 mL, 96-deepwell rack, Thermo Fisher Scientific) and precipitated by adding 400 µL of ISTD solution. Subsequently, the samples were vortexed on a Multi Tube Vortexer (VX-2500, VWR, Radnor, USA) for at least 1 min and centrifuged for 30 min at 10 °C and 3220 × g to produce a plasma protein free supernatant. After extraction, samples were kept in the autosampler at 10 °C until analysis.

Table 2
Tandem mass spectrometry settings applied for the quantification of mescaline and its metabolites.

Analyte	MRM (m/z) (Q1 → Q3)		RT [min]	DP [V]	EP [V]	CE [V]	CXP [V]
Mescaline	212.1 → 180.1	qualifier	2.04	76	10	43	16
	212.1 → 165.0	quantifier	2.04	76	10	22	14
TMPAA	227.0 → 181.1	qualifier	2.40	36	10	11	14
	227.0 → 148.0	quantifier	2.40	36	10	17	34
NAM	254.1 → 195.2	quantifier	2.53	126	10	34	12
	254.1 → 180.1	qualifier	2.53	126	10	37	20
4-desmethyl mescaline	198.2 → 181.2	quantifier	1.89	86	10	18	20
	198.2 → 166.2	qualifier	1.89	86	10	25	18
Mescaline- d_3	215.1 → 198.2	NA	2.03	86	10	15	22
	215.1 → 165.2	NA	2.03	86	10	31	18

4-desmethyl mescaline, 3,5-dimethoxy-4-hydroxyphenethylamine; CE, collision energy; CXP, collision cell exit potential; DP, declustering potential; EP, entrance potential; m/z , mass-to-charge ratio; MRM, multiple reaction monitoring; NA, not applicable; NAM, N-acetyl mescaline; Q1, quadrupole 1; Q3, quadrupole 3; RT, retention time; TMPAA, 3,4,5-trimethoxyphenylacetic acid; V, volt.

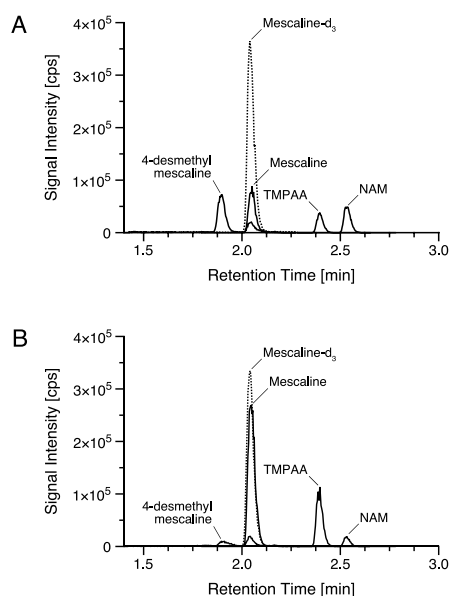


Fig. 2. Chromatographic separation of mescaline, 3,4,5-trimethoxyphenylacetic acid (TMPAA), N-acetyl mescaline (NAM), 3,5-dimethoxy-4-hydroxyphenethylamine (4-desmethyl mescaline), and mescaline- d_3 in human plasma. A: 4-desmethyl mescaline (25 ng/mL, retention time: 1.89 min), mescaline- d_3 (5 ng/mL, retention time: 2.03 min, dotted line), mescaline (250 ng/mL, retention time: 2.04 min), TMPAA (250 ng/mL, retention time: 2.40 min), and NAM (25 ng/mL, retention time: 2.53 min) in human plasma. B: Analysis of a clinical phase 1 study plasma sample. The healthy subject received an oral dose of 300 mg mescaline hydrochloride and the blood sample was withdrawn 2 h post-treatment.

2.6. Method validation

The validation of the method was conducted according to the Bio-analytical Method Validation Guidance for Industry of the United States Food and Drug Administration (FDA) [34]. The method was validated on an API 5000 LC-MS/MS system considering the following parameters: linearity, accuracy and precision, selectivity and sensitivity, extraction recovery and matrix effect, as well as analyte stability under various storage conditions.

2.6.1. Linearity

Each analytical run consisted of at least two discrete CAL lines, one measured at the beginning and the other at the end of the acquisition batch. A CAL line comprised of nine different concentration levels in increasing order, a blank, and a double blank sample. The blank sample was extracted with ISTD and measured before the LLOQ sample of the CAL. The double blank sample was processed with pure methanol and measured after the highest CAL to assess the proportion of analyte carry-over. The carry-over should be less than 20% of the peak area determined at the LLOQ.

A linear regression line was established in MultiQuant by plotting the nominal concentration of the CAL points against the ratio of the analyte peak area to the ISTD peak area. A weighing factor of $1/x^2$ was employed to reduce the error at low concentrations. The accuracy was calculated for each CAL point as the difference (%) between measured and nominal concentration. Only CAL points with an accuracy of 85 – 115% (LLOQ: 80 – 120%) were used to build CAL lines. However, a valid CAL had to include at least 75% of all values (e.g., 14 out of 18) and no less than one LLOQ and ULOQ sample. Finally, a correlation coefficient (R) of ≥ 0.99 was necessary to accept the CAL line.

2.6.2. Intra- and inter-assay accuracy and precision

Intra- and inter-assay accuracy and precision was determined by analyzing three validation runs on different days. Each validation run contained two CAL lines and seven replicates of each QC level (LLOQ, LQC, MQC, HQC, ULOQ). The accuracy was determined for each QC level as percentage difference (%) of the measured value to the nominal value within an assay (intra-assay: $n = 7$) and over three assays (inter-assay: $n = 21$). The coefficient of variation ($\%CV = \frac{\text{standard deviation}}{\text{mean}} \times 100$) was used as measurement of method precision (intra-assay: $n = 7$, inter-assay: $n = 21$ per QC level). An accuracy of 85 – 115% (LLOQ: 80 – 120%) and a precision of $\leq 15\%$ was accepted in this validation. All values, valid and in-valid, were used to calculate mean accuracy and to determine method precision. Altogether, at least half of the QC samples per level ($\geq 50\%$, 4 out of 7) and more than two thirds of all QC samples ($\geq 67\%$, 24 out of 35) had to exhibit an accuracy of 85 – 115% (LLOQ: 80 – 120%).

2.6.3. Selectivity and sensitivity

Method selectivity was assessed by analyzing plasma samples of seven different subjects. Double blank, blank, and LLOQ samples were prepared for each individual plasma. The analyte peak area at the LLOQ had to be at least five times larger than that of the noise signal in the blank and double blank samples. Furthermore, the accuracy of the LLOQ samples was determined based on two CAL lines. The mean accuracy and the individual accuracy of 4 out of 7 LLOQ samples ($\geq 50\%$) had to be within 80 – 120% to approve method sensitivity.

2.6.4. Extraction recovery and matrix effect

To assess the extraction recovery plasma samples of seven different subjects were spiked with equal amounts of analyte before and after extraction. Four QC levels (LLOQ, LQC, MQC, and HQC) were prepared to investigate the effect of the analyte concentration on the extraction recovery. The analyte peak area of the two conditions were pairwise compared to estimate the extraction recovery for each subject and QC

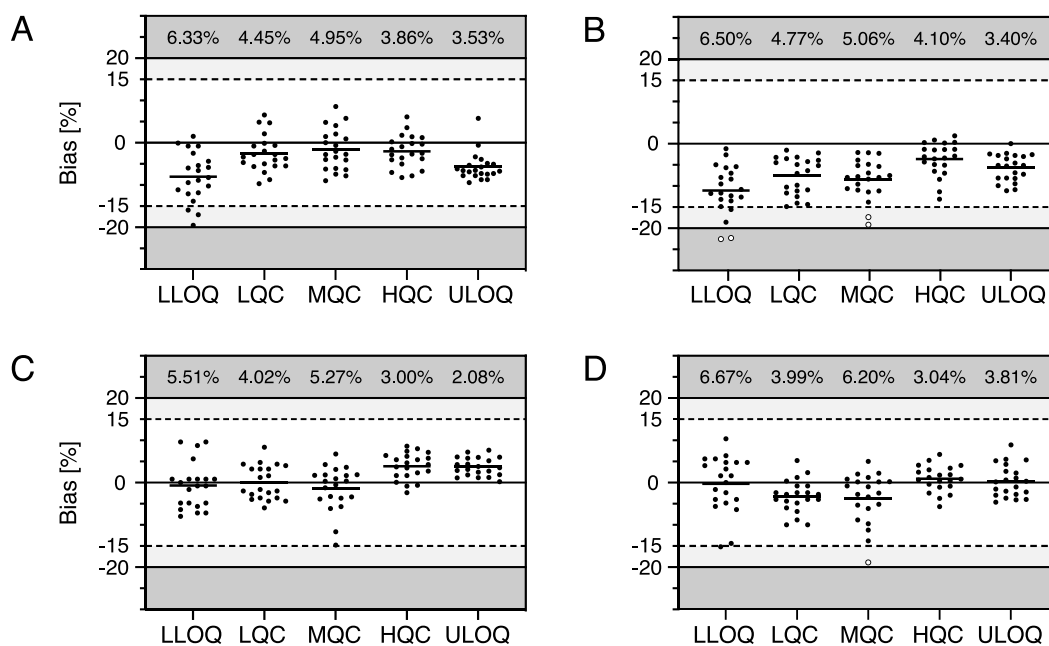


Fig. 3. Inter-assay accuracy and precision of mescaline (A), 3,4,5-trimethoxyphenylacetic acid (B), N-acetyl mescaline (C), and 3,5-dimethoxy-4-hydroxyphenethylamine (D) in human plasma. Inter-assay accuracy and precision was estimated by analyzing seven quality control (QC) samples at five concentration levels in three independent assays. The accuracy was calculated as percent bias (%) of the calculated to the nominal concentration. The inter-assay accuracy is shown as a black horizontal line. Data out of the acceptable range of $\pm 15\%$ (LLOQ: $\pm 20\%$) are illustrated in white. The Inter-assay precision (%CV) is displayed at the top of each graph.

level. The recovery of samples spiked after extraction was by definition 100%. The recovery had to be consistent between different plasma batches and QC levels ($\%CV \leq 15\%$).

The matrix effect was determined by comparing the analyte peak area of plasma samples, which were spiked after extraction, with matrix free samples containing water and ISTD solution (1:8, v/v). Therefore, equal amounts of the analytes were added to both sample types at four QC levels (LLOQ, LQC, MQC, and HQC). Inter-batch matrix variability was investigated by assessing plasma samples of seven subjects. Overall, matrix suppression and enhancement had to be consistent between plasma batches and QC levels indicated by a $\%CV$ of $\leq 15\%$ (LLOQ: $\%CV \leq 20\%$).

2.6.5. Stability

Several stability tests were performed for mescaline, TMPAA, NAM, and 4-desmethyl mescaline. The stability of seven replicates at each of the five QC levels (LLOQ, LQC, MQC, HQC, and ULOQ) were assessed under the following conditions. Extracted plasma samples were kept overnight in the autosampler at 10°C and re-analyzed on the following day (autosampler stability). Plasma samples were stored for 8 h at room temperature (benchtop stability), 1 month at -20°C (short-term stability), and 3 months at -20°C (medium-term stability). Plasma samples were subjected to three freeze and thaw cycles, keeping the samples at -80°C for at least 24 h and thawing them unassisted at room temperature (freeze-thaw stability). Stability of the QC samples was assessed using freshly prepared CAL lines. A deviation of the measured and nominal concentration of $\leq 15\%$ (LLOQ: $\leq 20\%$) indicated that the samples were stable under the particular storage condition.

2.7. Method application

The applicability of the method was tested by analyzing a subset of pharmacokinetic study samples ($n = 5$ participants) from a clinical phase 1 study, which was approved by the ethics committee of

Northwest and Central Switzerland (BASEC ID: 2019-02023) and registered at clinicaltrials.gov (ID: NCT04227756). The study was executed according to the Declaration of Helsinki and the International Conference of Harmonization for Good Clinical Practice guidelines.

Study participants received a single oral dose of 300 mg mescaline hydrochloride. Blood samples were drawn into lithium heparin coated S-Monovette tubes (Sarstedt) before treatment and 0.25, 0.5, 0.75, 1, 1.5, 2, 3, 3.5, 4, 5, 6, 7, 8, 10, 12, 14, 16, and 24 h post-treatment. Blood samples were centrifuged at $1811 \times g$ for 10 min to produce plasma and stored at -80°C until analysis. Sample extraction was carried out as described in Section 2.5. All 95 study samples were analyzed in one analytical run between two CAL lines, which were measured at the beginning and at the end of the run. In addition, four sets of QC samples of five different levels (LLOQ, LQC, MQC, HQC, and ULOQ) were equally distributed over the entire acquisition batch.

Pharmacokinetic parameters were calculated with Phoenix Win-Nonlin Software (Version 8.1.0, Certara, Princeton, USA). Plasma concentrations below the LLOQ were set to zero for the calculations. The elimination half-life ($t_{1/2}$, h) was calculated as $t_{1/2} = \ln(2)/\lambda$. The elimination constant (λ) was estimated by linear regression in the terminal elimination phase. The maximal plasma concentration (C_{\max} , ng/mL) and time to reach maximal concentration (t_{\max} , h) were directly obtained from the concentration-plots. The area under the curve (AUC_{0-24} , min*ng/mL) was calculated based on the linear trapezoidal rule from timepoint zero to the timepoint of the last quantifiable concentration.

3. Results and discussion

3.1. Method development

Mescaline is subject of growing interest for the use as a novel therapeutic agent for treatment of several psychiatric disorders. Quantification of mescaline and metabolite levels in blood circulation is essential

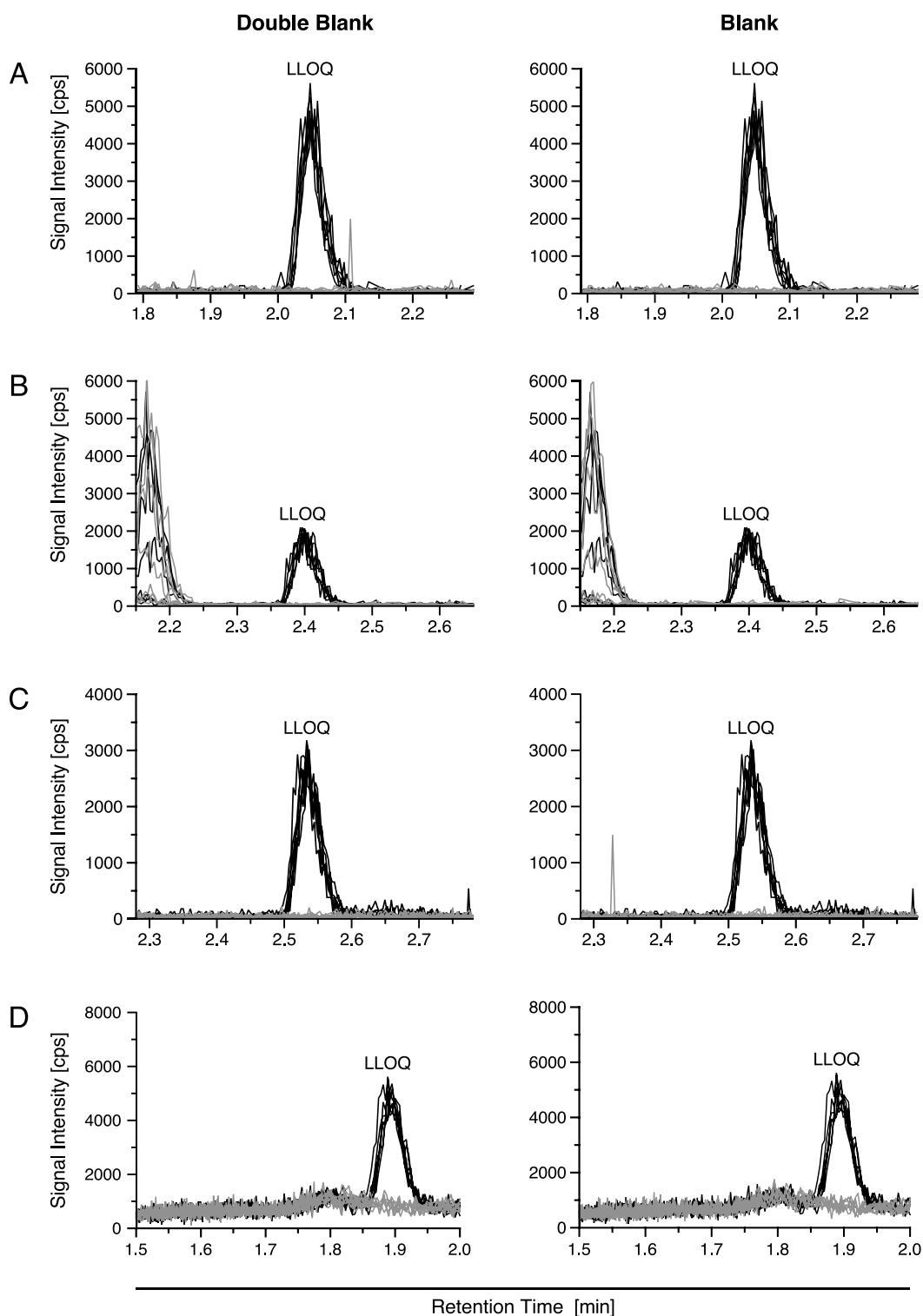


Fig. 4. Selectivity and sensitivity of mescaline (A), 3,4,5-trimethoxyphenylacetic acid (B), N-acetyl mescaline (C), and 3,5-dimethoxy-4-hydroxyphenethylamine (D) in human plasma. Overlay of seven double blank samples (left side, grey lines), seven blank samples (right side, grey lines), and seven lower limit of quantification samples (LLOQs, black lines) originating from different batches of human plasma. The signal-to-noise ratio at the LLOQ level was for all analytes > 5:1.

Table 3

Extraction recovery and matrix effect determined for mescaline, 3,4,5-trimethoxyphenylacetic acid (TMPAA), N-acetyl mescaline (NAM), and 3,5-dimethoxy-4-hydroxyphenethylamine (4-desmethyl mescaline) in human plasma.

Analyte	QC Level	Recovery	Mean	Matrix	Mean
		± %CV	Recovery ± %CV	Effect ± %CV	Matrix Effect ± %CV
		[%]	[%]	[%]	[%]
<i>Mescaline</i>	LLOQ	100 ± 8.15	99.2 ± 0.85	97.2 ± 3.75	92.4 ± 5.92
	LQC	98.2 ± 6.33		92.2 ± 3.70	
	MQC	98.7 ± 3.76		84.8 ± 2.81	
	HQC	100 ± 4.18		95.5 ± 2.20	
<i>TMPAA</i>	LLOQ	102 ± 6.72	104 ± 2.48	99.4 ± 3.93	96.8 ± 4.15
	LQC	107 ± 6.87		95.6 ± 2.87	
	MQC	102 ± 2.86		91.6 ± 2.26	
	HQC	103 ± 2.20		100 ± 2.28	
<i>NAM</i>	LLOQ	98.5 ± 9.02	102 ± 2.48	100 ± 6.45	97.1 ± 4.20
	LQC	102 ± 2.91		96.8 ± 2.83	
	MQC	104 ± 3.64		91.6 ± 3.26	
	HQC	103 ± 3.64		101 ± 2.13	
<i>4-desmethyl mescaline</i>	LLOQ	98.2 ± 7.97	98.3 ± 1.04	106 ± 5.07	100 ± 6.11
	LQC	97.7 ± 4.19		102 ± 3.20	
	MQC	100 ± 3.50		91.6 ± 2.38	
	HQC	97.5 ± 1.59		101 ± 3.28	

%CV, coefficient of variation; HQC, high quality control; LLOQ, lower limit of quantification; LQC, low quality control; MQC, medium quality control; ULOQ, upper limit of quantification.

to further our knowledge about its pharmacokinetic properties. It enables us to relate exposure with drug activity data or to evaluate interactions with co-medications such as antidepressants, which might influence treatment outcome and safety. So far, bioanalytical methods were mainly developed for forensic purposes without emphasizing analysis throughput and the pharmacological role of the mescaline metabolites. We aimed to address these gaps by developing and validating a bioanalytical method which allows an uncomplicated analysis of mescaline and its metabolites even in minute quantities of human plasma.

The method development was initiated by infusing each analyte into the mass spectrometer to optimize ionization parameters and elucidate their fragmentation pattern. Mescaline, mescaline- d_3 , NAM, and 4-desmethyl mescaline were ionized in the positive mode, whereas the ionization of TMPAA was tested in the positive and negative mode due to its acetic acid moiety. Mescaline (m/z 211.1 + 1 H⁺) fragmented predominantly into the three fragments m/z 195.1, m/z 180.1, and m/z 165.0. Best initial signal intensities and signal-to-noise ratios were recorded for fragments m/z 195.1 and m/z 165.0. Indeed, these two fragments were also detected and employed in other studies [19,27,32,33]. For mescaline- d_3 (m/z 214.1 + 1 H⁺) we found the fragments m/z 198.2, m/z 183.0, and m/z 165.2 corresponding to the mass fragments observed for mescaline but containing all three deuterium atoms. In addition, NAM (m/z 253.1 + 1 H⁺) produced the same fragments as mescaline (m/z 195.2 and m/z 180.1). TMPAA could be analyzed in the positive and negative mode. However, we selected positive ionization

(m/z 226.0 + 1 H⁺) to avoid polarity switching. The mass transitions to m/z 181.1 and m/z 148.0 were integrated into our method. Finally, 4-desmethyl mescaline (m/z 197.2 + 1 H⁺) fragmented best into m/z 181.2 and m/z 166.2 as observed by Ma and colleagues [32]. Product ion spectra of all analytes are depicted in [Supplementary Fig. S1](#).

In a next step, we optimized separation and retention of the analytes by screening various chromatographic columns and mobile phases. We examined C₁₈, pentafluorophenyl, and biphenyl phase HPLC columns. C₁₈ phase columns were in general able to retain and separate the polar and aromatic compounds most effectively. Overall, best peak shapes and analyte separation was achieved with an Acquity C₁₈ column (1.8 μm, 2.1 × 100 mm). Water was used as mobile phase A and combined with methanol or acetonitrile as mobile phase B. Acetonitrile reduced the retention of most analytes but did not improve method sensitivity or chromatographic resolution. Various mobile phase additives were investigated including acetic and formic acid (0.01%, 0.02%, 0.05%, and 0.1% v/v) aiming to improve ionization by creating an environment where e.g., amine containing analytes are sufficiently protonated [35]. In addition, we screened different concentrations of ammonium formate and acetate (2.5, 5, and 10 mM) dissolved in mobile phase A. Notably, 0.1% acetic acid was with our setting superior to other concentrations and also to formic acid regarding peak shape and separation. Importantly, the addition of ammonium acetate but not formate enhanced peak separation. A representative chromatogram is given in [Fig. 2](#) using an aqueous ammonium acetate solution (10 mM, 0.1% acetic acid, pH 4.4) and methanol (0.1% acetic acid) as mobile phases A and B, respectively.

We aimed to use a simple protein precipitation method for plasma sample extraction to reduce the work steps considering that hundreds of samples must be processed for PK studies. Moreover, we selected a volume of 50 μL plasma which is convenient to handle and allows for repetitive analyses also when only small amounts of blood are withdrawn from study participants. Plasma samples were extracted with methanol in order to precipitate proteins which were subsequently spun down by centrifugation. We injected an aliquot of pure methanolic supernatant into the LC-MS/MS system. The sample was diluted online within a T-union with mobile phase A (transported by pump C) before reaching the analytical column. Mixing the methanolic sample with water (mobile phase A) improved the retention of the polar analytes on the stationary phase. For this analysis the peak shape of 4-desmethyl mescaline was inadequate without an online dilution flow program.

In the last development step, we quantified the analytes in plasma samples of participants given an oral dose of 300 mg mescaline hydrochloride. Based on these findings, we defined the calibration range for each analyte. Peak intensities of TMPAA and NAM were beyond the linear range of the employed mass detector, thus we quenched their signal strength by reducing the collision energy. By this approach, the signal intensity of the other analytes was not affected and samples must not be additionally diluted making PK study sample analysis overall more practicable.

3.2. Method validation

3.2.1. Method linearity

The method was linear from 12.5 to 5'000 ng/mL for mescaline and TMPAA and from 1.25 to 500 ng/mL for NAM and 4-desmethyl mescaline. Calibration curves were fitted by linear regression using a weighting of 1/x² to improve the accuracy at low concentrations. The correlation coefficients (R) of all validation runs were above 0.998 and none of the calibration points had to be excluded for establishing the linear regressions as the deviation from the nominal value was throughout ≤ 15% (LLOQ ≤ 20%). Intra- and inter-assay linearity of all analytes are summarized in [Supplementary Table S1](#). Importantly, the chosen calibration range was at least two times higher than the maximal concentrations observed in clinical study samples. In addition, the sensitivity was sufficient to monitor the PK of mescaline over 24 h (see

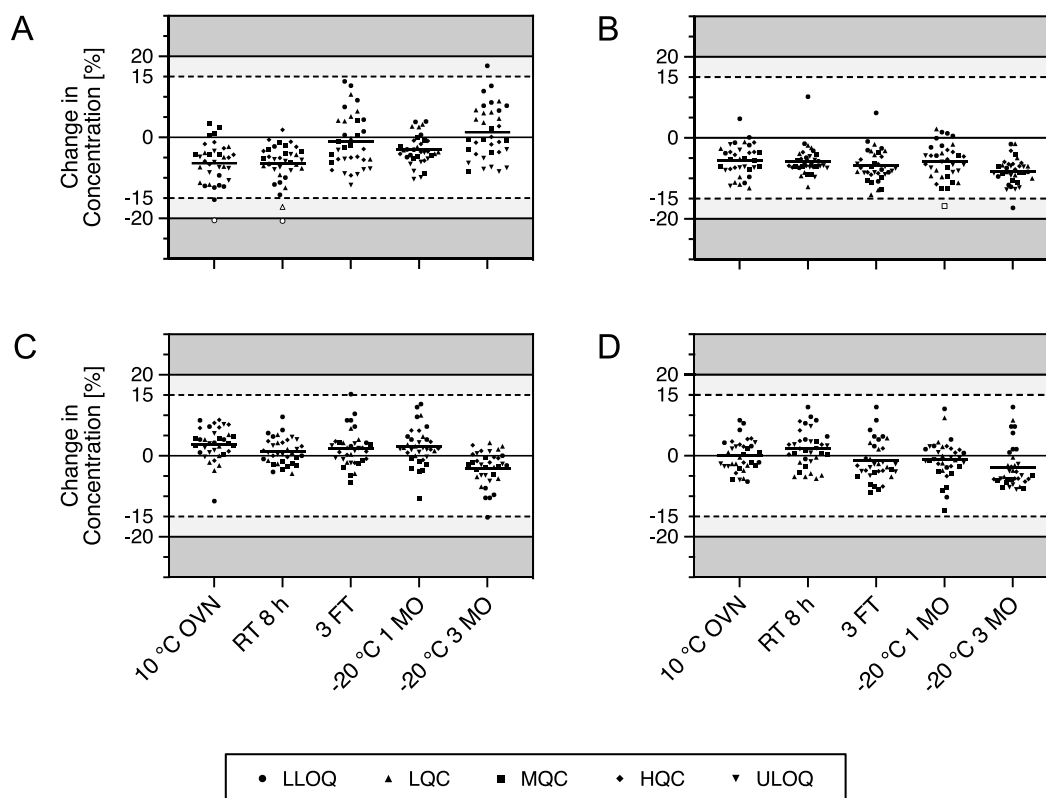


Fig. 5. Stability of mescaline and its metabolites under various storage conditions. Autosampler stability (10 °C overnight [OVN]), benchtop stability (room temperature [RT] for 8 h), freeze-thaw stability (three freeze-thaw cycles [3 FT]), short-term stability (– 20 °C for 1 month [1 MO]), and medium-term stability (– 20 °C for 3 months [3 MO]) of mescaline (A), 3,4,5-trimethoxyphenylacetic acid (B), N-acetyl mescaline (C), and 3,5-dimethoxy-4-hydroxyphenethylamine (D) were determined in human plasma samples. Stability was assessed in seven replicates ($n = 7$, black dots) at five quality control levels. Results are shown as change in concentration (%) of the measured values compared to freshly prepared calibrators (CALs). Data out of the valid range of $\pm 15\%$ (LLOQ: $\pm 20\%$) are illustrated in white.

Section 3.2.4).

3.2.2. Analyte carry-over

After injecting a ULOQ sample, the measured carry-over was negligible as signals in double blank samples were below 20% of the signals recorded for LLOQ samples. In detail, we observed a carry-over of 5.69–10.8% for mescaline, 1.29–2.93% for TMPAA, 2.37–2.98% for NAM, and 11.2–17.2% for 4-desmethyl mescaline. Therefore, no additional blank samples must be included in the analysis sequence after injecting high concentration samples.

3.2.3. Accuracy and precision

We assessed intra- and inter-assay precision at the LLOQ, LQC, MQC, HQC, and ULOQ using seven replicates per level analyzed on three different days. Accuracy and precision data are summarized in Fig. 3 and Supplementary Table S2. We calculated an intra-assay accuracy between 89.1% and 101% for mescaline, 84.9% and 99.3% for TMPAA, 94.0% and 106% for NAM, and 90.3% and 105% for 4-desmethyl mescaline. The inter-assay deviation of the assessed to the nominal value was for all analytes and QC levels between 88.9% and 104%. The intra- and inter-assay precision (%CV) was $\leq 7.33\%$ and $\leq 6.67\%$, respectively, considering all analytes and QC levels. The method demonstrated to be highly reliable considering that out of 105 measurements none were out of specification for mescaline and NAM and only four values for TMPAA and one for 4-desmethyl mescaline were outside the acceptable limits (Fig. 3).

3.2.4. Selectivity and sensitivity

Seven blank human plasma samples from different donors were investigated to assess the methods' selectivity and sensitivity. No interferences were monitored between analytes and endogenous human plasma components. The peak area of the noise signal in blank and double blank samples was for all analyte less than 20% compared to the LLOQ peak area (signal-to-noise ratio $> 5:1$). These findings are depicted in Fig. 4 and Supplementary Table S3. We further spiked seven different blank plasma samples and assessed their accuracy and precision at the LLOQ level. The mean accuracy of all samples was between 103% and 109% and the mean precision was smaller than 5.26%, demonstrating that chosen LLOQ level can be consistently measured for all analytes.

3.2.5. Extraction recovery and matrix effect

Using a simple protein precipitation method, we reached a complete extraction with a mean recovery of 99.2% for mescaline, 104% for TMPAA, 102% for NAM, and 98.3% for 4-desmethyl mescaline (Table 3). Importantly, we observed a very consistent extraction recovery that was neither influenced by inter-subject variations (%CV $\leq 9.02\%$) nor by the applied concentration (%CV $\leq 2.48\%$). Furthermore, we found only a negligible matrix effect for mescaline ($92.4 \pm 5.92\%$), TMPAA ($96.8 \pm 4.15\%$), NAM ($97.1 \pm 4.20\%$), and 4-desmethyl mescaline ($100 \pm 6.11\%$), which was independent of the plasma batch ($n = 7$) and concentration level (Table 3).

Overall, the developed extraction method led to a complete and consistent extraction recovery, while plasma matrix did not affect the

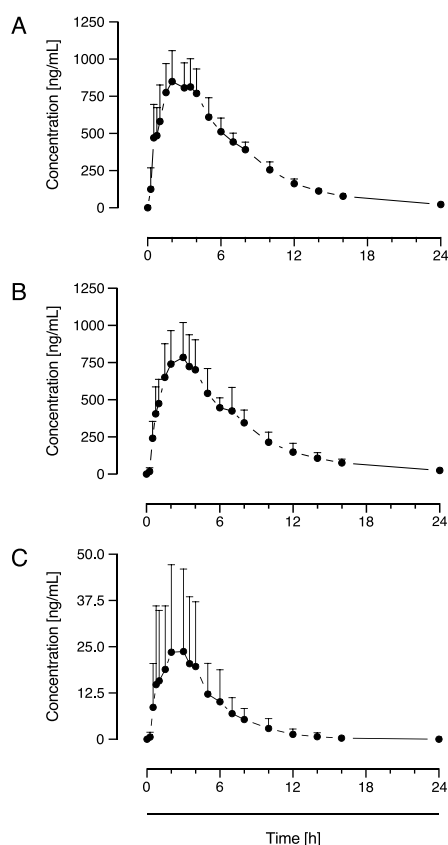


Fig. 6. Pharmacokinetic profiles of mescaline (A), 3,4,5-trimethoxyphenylacetic acid (B), and N-acetyl mescaline (C) in human plasma. Five healthy subjects received a single oral dose of 300 mg mescaline hydrochloride. Blood samples were collected over a time period of 24 h to determine the concentration of mescaline, TMPAA, and NAM in plasma. Mean concentrations and standard deviations are depicted in concentration-time profiles.

reliability of the analysis.

3.2.6. Stability

Autosampler, benchtop, freeze-thaw, short-term, and medium-term stability were determined for mescaline and its metabolites. The mean difference of stability samples compared to freshly prepared calibrators was less than 15% (LLOQ: 20%) for all analytes.

Out of 175 samples, three mescaline, one TMPAA, and zero NAM and 4-desmethyl mescaline determinations were outside $\pm 15\%$ (LLOQ: 20%) limits. In summary, mescaline concentrations only differed between -6.45 and $+1.27\%$ on average, taking all storage conditions into account. Similarly, we observed a change in TMPAA, NAM, and 4-desmethyl mescaline concentration of -8.20 to -5.57% , -3.02 to $+2.89\%$, and -2.80 to $+1.78\%$, respectively (Fig. 5, Supplementary Table S4). The stability of mescaline was also previously assessed by others with similar outcomes [22,24,26,33]. For mescaline's metabolites there is as far as we are aware no data available.

In conclusion, mescaline and its metabolites are stable at room temperature for at least 8 h and at -20°C for at least 3 months. Samples were stable also after repetitive thawing and re-freezing and extracted plasma samples can be re-injected on the next day in case the analytical run aborted overnight.

3.2.7. Clinical application

The applicability of the herein developed and validated method was

tested by measuring PK samples of five different healthy subjects who received a single oral dose of 300 mg mescaline hydrochloride. The obtained PK profiles of mescaline were characterized by a rapid drug invasion reaching a mean maximal plasma concentration (C_{max}) of 895 ± 196 ng/mL (mean \pm SD) after 2.09 ± 0.80 h (t_{max}), which concurred with the maximal psychoactive effect described in the literature (Fig. 6) [5]. We observed a terminal plasma elimination half-life ($t_{1/2}$) of 4.10 ± 0.40 h, which is somewhat faster but still in the same range as reported in literature [16]. TMPAA (2.36 ± 0.73 h) and NAM (2.42 ± 0.82 h) concentration peaked slightly later than mescaline reaching maximal plasma levels of 794 ± 235 ng/mL and 24.7 ± 23.1 ng/mL, respectively (Fig. 6). The half-life of TMPAA (4.51 ± 0.85 h) was comparable to the one calculated for mescaline, whereas NAM displayed a more rapid elimination (2.72 ± 0.72 h). Total exposure was similar for mescaline and TMPAA considering that the calculated AUC_{0-24} was $408'000 \pm 68'300$ min*ng/mL and $364'000 \pm 97'500$ min*ng/mL, respectively. In contrast, the AUC_{0-24} of NAM was approximately fifty times lower ($7'730 \pm 7'000$ min*ng/mL). Raw data of the concentration-time profiles are listed in Supplementary Table S5.

Accurate quantification of 4-desmethyl mescaline was not possible, because concentrations were very low and an interfering peak was monitored in PK but not in CAL and QC samples (Supplementary Fig. S2). The interference corresponded likely to the 3-desmethyl mescaline metabolite, which has previously been described in literature as a minor metabolite of mescaline [2,15]. It is an isomer of 4-desmethyl mescaline and likely produces the same daughter ions (m/z 181.2, m/z 166.2), thus cannot be distinguished from 4-desmethyl mescaline in the MRM mode. The interference could chromatographically be separated, however this affected peak symmetry of the other analytes. Since O-demethylated metabolites were minor metabolites (~ 7.00 ng/mL) compared to TMPAA and NAM, we did not further optimize or even re-validate the method in order to discriminate those two metabolites.

Overall, the accuracy of QC samples ($n = 4$ replicates, $n = 5$ concentration levels) was in-between 88.1% and 104% for mescaline, TMPAA, and NAM and the precision was $\leq 5.61\%$ verifying the performance of the analytical run. The method was suitable for the quantification of mescaline, TMPAA, and NAM in human plasma but not for the selective bioanalysis of 4-desmethyl mescaline in PK samples.

4. Conclusion

We developed and validated a highly reliable bioanalytical assay to quantify mescaline and its two major metabolites in human plasma. The usability of our method stands out, as we require only a small amount of plasma which is processed by a straightforward protein precipitation and analyzed within only four minutes. The employed extraction protocol led to a complete analyte recovery ($\geq 98.3\%$) as well as no matrix suppression. Importantly, both parameters remained unaffected by the plasma batch. In addition, the accuracy and precision of the method was in line with regulatory guidelines. We demonstrated that the method can be used to assess the clinical pharmacokinetics of mescaline and simultaneously of its major metabolites TMPAA and NAM. However, O-demethylation of mescaline cannot be determined with sufficient selectivity by the applied gradient program. Overall, this method facilitates the bioanalysis of mescaline in human plasma, making it attractive for forensic investigations and in-depth pharmacokinetic and drug-drug interaction studies.

Funding

This work was supported by the Swiss National Science Foundation (SNF, Grant No. 32003B_185111/1) to Matthias E. Liechti and Mind Medicine Inc.

CRedit authorship contribution statement

Jan Thomann: Methodology, Investigation, Validation, Formal analysis, Visualization, Writing - original draft. **Laura Ley:** Resources, Writing - review & editing. **Aaron Klaiber:** Resources, Writing - review & editing. **Matthias E. Liechti:** Conceptualization, Supervision, Funding acquisition, Writing - review & editing. **Urs Duthaler:** Conceptualization, Methodology, Formal analysis, Visualization, Supervision, Writing - review & editing.

Data Availability

Data will be made available on request.

Acknowledgments

The authors thank Beatrice Vetter for providing technical assistance.

Declaration of Competing Interest

The authors declare the following financial interests and personal relationships which may be considered as potential competing interests: Matthias E. Liechti is a consultant for Mind Medicine Inc. All other authors do not have any conflicts of interest to declare for this work. Knowhow and data associated with this work and owned by the University Hospital Basel were licensed by Mind Medicine Inc. Mind Medicine Inc. had no role in planning or conducting the present study or the present publication.

Appendix A. Supporting information

Supplementary data associated with this article can be found in the online version at doi:10.1016/j.jpba.2022.114980.

References

- [1] S.D. Carstairs, F.L. Cantrell, Peyote and mescaline exposures: a 12-year review of a statewide poison center database, *Clin. Toxicol.* 48 (4) (2010) 350–353.
- [2] R.J. Dinis-Oliveira, C.L. Pereira, D.D. Da Silva, Pharmacokinetic and pharmacodynamic aspects of peyote and mescaline: clinical and forensic repercussions, *Curr. Mol. Pharmacol.* 12 (3) (2019) 184–194.
- [3] B.K. Cassels, P. Sáez-Briones, Dark classics in chemical neuroscience: mescaline, *ACS Chem. Neurosci.* 9 (10) (2018) 2448–2458.
- [4] H.R. El-Seedi, P.A.G.M. De Smet, O. Beck, G. Possnert, J.G. Bruhn, Prehistoric peyote use: alkaloid analysis and radiocarbon dating of archaeological specimens of *Lophophora* from Texas, *J. Ethnopharmacol.* 101 (1) (2005) 238–242.
- [5] A. Dasgupta, Abuse of magic mushroom, peyote cactus, LSD, khat, and volatiles, *Critical Issues in Alcohol and Drugs of Abuse Testing*, Elsevier, 2019, pp. 477–494.
- [6] International Narcotics Control Board, List of psychotropic substances under international control, (2020).
- [7] B.J. Albaugh, P.O. Anderson, Peyote in the treatment of alcoholism among American Indians, *Am. J. Psychiatry* 131 (11) (1974) 1247–1250.
- [8] J.J. Rucker, J. Iliff, D.J. Nutt, Psychiatry & the psychedelic drugs. Past, present & future, *Neuropharmacology* 142 (2018) 200–218.
- [9] A.C.M. Garcia, L.O. Maia, The therapeutic potential of psychedelic substances in hospice and palliative care, *Prog. Palliat. Care* 30 (1) (2022) 1–3.
- [10] F. Holze, P. Vizeli, L. Ley, F. Müller, P. Dolder, M. Stocker, U. Duthaler, N. Varghese, A. Eckert, S. Borgwardt, Acute dose-dependent effects of lysergic acid diethylamide in a double-blind placebo-controlled study in healthy subjects, *Neuropsychopharmacology* 46 (3) (2021) 537–544.
- [11] F.X. Vollenweider, M.F. Vollenweider-Scherpenhuyzen, A. Bähler, H. Vogel, D. Hell, Psilocybin induces schizophrenia-like psychosis in humans via a serotonin-2 agonist action, *Neuroreport* 9 (17) (1998) 3897–3902.
- [12] K.E. Kolaczynska, D. Luethi, D. Trachsel, M.C. Hoener, M.E. Liechti, Receptor interaction profiles of 4-alkoxy-3,5-dimethoxy-phenethylamines (mescaline derivatives) and related amphetamines, *Front. Pharmacol.* 12 (2021), 794254.
- [13] A. Rickli, O.D. Moning, M.C. Hoener, M.E. Liechti, Receptor interaction profiles of novel psychoactive tryptamines compared with classic hallucinogens, *Eur. Neuropsychopharmacol.* 26 (8) (2016) 1327–1337.
- [14] D.E. Nichols, Hallucinogens, *Pharmacol. Ther.* 101 (2) (2004) 131–181.
- [15] F. Holze, L. Ley, F. Müller, A.M. Becker, I. Straumann, P. Vizeli, S.S. Kuehne, M. A. Roder, U. Duthaler, K.E. Kolaczynska, Direct comparison of the acute effects of lysergic acid diethylamide and psilocybin in a double-blind placebo-controlled study in healthy subjects, *Neuropsychopharmacology* 47 (6) (2022) 1180–1187.
- [16] K. Charalampous, K. Walker, J. Kinross-Wright, Metabolic fate of mescaline in man, *Psychopharmacologia* 9 (1) (1966) 48–63.
- [17] A.J. Friedhoff, L.E. Hollister, Comparison of the metabolism of 3, 4-dimethoxy-phenylethylamine and mescaline in humans, *Biochem. Pharmacol.* 15 (3) (1966) 269–273.
- [18] J. Daly, J. Axelrod, B. Witkop, Methylation and demethylation in relation to the in vitro metabolism of mescaline, *Ann. N. Y. Acad. Sci.* 96 (1) (1962) 37–43.
- [19] K. Björnstad, A. Helander, O. Beck, Development and clinical application of an LC-MS-MS method for mescaline in urine, *J. Anal. Toxicol.* 32 (3) (2008) 227–231.
- [20] R. Casado, I. Uriarte, R.Y. Cavero, M.I. Calvo, LC-PAD determination of mescaline in cactus “peyote” (*Lophophora williamsii*), *Chromatographia* 67 (7) (2008) 665–667.
- [21] C. Gabelunghe, R. Marsili, K. Aroni, M. Bacchi, R. Rossi, GC-MS and GC-MS/MS in PCI mode determination of mescaline in peyote tea and in biological matrices, *J. Forensic Sci.* 58 (1) (2013) 270–278.
- [22] D. Battal, A.J. Barnes, M.S. Castaneto, T.M. Martin, K.L. Klette, M.A. Huestis, Urine mescaline screening with a biochip array immunoassay and quantification by gas chromatography–mass spectrometry, *Ther. Drug Monit.* 37 (6) (2015) 805–811.
- [23] C.M. Longo, R.A. Musah, An efficient ambient ionization mass spectrometric approach to detection and quantification of the mescaline content of commonly abused cacti from the *Echinopsis* genus, *J. Forensic Sci.* 65 (1) (2020) 61–66.
- [24] S. Yang, Y. Shi, Z. Chen, M. Chen, X. Liu, W. Liu, M. Su, B. Di, Detection of mescaline in human hair samples by UPLC-MS/MS: application to 19 authentic forensic cases, *J. Chromatogr. B* 1195 (2022), 123202.
- [25] J.L. Valentine, R. Middleton, GC-MS identification of sympathomimetic amine drugs in urine: rapid methodology applicable for emergency clinical toxicology, *J. Anal. Toxicol.* 24 (3) (2000) 211–222.
- [26] V. Habrdova, F.T. Peters, D.S. Theobald, H.H. Maurer, Screening for and validated quantification of phenethylamine-type designer drugs and mescaline in human blood plasma by gas chromatography/mass spectrometry, *J. Mass Spectrom.* 40 (6) (2005) 785–795.
- [27] J. Beyer, F.T. Peters, T. Kraemer, H.H. Maurer, Detection and validated quantification of nine herbal phenalkylamines and methcathinone in human blood plasma by LC-MS/MS with electrospray ionization, *J. Mass Spectrom.* 42 (2) (2007) 150–160.
- [28] J.Y. Kim, K.S. Jung, M.K. Kim, J.I. Lee, M.K. In, Simultaneous determination of psychotropic phenylalkylamine derivatives in human hair by gas chromatography/mass spectrometry, *Rapid Commun. Mass Spectrom.* 21 (11) (2007) 1705–1720.
- [29] S. Pichini, E. Marchei, O. García-Algar, A. Gomez, R. Di Giovannandrea, R. Pacifici, Ultra-high-pressure liquid chromatography tandem mass spectrometry determination of hallucinogenic drugs in hair of psychedelic plants and mushrooms consumers, *J. Pharm. Biomed. Anal.* 100 (2014) 284–289.
- [30] K. Francisco da Cunha, K.D. Oliveira, M.A. Huestis, J.L. Costa, Screening of 104 new psychoactive substances (NPS) and other drugs of abuse in oral fluid by LC-MS-MS, *J. Anal. Toxicol.* 44 (7) (2020) 697–707.
- [31] H.J. Helmlin, R. Brenneisen, Determination of psychotropic phenylalkylamine derivatives in biological matrices by high-performance liquid chromatography with photodiode-array detection, *J. Chromatogr.* 593 (1–2) (1992) 87–94.
- [32] W. Ma, X. Jiang, R. Cooks, J. McLaughlin, A. Gibson, F. Zeylemaker, C. Ostolaza, Cactus alkaloids, LXI. Identification of mescaline and related compounds in eight additional species using TLC and MS/MS, *J. Nat. Prod.* 49 (4) (1986) 735–737.
- [33] M. Sergi, D. Compagnone, R. Curini, G. D’Ascenzo, M. Del Carlo, S. Napoletano, R. Risoluti, Micro-solid phase extraction coupled with high-performance liquid chromatography–tandem mass spectrometry for the determination of stimulants, hallucinogens, ketamine and phencyclidine in oral fluids, *Anal. Chim. Acta* 675 (2) (2010) 132–137.
- [34] U.S. Food and Drug Administration, Bioanalytical method validation guidance for industry, (2018).
- [35] Y. Hua, D. Jenke, Increasing the sensitivity of an LC-MS method for screening material extracts for organic extractables via mobile phase optimization, *J. Chromatogr. Sci.* 50 (3) (2012) 213–227.

3.2 Manuscript 2

Development and validation of an LC-MS/MS method for quantifying diamorphine and its major metabolites 6-monoacetylmorphine, morphine, morphine-3-glucuronide, and morphine-6-glucuronide in human plasma

Jan Thomann^{a,b}, Severin B. Vogt^{a,b}, Adrian Guessoum^c, Maximilian Meyer^c, Marc Vogel^c, Matthias E. Liechti^{a,b}, Dino Luethi^{a,b,†,*}, Urs Duthaler^{a,b,d,e,†}

^a Division of Clinical Pharmacology and Toxicology, Department of Biomedicine, University Hospital Basel, Basel, Switzerland

^b Division of Clinical Pharmacology and Toxicology, Department of Pharmaceutical Sciences, University of Basel, Basel, Switzerland

^c University Psychiatric Clinics Basel, University of Basel, Basel, Switzerland

^d Institute of Forensic Medicine, Department of Biomedical Engineering, University of Basel, Basel, Switzerland

^e Institute of Forensic Medicine, Health Department Basel-Stadt, Basel, Switzerland

* Corresponding author

† Equal contribution

J Chromatogr B. 2024 Apr 15:1237:124104

DOI: 10.1016/j.jchromb.2024.124104



Contents lists available at ScienceDirect

Journal of Chromatography B

journal homepage: www.elsevier.com/locate/jchromb

Development and validation of an LC-MS/MS method for quantifying diamorphine and its major metabolites 6-monoacetylmorphine, morphine, morphine-3-glucuronide, and morphine-6-glucuronide in human plasma

Jan Thomann^{a,b}, Severin B. Vogt^{a,b}, Adrian Guessoum^c, Maximilian Meyer^c, Marc Vogel^c, Matthias E. Liechti^{a,b}, Dino Luethi^{a,b,1,*}, Urs Duthaler^{a,b,d,e,1}

^a Division of Clinical Pharmacology and Toxicology, Department of Biomedicine, University Hospital Basel, Basel, Switzerland

^b Division of Clinical Pharmacology and Toxicology, Department of Pharmaceutical Sciences, University of Basel, Basel, Switzerland

^c University Psychiatric Clinics Basel, University of Basel, Basel, Switzerland

^d Institute of Forensic Medicine, Department of Biomedical Engineering, University of Basel, Basel, Switzerland

^e Institute of Forensic Medicine, Health Department Basel-Stadt, Basel, Switzerland

ARTICLE INFO

Keywords:

Method development
Method validation
Diamorphine
Metabolites
Pharmacokinetics
LC-MS/MS

ABSTRACT

Diamorphine, commonly known as heroin, is a semi-synthetic opioid analgesic. In the context of heroin-assisted treatment for opioid-dependent patients, diamorphine is mostly administered intravenously. However, recent attention has shifted towards intranasal administration as a better-tolerated alternative to the intravenous route. Here, we developed and validated a rapid bioanalytical method for the simultaneous quantification of diamorphine and its major metabolites 6-monoacetylmorphine, morphine, morphine-3-glucuronide, and morphine-6-glucuronide in human plasma using liquid chromatography-tandem mass spectrometry (LC-MS/MS).

A straightforward protein precipitation extraction step was used for sample preparation. Chromatographic analyte separation was achieved using a Kinetex EVO C₁₈ analytical column and a mobile phase gradient comprising an aqueous solution of ammonium hydrogen carbonate and methanol supplied with formic acid. Employing positive electrospray ionization and scheduled multiple reaction monitoring, we established a quantification range of 1–1,000 ng/mL for all analytes.

Our validation results demonstrate a mean intra-assay accuracy of 91–106% and an intra-assay precision (CV) between 2 and 9% for all analytes and over three validation runs. The method exhibits a high extraction recovery (> 87%) and a negligible matrix effect (99–125%). Furthermore, no interferences with endogenous plasma compounds were detected. Lastly, we applied the method to assess the plasma concentrations of an opioid-dependent patient after the intranasal administration of diamorphine in a clinical study.

In summary, we have successfully developed a rapid, highly reliable, and straightforward bioanalytical method for quantifying diamorphine and its metabolites in low amounts of clinical plasma samples.

1. Introduction

Diamorphine (DAM, heroin) is a semi-synthetic opioid and a potent analgesic derived from morphine (MOR). DAM crosses the blood–brain barrier more rapidly compared to MOR and exerts a more immediate psychoactive effect [1,2]. However, DAM can be characterized as a prodrug since it mainly acts through its active metabolites, which exhibit a higher affinity for opioid receptors than DAM itself [1]. Oral DAM has a substantial first-pass effect in the liver and thus a reduced

bioavailability. The half-life of DAM is about 2–5 min [3–5]. Metabolism primarily occurs in the liver and the serum and is predominantly catalyzed by several types of esterases. Main metabolic pathways involve the deacetylation of DAM to the active 6-monoacetylmorphine (6-MAM), which is further deacetylated to the potent analgesic MOR (Fig. 1) [2,6]. MOR is substantially contributing to the pain-relieving effects of DAM [5]. MOR is subject to glucuronidation predominantly by UGT2B7 to form morphine-3-glucuronide (M3G) or morphine-6-glucuronide (M6G; Fig. 1). M6G has analgesic properties equipotent to MOR but shows

* Corresponding author at: Division of Clinical Pharmacology and Toxicology, University Hospital Basel, Hebelstrasse 20, 4031 Basel, Switzerland.

E-mail address: dino.luethi@unibas.ch (D. Luethi).

¹ Equal contribution

<https://doi.org/10.1016/j.jchromb.2024.124104>

Received 26 February 2024; Received in revised form 19 March 2024; Accepted 23 March 2024

Available online 25 March 2024

1570-0232/© 2024 The Author(s). Published by Elsevier B.V. This is an open access article under the CC BY license (<http://creativecommons.org/licenses/by/4.0/>).

fewer adverse effects [1,5,7]. The plasma levels and metabolism of DAM can vary among individuals due to e.g., genetic factors, route of administration, and concurrent drug use [2,7].

Pharmaceutical DAM is used in pain management but mainly in the treatment of opioid use disorder [2,8,9]. First line treatment of opioid dependence is opioid agonist treatment (OAT) including methadone, buprenorphine, and slow-release oral morphine [10,11]. Alternatively, heroin-assisted treatment (HAT) with DAM can be an option where conventional OAT is not effective [12]. Pharmaceutical DAM is either orally ingested or intravenously injected under the supervision of clinical professionals [12]. However, patients with several years of intravenous drug use often have deteriorated peripheral veins, impeding intravenous drug injection [13]. Other routes of parenteral administration can be inguinal, intramuscular, or subcutaneous injections [13–16]. However, these administration routes have some disadvantages such as muscle tissue indurations, abscesses, pain, and skin lesions [8,16,17]. Intranasal DAM administration on the other hand offers unique advantages over injectable routes of administration [8,9]. Intranasal administration is generally considered safer than intravenous drug use, as it bypasses the risks associated with injection, such as bacterial infections and abscesses, collapsed veins, and vascular damage. Furthermore, it significantly reduces the risk of bloodborne infections like HIV and hepatitis C [8,18,19]. Even though it takes longer to reach peak plasma levels with intranasal compared to intravenous administration, it can still satisfy the desire for a subjective “drug high” in many patients. The “drug high” is usually considered a prerequisite for treatment success in HAT patients [8]. This alternative OAT may thus enhance medication adherence as it offers a less stigmatized method of administration compared to injection [20,21]. It may also prove beneficial for patients who primarily sniff DAM, as they usually receive DAM tablets that do not produce a “drug high”.

Several bioanalytical methods to detect DAM and its metabolites 6-MAM, MOR, M3G, and M6G have been published. These methods were developed to quantify DAM in various matrices such as plasma, serum, urine, brain tissue, and wastewater [3,4,22–27]. However, most methods employ a time and work-intensive sample preparation or an elongated run time (> 8 min) [3,4,22–26]. To analyze plasma samples of a clinical study with patients receiving intranasal DAM, a fast and reliable bioanalytical method is crucial. Thus, we here developed a method with a short run time and non-laborious sample preparation to analyze numerous clinical study samples in a reasonable time. Additionally, our method allows for the efficient analysis of small sample volumes, enhancing its versatility and practicality in various research settings.

2. Material and methods

2.1. Chemicals, reagents, and reference compounds

Calibrated stock solutions of diamorphine (99.9% purity), 6-monoacetylmorphine hydrochloride (99.8% purity), morphine monohydrate (99.2% purity), morphine-3- β -D-glucuronide (98.8% purity), and morphine-6- β -D-glucuronide (97.8% purity) were obtained as 1 mg/mL solutions from Lipomed (Arlesheim, Switzerland). The respective internal standards, diamorphine- d_9 (99.6% purity), 6-monoacetylmorphine- d_3 hydrochloride trihydrate (99.1% purity), morphine- d_3 monohydrate (99.9% purity), morphine-3- β -D-glucuronide- d_3 (99.0% purity), and morphine-6- β -D-glucuronide- d_3 (99.6% purity) were purchased as 0.1 mg/mL solutions from Lipomed.

LC-MS grade water, methanol, and ammonium hydrogen carbonate (NH_4HCO_3) were acquired from Merck (Darmstadt, Germany), while LC-MS grade formic acid was obtained from Carl Roth (Karlsruhe, Germany). Dimethyl sulfoxide (DMSO) was acquired from Sigma-Aldrich (Buchs, Switzerland).

Human blood for the method development and validation was collected at the University Hospital Basel and drawn into fluoride/EDTA-coated S-Monovette tubes (Sarstedt, Nümbrecht, Germany). After collection, the blood was centrifuged at $1811 \times g$ for 10 min (5810 R centrifuge, Eppendorf, Hamburg, Germany) to separate the plasma.

2.2. Stock solution preparation

For each analyte, separate calibration (CAL) and quality control (QC) working solutions were prepared from different stock solutions. Each analyte was 1:5 diluted in DMSO. All internal standards were diluted in methanol to receive an internal standard working solution (ISTD) with a concentration of 10 ng/mL for each standard. Stock and working solutions were stored at -20°C .

2.3. Calibration and quality control sample preparation

CAL dilution series (0.1–100 $\mu\text{g/mL}$) were prepared in DMSO by serially diluting the CAL working solution. The dilution series was used to spike a blank pool of human plasma ($n = 8$ donors) at a ratio of 1:100 (v/v) to obtain a calibration range of 1–1000 ng/mL for DAM, 6-MAM, MOR, M3G, and M6G.

For QCs, the dilution procedure was repeated using the QC working solution. QC samples were prepared at the lower limit of quantification

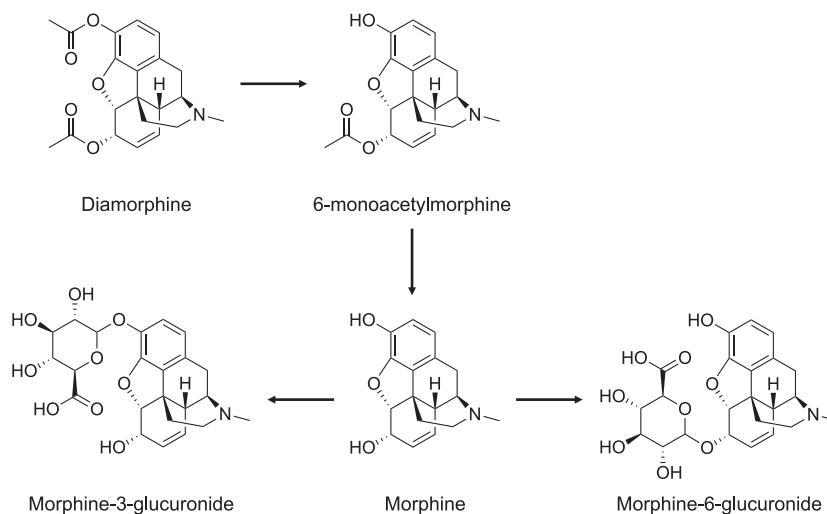


Fig. 1. Metabolic pathway of diamorphine and its metabolites.

(LLOQ) and at low (LQC), medium (MQC), and high (HQC) concentrations by spiking the blank pool of human plasma at a ratio of 1:100 (v/v). The following QC levels were prepared: 1 ng/mL (LLOQ), 2.5 ng/mL (LQC), 50 ng/mL (MQC), and 500 ng/mL (HQC). Additionally, a QC solution with a concentration of 2000 ng/mL was prepared and 1:10 (v/v) diluted in blank plasma to receive a 200 ng/mL diluted QC sample (dilQC).

2.4. LC-MS/MS instrumentation and setting

The system consisted of a modular high-performance liquid chromatograph (HPLC, Shimadzu, Kyoto, Japan) coupled to an API 5000 triple quadrupole tandem mass spectrometer (AB Sciex, Ontario, Canada). Analyte separation was performed with a Kinetex EVO C₁₈ analytical column (2.6 µm, 100 Å, 50 × 4.6 mm, Phenomenex, Torrance, CA, USA). The modular HPLC system consisted of an autosampler (set to 10 °C), a system controller, three pumps (A, B, and C), two degassing units, and a column oven (set to 45 °C). An aqueous solution of ammonium hydrogen carbonate (20 mM, pH 9.0) was used as mobile phase A. Mobile phase B consisted of methanol supplied with 0.1% (v/v) formic acid. 5 µL of the sample was injected and transported to a T-union by pumps A and B where it was further diluted with mobile phase A (delivered by pump C, 0.5 mL/min) for the first 0.5 min. The aqueous dilution of the sample enhances the interaction between the methanolic sample and the analytical column. Before the analytical column, a pre-column filter was installed to remove any impurities. The initial total flow of pumps A (70%) and B (30%) was 0.2 mL/min for 0.5 min, which was then raised to 0.5 mL/min. The concentration of mobile phase B linearly increased from 30% to 95% from 0.5 min to 2.5 min. Subsequently, the column was washed with 95% mobile phase B for 1.0 min and was reconditioned at 30% mobile phase B from 3.5 to 4.0 min. Between 1.5 and 3.2 min the eluent was directed into the mass spectrometer and otherwise into the waste. The total run time of a single sample analysis was 4.0 min.

In the mass spectrometer, the analytes were ionized by electron spray ionization and were detected using scheduled multiple reaction monitoring (sMRM). Parameters were as follows: ion spray voltage, 5500 V; temperature, 500 °C; curtain gas, 10 psi; nebulizer gas (ion source gas 1), 60 psi; heater gas (ion source gas 2) 50 psi; collision gas, 4 psi. Elemental nitrogen (N₂) was used as gas supply. For each analyte, a quantifier ion was utilized for identification and quantitation, along with a qualifier ion solely for identification purposes. Detailed information regarding

the exact mass transitions for each analyte and specific mass spectrometer settings can be found in Table 1. Analyst Instrumental Control and Data Processing Software (Version 1.7.2, AB Sciex) and MultiQuant Software (Version 3.0.3, AB Sciex) were used for system operation and data analysis, respectively.

2.5. Sample extraction

50 µL of plasma per sample were aliquoted into matrix tubes (0.7 mL, 96-deepwell rack, Thermo Fisher Scientific, Waltham, MA, USA) and extracted with 400 µL ISTD to precipitate plasma proteins. After vortexing, the samples were centrifuged for 30 min at 15 °C and 3220 × g (5810 R centrifuge, Eppendorf) to create a protein-free supernatant which was later injected directly into the HPLC.

2.6. Method validation

The validation of this bioanalytical method was conducted according to the Bioanalytical Method Validation Guidance for Industry of the United States Food and Drug Administration (FDA) [28]. The LC-MS/MS system was validated for linearity, accuracy, precision, selectivity, sensitivity, extraction recovery, matrix effect, and analyte stability.

2.6.1. Linearity

In each analytical run, a CAL line was measured at the beginning and the end. For all analytes, a CAL line consisted of 10 samples over a range of 1–1,000 ng/mL (1, 2.5, 5, 10, 25, 50, 100, 250, 500, and 1,000 ng/mL). Prior to a CAL line, a blank plasma sample (extracted with ISTD) was analyzed and after each CAL line, a double blank plasma sample (extracted with pure methanol) was measured. If the analyte carry-over exceeds 20% of the LLOQ peak area, additional solvent samples must be inserted after samples containing high analyte concentrations. A linear regression line was established using MultiQuant by plotting the nominal concentration of CAL samples against the ratio of the analyte peak area to the ISTD peak area. To mitigate errors at low concentrations, a weighting factor of 1/x² was applied. The accuracy of each CAL sample was determined by calculating the percentage difference between the measured and nominal concentrations. Only CAL samples within 85% to 115% accuracy (80% to 120% accuracy for the LLOQ) were included in the calibration lines. A valid CAL line needed to incorporate a minimum of 75% of all data points, including at least one LLOQ and one ULOQ sample, and display a correlation coefficient (R) of ≥ 0.99.

Table 1

Mass spectrometry settings for the quantification of DAM, 6-MAM, MOR, M3G, M6G, and their deuterated internal standards.

Analyte	Type	Q1	Q3	RT	DP	EP	CE	CXP
		[Da]	[Da]	[min]	[V]	[V]	[V]	[V]
DAM	quantifier	370.2	165.2	3.05	151	10	65	20
	qualifier	370.2	268.1	3.05	151	10	26	32
DAM-d ₉	internal standard	379.2	165.2	3.04	96	10	65	18
	internal standard	379.2	272.2	3.04	96	10	39	30
6-MAM	quantifier	328.1	165.1	2.81	106	10	61	26
	qualifier	328.2	211.2	2.81	116	10	19	24
6-MAM-d ₃	internal standard	331.2	165.0	2.80	106	10	83	26
	internal standard	331.2	211.1	2.80	116	10	35	24
MOR	quantifier	286.2	201.3	2.60	181	10	33	22
	qualifier	286.2	152.1	2.60	161	10	51	18
MOR-d ₃	internal standard	289.2	201.1	2.58	91	10	35	22
	internal standard	289.2	152.1	2.58	96	10	79	24
M3G	quantifier	462.2	286.2	1.76	161	10	29	32
	qualifier	462.2	201.1	1.76	161	10	59	22
M3G-d ₃	internal standard	465.2	289.2	1.74	131	10	43	18
	internal standard	465.2	201.1	1.74	131	10	59	22
M6G	quantifier	462.2	286.1	2.06	111	10	34	20
	qualifier	462.2	201.1	2.06	161	10	57	24
M6G-d ₃	internal standard	465.2	289.2	2.05	96	10	43	32
	internal standard	465.2	201.1	2.05	106	10	55	24

CE, collision energy; CXP, collision cell exit potential; DP, declustering potential; EP, entrance potential; Q1, quadrupole 1; Q3, quadrupole 3; RT, retention time.

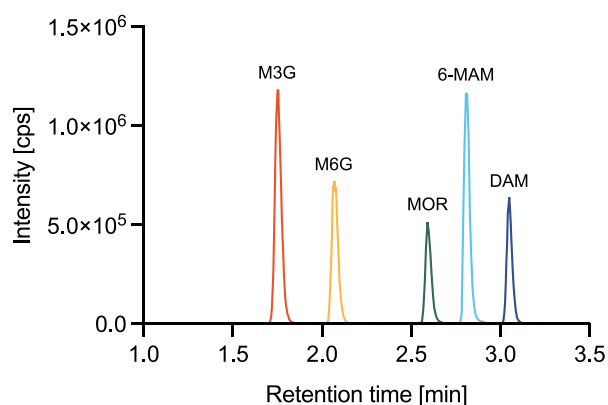


Fig. 2. Chromatographic separation of 500 ng/mL diamorphine (DAM), 6-monoacetylmorphine (6-MAM), morphine (MOR), morphine-3-glucuronide (M3G), and morphine-6-glucuronide (M6G) in human plasma.

2.6.2. Intra- and inter-assay accuracy and precision

Accuracy and precision were assessed in three individual analytical runs on three different days. Two distinct CAL lines and seven replicates of each QC level (LLOQ, LQC, MQC, and HQC) were assessed. Accuracy was determined as the percentage difference in concentration of the QC level to its nominal value. The intra- ($n = 7$) and inter-assay ($n = 21$) accuracy of QC samples of one level needed to be 85–115% (80–120% for the LLOQ). To assess precision, the coefficient of variation ($CV = \text{standard deviation} / \text{mean} \times 100$) was used. The intra- ($n = 7$) and inter-

Table 2

Intra- and inter-assay accuracy and precision of DAM, 6-MAM, MOR, M3G, and M6G in human plasma.

Analyte	Nominal concentration	Intra-assay accuracy	Inter-assay accuracy	Intra-assay precision	Inter-assay precision
	[ng/mL]	[%]	[%]	[CV%]	[CV%]
DAM	1	95.2	94.4	4.1	7.7
	2.5	95.1	95.2	3.7	4.4
	50	97.3	97.4	1.6	2.1
	500	93.7	93.7	1.6	2.3
	2,000*	94.0	93.5	2.7	3.9
6-MAM	1	90.7	89.0	5.5	9.4
	2.5	93.9	93.3	3.8	4.6
	50	97.7	97.7	2.6	2.8
	500	94.4	94.4	2.7	2.7
	2,000*	105.7	105.0	3.5	4.2
MOR	1	97.1	96.0	9.1	14.2
	2.5	96.4	95.2	3.8	7.1
	50	98.5	98.4	3.2	3.7
	500	96.9	96.9	2.5	2.4
	2,000*	103.0	103.0	3.1	3.4
M3G	1	95.0	91.5	4.1	6.7
	2.5	98.0	90.1	3.0	3.9
	50	100.1	101.0	2.0	1.9
	500	95.4	92.6	1.7	2.0
	2,000*	101.4	100.0	3.2	4.5
M6G	1	91.8	95.0	5.2	6.7
	2.5	91.0	98.0	4.9	4.8
	50	101.0	100.0	1.6	1.8
	500	92.6	95.4	1.8	2.4
	2,000*	100.2	101.0	3.7	4.7

* diluted in a ratio of 1:10.

assay ($n = 21$) CV needed to be $< 15\%$ ($< 20\%$ for the LLOQ). At least 50% of the QC samples of one level (at least 4 out of 7) and 67% of all QC samples (at least 19 out of 28) needed to meet these criteria. All QC samples including outliers were used to calculate accuracy and precision.

Additionally, the accuracy and precision of a QC sample outside the calibration range were examined after dilution (dilQC). QC samples ($n = 7$) spiked at a concentration of 2,000 ng/mL were 1:10 diluted in pooled plasma ($n = 8$ donors) to reach a final concentration of 200 ng/mL. Intra- and inter-assay accuracy and precision were assessed using the same criteria as for the other QC levels.

2.6.3. Selectivity and sensitivity

Method selectivity and sensitivity were assessed by analyzing double blank, blank, and LLOQ samples prepared with the plasma of six different donors. A LLOQ sample in each individual's plasma was measured in triplicate. To accept method selectivity, the peak area of the LLOQ signal needed to be at least five times higher than the noise signal (peak area) of a double blank and blank sample. The method was considered sufficiently sensitive if the mean accuracy of the LLOQ samples was between 80 and 120% and $\geq 50\%$ of the individual QC samples (at least 3 out of 6) were within this range.

2.6.4. Extraction recovery and matrix effect

Extraction recovery was assessed in the plasma of six individuals by comparing the analyte peak area of QC samples (LLOQ, LQC, MQC, and HQC) spiked before extraction with the same QC levels spiked after extraction. The peak area of supernatants spiked after extraction corresponded to 100% recovery. Recovery was required to be consistent, precise, and reproducible with a $CV \leq 15\%$ ($\leq 20\%$ for the LLOQ) at all QC levels and over different plasma batches.

The matrix effect was determined as the ratio of the analyte peak area in the presence of a matrix compared to the analyte peak area in the absence of a matrix. The peak areas determined in spiked plasma supernatants of six individual donors were compared to the peak areas determined in a mixture of water and ISTD (ratio of 1:9, v/v). The matrix effect was assessed at LLOQ, LQC, MQC, and HQC levels. The matrix suppression or enhancement had to be consistent at all QC levels and overall plasma batches with a $CV \leq 15\%$ (20% for the LLOQ).

2.6.5. Analyte stability

Several tests were performed to assess analyte stability. The stability of seven replicates of LQC, MQC, and HQC samples was evaluated under the following conditions: extracted and analyzed samples were stored in the HPLC autosampler overnight at 10 °C (autosampler stability) or stored at -20 °C for one week before being reanalyzed (extract stability). These stability tests were performed to assess the option of re-injection in case of a system failure. The same acceptance requirements as for accuracy and precision runs were applied.

Furthermore, samples were thawed and kept at room temperature for 8 h (bench-top stability), at -20 °C and -80 °C for 1 month (short-term stability), at -80 °C for 3 months (medium-term stability), at -80 °C for 6 months (long-term stability), or were subject to 3 freeze-thaw cycles (freeze-thaw stability). The samples' freeze-thaw stability was assessed by thawing them unassisted and then refreezing them for at least 24 h. The stability was evaluated using two freshly prepared CAL lines and three replicates of freshly prepared QC samples of each level. The acceptance criteria for accuracy and precision runs were applied.

2.7. Method application

The application of the method was assessed by analyzing blood samples from a prospective observational study that examines the feasibility and acceptability of intranasal DAM administration in opioid-dependent patients [29]. The full pharmacokinetic profile of one study participant was analyzed for this method validation. The study was

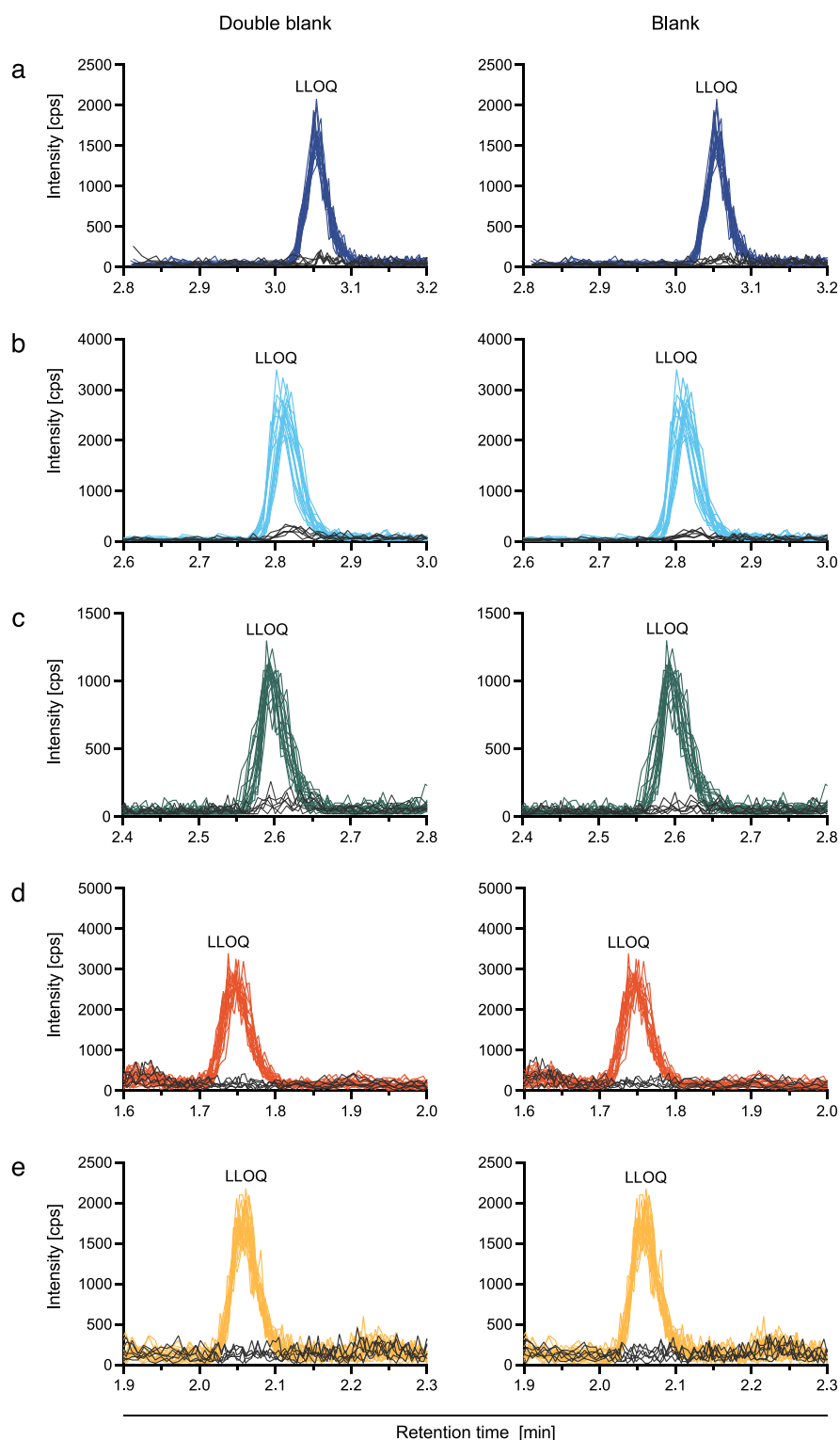


Fig. 3. Selectivity and sensitivity of diamorphine (DAM; a), 6-monoacetylmorphine (6-MAM; b), morphine (MOR; c), morphine-3-glucuronide (M3G; d), and morphine-6-glucuronidation (M6G; e) in human plasma. The chromatograms are shown as an overlay of six double blank samples (left side, black lines), six blank samples (right side, black lines), and six lower limit of quantification (LLOQ; colored lines) samples from six different batches of human plasma in triplicate. The signal-to-noise ratio at each LLOQ level was $> 5:1$.

Table 3

Extraction recovery and matrix effect determined for DAM, 6-MAM, MOR, M3G, and M6G in human plasma calculated using area ratios.

Analyte	Nominal concentration	Recovery (CV)	Mean recovery (CV)	Matrix effect (CV)	Mean matrix effect (CV)
	[ng/mL]	[%]	[%]	[%]	[%]
DAM	1	91.7 (14.7)	86.8 (3.9)	104.0 (10.4)	111.3 (4.5)
	2.5	86.4 (8.8)		112.1 (3.7)	
	50	85.0 (4.2)		114.1 (2.9)	
	500	84.2 (5.1)		115.0 (5.7)	
6-MAM	1	96.3 (11.8)	86.7 (9.6)	108.6 (5.8)	124.5 (12.0)
	2.5	91.2 (5.2)		115.0 (3.7)	
	50	79.6 (4.2)		139.1 (1.4)	
	500	79.8 (4.9)		135.4 (3.9)	
MOR	1	108.7 (17.4)	101.9 (4.8)	92.1 (11.8)	98.9 (5.6)
	2.5	100.7 (9.1)		102.8 (6.3)	
	50	97.0 (3.8)		104.0 (2.3)	
	500	101.3 (2.1)		96.5 (1.6)	
M3G	1	98.2 (7.0)	97.0 (4.1)	94.9 (2.4)	101.8 (5.3)
	2.5	101.9 (14.7)		100.4 (4.8)	
	50	95.6 (6.4)		104.9 (2.2)	
	500	92.4 (3.0)		107.0 (1.4)	
M6G	1	87.6 (10.2)	95.4 (6.0)	102.6 (9.2)	103.6 (3.2)
	2.5	101.4 (6.9)		99.5 (4.6)	
	50	95.8 (4.5)		107.1 (1.8)	
	500	96.8 (3.0)		105.2 (1.3)	

approved by the Ethics Committee of Northwest and Central Switzerland (BASEC ID:2020-00354) and was conducted according to the Declaration of Helsinki and the International Conference of Harmonization for Good Clinical Practice guidelines.

The study participant self-administered an individually prescribed dose of DAM intranasally using a mucosal atomization device (MAD Nasal). The study participant who provided the samples for this method validation administered a dose of 400 mg DAM (4 mL of Diaphin® IV 100 mg/mL, DiaMo Narcotics, Thun, Switzerland) within 5 min. Prior to the dose administration, a baseline blood sample was drawn ($t = 0$ min). Subsequent blood samples were collected at 2, 5, 10, 15, 20, 30, 40, 50, 60, 120, and 180 min after DAM administration. All samples were collected in fluoride/EDTA-coated S-Monovette tubes (Sarstedt) and were immediately put in an ice bath for 1–2 min before centrifugation at 3,000 rpm for 10 min at 4 °C. Subsequently, the plasma was extracted and the samples were stored on dry ice before being transferred and preserved at -80 °C until analysis.

Two CAL lines and four sets of QCs (LQC, MQC, HQC, and dilQC) were equally distributed over the analytical run and used to determine the plasma concentrations of the analytes in the pharmacokinetic sample. Plasma concentration curves were plotted using GraphPad Prism (Version 10.1.1, GraphPad Software, Boston, MA, USA) and the maximal plasma concentration (C_{max}) was a direct readout of the graphical plots.

3. Results and discussion

3.1. Method development

Existing bioanalytical methods to analyze DAM and metabolites in plasma or urine mostly include a long sample run time or employ laborious sample preparation like solid-phase extraction or evaporation steps. Here, we aimed to develop an improved bioanalytical method for fast sample analysis, thus suitable for measuring numerous clinical study samples.

Initially, the analytes and their internal standards were infused into the mass spectrometer to optimize ionization parameters and detect their fragmentation pattern. All analytes were detected in positive electron spray ionization mode. The two most suitable transitions for each analyte were selected to define one mass transition for quantification and identification (quantifier) and one solely for identification (qualifier) of the analyte (Table 1). The mass transition with higher intensity was generally chosen as the quantifier. Most of the here used mass transitions were previously described by others [3,22–26].

As good separation and symmetry were achieved with a Kinetex EVO C₁₈ analytical column (2.6 μm, 100 Å, 50 × 4.6 mm, Phenomenex) no further analytical columns were evaluated. A representative chromatogram is shown in Fig. 2.

A straightforward and non-laborious protein precipitation method based on previously developed analytical methods was employed as sample pre-treatment [30–34]. A small sample volume of 50 μL extracted with 400 μL ISTD and an injection volume of 5 μL ensured the possibility of repeated sample analysis.

3.2. Method validation

3.2.1. Method linearity

The herein developed bioanalytical method was linear in the range of 1–1,000 ng/mL for DAM, 6-MAM, MOR, M3G, and M6G. The correlation coefficient (R) for each calibration line was >0.998. Calibration curves were fitted by linear regression and a weighting factor of $1/x^2$ was applied. The limit of deviation from the nominal value was ≤ 15% (≤ 20% for the LLOQ). All DAM, 6-MAM, MOR, and M6G CAL values were within those limits (60 for each analyte), while just one CAL value for M3G was excluded over three runs (59 of 60 within limits).

3.2.2. Analyte carry-over

We observed carry-over of more than 20% of the LLOQ signal in the first double-blank samples after injection of ULOQ samples for most analytes. Carry-over expressed as a percentage of the LLOQ signal was 15–24% for DAM, 24–57% for 6-MAM, 23–71% for MOR, and 1–29% for M3G in the first double blank sample after a ULOQ sample. M6G did not show any relevant carry-over effect (2–5% of LLOQ signal). Carry-over in the subsequent (second) blank sample was 14–32% for 6-MAM, 23–39% for MOR, and 1–31% for M3G. The carry-over for DAM (7–17%) and M6G (2–5%) was within limits after the second double blank sample.

Thus, study samples should not be randomized and an additional blank sample must be included after high concentration samples to counteract and minimize carry-over.

3.2.3. Accuracy and precision

Intra- and inter-assay accuracy and precision at the LLOQ, LQC, MQC, HQC, and dilQC levels are shown in Table 2. Seven replicates of each QC level were analyzed on three different days. Intra-assay accuracy was 91–102% for DAM, 85–107% for 6-MAM, 90–107% for MOR, 86–109% for M3G, and 90–104% for M6G. Inter-assay accuracy was

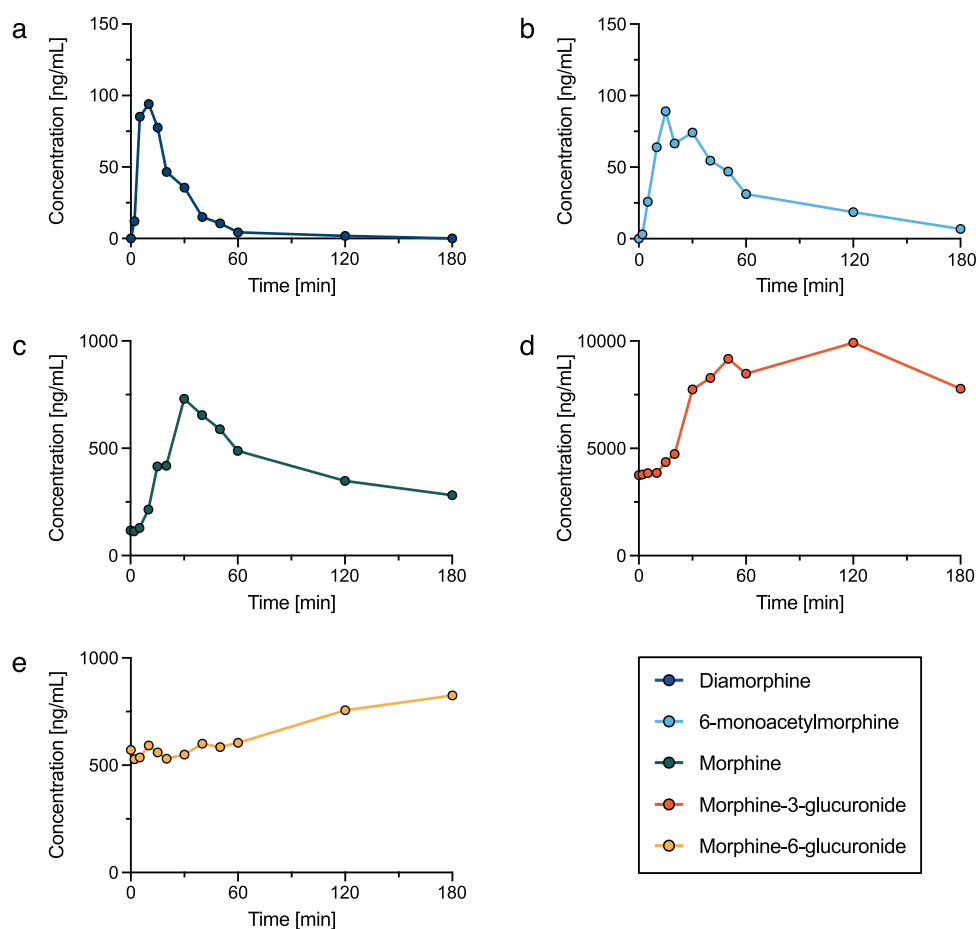


Fig. 4. Pharmacokinetic profiles of diamorphine (DAM; a), 6-monoacetylmorphine (6-MAM; b), morphine (MOR; c), morphine-3-glucuronide (M3G; d), and morphine-6-glucuronide (M6G; e) in the plasma of a clinical study participant after intranasal administration of 400 mg DAM within 5 min.

between 89 and 105% for all analytes and QC levels. Intra- and inter-assay precision (CV) were in the range of 1–12% and 2–14%, respectively, for all analytes and QC levels. The intra- and inter-assay accuracy for the dilution of a 2,000 ng/mL sample (dilQC) at a ratio of 1:10 was 93–108% and 94–105%, respectively (Table 2).

3.2.4. Selectivity and sensitivity

Six individual double blank and blank samples were analyzed and compared to LLOQ samples to assess the selectivity and sensitivity of the method. No interferences of endogenous plasma compounds with any of the analytes were detected. The signal-to-noise ratio (peak area) in double blank and blank samples compared to the LLOQ was > 5:1. Detailed results are depicted in Fig. 3 and Supplementary Table 1. Mean accuracy at the LLOQ level was between 87 and 94% for all analytes. The mean precision (CV) was $\leq 6.8\%$ throughout the assay, confirming the validated limits of quantification.

3.2.5. Extraction recovery and matrix effect

Extraction recovery results are shown in Table 3. By applying a straightforward extraction method, we reached a mean recovery of 87%, 87%, 102%, 97%, and 95% for DAM, 6-MAM, MOR, M3G, and M6G, respectively. Additionally, extraction recovery was consistent over the entire concentration range (CV $\leq 10\%$) and did not show any relevant inter-subject variations (CV $\leq 15\%$).

The matrix effect was neither affected by the plasma batch (CV $\leq 12\%$) nor the QC levels (CV $\leq 12\%$) and was negligible for all

compounds. The mean observed matrix effect was 111% for DAM, 125% for 6-MAM, 99% for MOR, 102% for M3G, and 104% for M6G.

3.2.6. Stability

Autosampler, extract, bench-top, freeze-thaw, short-term, medium-term, and long-term stability for DAM and its metabolites are summarized in Supplementary Table 2. DAM was stable when reinjected after extraction (autosampler and extract stability), after undergoing three freeze-thaw cycles (freeze-thaw stability), or when kept at room temperature for 8 h (bench-top stability). The accuracy under these conditions ranged from 89 to 98%, and precision (CV) was consistently within the range of 1 to 7%. However, a notable decrease in DAM concentration was observed following storage at $-20\text{ }^{\circ}\text{C}$ for 1 month, resulting in an accuracy of 78 to 84% and a precision (CV) of 1 to 8%. The degradation of DAM in plasma and other matrices was previously described by others [3,27,35]. Under the same condition, 6-MAM levels tended to be slightly elevated, suggesting the possibility of DAM being deacetylated to this metabolite under these circumstances. The decrease in accuracy could be counteracted when DAM samples were instead stored at $-80\text{ }^{\circ}\text{C}$ for 1 month, which resulted in accuracy of 90 to 99% and precision (CV) of 2 to 8%, respectively. After 3 months at $-80\text{ }^{\circ}\text{C}$, the accuracy of DAM samples was between 90 and 92% while precision (CV) was between 2 and 3%. Furthermore, after 6 months of storage at $-80\text{ }^{\circ}\text{C}$, DAM samples displayed an accuracy between 93 and 95% and a precision (CV) between 2 and 5%. Thus, to ensure the stability of DAM samples for at least 6 months, storage at $-80\text{ }^{\circ}\text{C}$ is required.

The metabolites 6-MAM, MOR, M3G, and M6G displayed stability under all assessed conditions. The accuracy of respective samples was consistently within the range of 89 to 114%, with CV values ranging from 1 to 15%. Overall, 6-MAM, MOR, M3G, and M6G were stable at room temperature for at least 8 h and during three freeze-thaw cycles. The reinjection of extracted samples after 1 day at 10 °C or 7 days at -20 °C did not affect analyte concentration. Furthermore, storage at -20 °C for 1 month resulted in sufficient stability for the metabolites. Consequently short-term, medium-term, and long-term storage at -80 °C did also not affect the analyte concentration.

3.2.7. Clinical application

Blood samples from a multicenter observational study that assesses the acceptability and feasibility of intranasal DAM administration in HAT were analyzed as proof-of-concept. For the analysis, the full pharmacokinetic profile of one study participant was used. The pharmacokinetic profiles obtained for DAM, 6-MAM, MOR, M3G, and M6G are depicted in Fig. 4. The C_{max} of DAM was 94 ng/mL and was reached after 10 min (t_{max}). 6-MAM concentrations peaked at 89 ng/mL after 15 min, while morphine reached 731 ng/mL after 30 min. The glucuronidated metabolites M3G and M6G exhibited substantial differences in plasma concentration. M3G reached a C_{max} of 9,922 ng/mL, whereas M6G peaked at 826 ng/mL after 180 min. As M3G was detected in plasma at concentrations exceeding the ULOQ, all plasma samples were 1:10 diluted in blank plasma and reanalyzed for this metabolite. The final concentrations of the diluted samples were determined through back-calculation. A set of dilQC samples were incorporated to ensure the quality and reliability of the analysis. The metabolites MOR, M3G, and M6G were present in the participant's plasma at the baseline measurement ($t = 0$ min), indicating a recent DAM application. Study samples were analyzed in the order of collection and sufficient blank samples were added after high concentration samples (e.g., ULOQ) to minimize carry-over. The accuracy and precision (CV) of four sets of LQC, MQC, HQC, and dilQC samples were 92–99% and < 6%, respectively, thus confirming the reliability of the analytical run. Consequently, the method proves suitable for the rapid bioanalysis of DAM, 6-MAM, MOR, M3G, and M6G in plasma samples.

4. Conclusion

The herein presented bioanalytical method is reliable and sensitive for the quantification of DAM and its metabolites 6-MAM, MOR, M3G, and M6G in human plasma. A rapid and non-laborious extraction protocol, a small sample volume, and a short analytical run time make the method stand out. Linearity, accuracy, and precision were all in line with regulatory guidelines. Furthermore, we observed a consistent extraction recovery and a negligible matrix effect. Finally, we successfully applied the method to analyze samples of a clinical study employing intranasal DAM administration in HAT. The use of only a small sample volume holds promise for developing micro-sampling techniques, such as the dried blood spot method, which offers significant advantages in collecting samples from patients with deteriorated peripheral veins. Overall, our method is capable of facilitating the analysis of DAM and metabolites in pharmacokinetic analysis, forensic investigations, and drug-drug interaction studies.

Funding

This work was supported by the University Hospital Basel and a grant by the Federal Office of Public Health (No. 142,004,283/321–446/4) to MV.

CRediT authorship contribution statement

Jan Thomann: Writing – review & editing, Writing – original draft, Visualization, Validation, Methodology, Investigation, Formal analysis.

Severin B. Vogt: Writing – review & editing, Resources, Investigation. **Adrian Guessoum:** Writing – review & editing, Resources, Investigation. **Maximilian Meyer:** Writing – review & editing, Resources, Investigation. **Marc Vogel:** Writing – review & editing, Resources, Investigation. **Matthias E. Liechti:** Writing – review & editing, Supervision, Resources, Project administration, Funding acquisition. **Dino Luethi:** Writing – review & editing, Supervision, Project administration, Investigation, Formal analysis, Conceptualization. **Urs Duthaler:** Writing – review & editing, Supervision, Project administration, Investigation, Conceptualization.

Declaration of competing interest

The authors declare the following financial interests and personal relationships: MV reports consultancy and speaker fees from Camurus, Takeda, and Hexal. The other authors do not have any conflicts of interest to declare for this work.

Data availability

Data will be made available on request.

Acknowledgments

The authors thank Beatrice Vetter for providing technical assistance.

Appendix A. Supplementary data

Supplementary data to this article can be found online at <https://doi.org/10.1016/j.jchromb.2024.124104>.

References

- [1] H.H. Maurer, C. Sauer, D.S. Theobald, Toxicokinetics of drugs of abuse: current knowledge of the isoenzymes involved in the human metabolism of tetrahydrocannabinol, cocaine, heroin, morphine, and codeine, *Ther. Drug Monit.* 28 (3) (2006) 447–453.
- [2] E.J. Rook, A.D. Huitema, W. van den Brink, J.M. van Ree, J.H. Beijnen, Pharmacokinetics and pharmacokinetic variability of heroin and its metabolites: review of the literature, *Curr. Clin. Pharmacol.* 1 (1) (2006) 109–118.
- [3] R. Karinen, J.M. Andersen, A. Ripel, I. Hasvold, A.B. Hopen, J. Morland, A. S. Christophersen, Determination of heroin and its main metabolites in small sample volumes of whole blood and brain tissue by reversed-phase liquid chromatography-tandem mass spectrometry, *J. Anal. Toxicol.* 33 (7) (2009) 345–350.
- [4] P. Zuccaro, R. Ricciarello, S. Pichini, R. Pacifici, I. Altieri, M. Pellegrini, G. D'Ascenzo, Simultaneous determination of heroin 6-monoacetylmorphine, morphine, and its glucuronides by liquid chromatography-atmospheric pressure ionspray-mass spectrometry, *J. Anal. Toxicol.* 21 (4) (1997) 268–277.
- [5] K.M. Rentsch, G.A. Kullak-Ublick, C. Reichel, P.J. Meier, K. Fattinger, Arterial and venous pharmacokinetics of intravenous heroin in subjects who are addicted to narcotics, *Clin. Pharmacol. Ther.* 70 (3) (2001) 237–246.
- [6] A. Dienes-Nagy, L. Rivier, C. Giroud, M. Augsburg, P. Mangin, Method for quantification of morphine and its 3- and 6-glucuronides, codeine, codeine glucuronide and 6-monoacetylmorphine in human blood by liquid chromatography-electrospray mass spectrometry for routine analysis in forensic toxicology, *J. Chromatogr. A* 854 (1–2) (1999) 109–118.
- [7] H.S. Smith, Opioid metabolism, *Mayo Clin. Proc.* 84 (7) (2009) 613–624.
- [8] M. Vogel, M. Meyer, J.N. Westenber, A. Kormann, O. Simon, R. Salim Hassan Fadleseed, M. Kurmann, R. Bröer, N. Devaud, U. Sanwald, S. Baumgartner, H. Binder, J. Strasser, R.M. Krausz, T. Beck, K.M. Dürsteler, L. Falcato, Safety and feasibility of intranasal heroin-assisted treatment: 4-week preliminary findings from a swiss multicentre observational study, *Harm Reduct. J.* 20 (1) (2023) 2.
- [9] J.M. Kendall, V.S. Latter, Intranasal diamorphine as an alternative to intramuscular morphine: pharmacokinetic and pharmacodynamic aspects, *Clin. Pharmacokinet.* 42 (6) (2003) 501–513.
- [10] C. Nordt, M. Vogel, M. Dey, A. Moldovanyi, T. Beck, T. Berthel, M. Walter, E. Seifritz, K.M. Dürsteler, M. Herdener, One size does not fit all—evolution of opioid agonist treatments in a naturalistic setting over 23 years, *Addiction* 114 (1) (2019) 103–111.
- [11] World Health Organization, Guidelines for Psychosocially Assisted Pharmacological Treatment of Opiate Dependence. https://iris.who.int/bitstream/handle/10665/43948/9789241547543_eng.pdf?sequence=1, 2009 (accessed 21.02.2024).
- [12] J. Strang, T. Groshkova, A. Uchtenhagen, W. van den Brink, C. Haasen, M. T. Schechter, N. Lintzeris, J. Bell, A. Pirona, E. Oviedo-Joekes, Heroin on trial:

- systematic review and meta-analysis of randomised trials of diamorphine-prescribing as treatment for refractory heroin addiction, *Br. J. Psychiatry* 207 (1) (2015) 5–14.
- [13] D. Ciccarone, M. Harris, Fire in the vein: heroin acidity and its proximal effect on users' health, *Int. J. Drug Policy* 26 (11) (2015) 1103–1110.
- [14] M. Vogel, K. Dürsteler, J. Strasser, O. Schmid, E. Müller, P. Himmelheber, U. Lang, M. Walter, M. Krausz, Injektionen in die leistevene: prävalenz und umgang in heroingestützter behandlung, *Suchtmedizin* 17 (2) (2015) 57–62.
- [15] V. Hope, J. Parry, F. Ncube, M. Hickman, Not in the vein: 'missed hits', subcutaneous and intramuscular injections and associated harms among people who inject psychoactive drugs in Bristol, United Kingdom, *Int. J. Drug Policy* 28 (2016) 83–90.
- [16] S. Larney, A. Peacock, B.M. Mathers, M. Hickman, L. Degenhardt, A systematic review of injecting-related injury and disease among people who inject drugs, *Drug Alcohol Depend.* 171 (2017) 39–49.
- [17] M. Meyer, R. Eichenberger, J. Strasser, K.M. Dürsteler, M. Vogel, «One prick and then it's done»: a mixed-methods exploratory study on intramuscular injection in heroin-assisted treatment, *Harm Reduct. J.* 18 (1) (2021) 1–10.
- [18] F.T. Delaney, E. Stanley, F. Bolster, The needle and the damage done: musculoskeletal and vascular complications associated with injected drug use, *Insights Imaging* 11 (1) (2020) 98.
- [19] K.T. Phillips, M.D. Stein, Risk practices associated with bacterial infections among injection drug users in Denver, Colorado, *Am J Drug Alcohol Abuse* 36 (2) (2010) 92–97.
- [20] E. Cama, L. Brener, H. Wilson, C. von Hippel, Internalized stigma among people who inject drugs, *Subst. Use Misuse* 51 (12) (2016) 1664–1668.
- [21] D.L. Biancarelli, K.B. Biello, E. Childs, M. Drainoni, P. Salhaney, A. Edeza, M. J. Mimiaga, R. Saitz, A.R. Bazzi, Strategies used by people who inject drugs to avoid stigma in healthcare settings, *Drug Alcohol Depend.* 198 (2019) 80–86.
- [22] L. Wang, C. Ni, H. Shen, Z. Sheng, C. Liang, R. Wang, Y. Zhang, Comparison of the detection windows of heroin metabolites in human urine using online SPE and LC-MS/MS: importance of morphine-3-glucuronide, *J. Anal. Toxicol.* 44 (1) (2020) 22–28.
- [23] R. Moreno-Vicente, Z. Fernández-Nieva, A. Navarro, I. Gascón-Crespí, M. Farré-Albaladejo, M. Igartua, R.M. Hernández, J.L. Pedraz, Development and validation of a bioanalytical method for the simultaneous determination of heroin, its main metabolites, naloxone and naltrexone by LC-MS/MS in human plasma samples: application to a clinical trial of oral administration of a heroin/naloxone formulation, *J. Pharm. Biomed. Anal.* 114 (2015) 105–112.
- [24] G. Jakobsson, M.T. Truver, S.A. Wrobel, H. Gréen, R. Kronstrand, Heroin-related compounds and metabolic ratios in postmortem samples using LC-MS-MS, *J. Anal. Toxicol.* 45 (3) (2021) 215–225.
- [25] W. Gul, B. Stamper, M. Godfrey, S.W. Gul, M.A. ElSohly, LC-MS-MS method for analysis of opiates in wastewater during football games II, *J. Anal. Toxicol.* 40 (5) (2016) 330–337.
- [26] E.J. Rook, M.J. Hillebrand, H. Rosing, J.M. van Ree, J.H. Beijnen, The quantitative analysis of heroin, methadone and their metabolites and the simultaneous detection of cocaine, acetylcodeine and their metabolites in human plasma by high-performance liquid chromatography coupled with tandem mass spectrometry, *J. Chromatogr. B Anal. Technol. Biomed. Life Sci.* 824 (1–2) (2005) 213–221.
- [27] J.M. Jones, M.D. Raleigh, P.R. Pentel, T.M. Harmon, D.E. Keyler, R.P. Remmel, A. K. Birnbaum, Stability of heroin, 6-monoacetylmorphine, and morphine in biological samples and validation of an LC-MS assay for delayed analyses of pharmacokinetic samples in rats, *J. Pharm. Biomed. Anal.* 74 (2013) 291–297.
- [28] United States Food and Drug Administration (FDA), Bioanalytical Method Validation Guidance for Industry. <https://www.fda.gov/files/drugs/published/Bioanalytical-Method-Validation-Guidance-for-Industry.pdf>, 2018 (accessed 10.10.2023).
- [29] J.N. Westenberg, M. Meyer, J. Strasser, M. Krausz, K.M. Dürsteler, L. Falcato, M. Vogel, Feasibility, safety, and acceptability of intranasal heroin-assisted treatment in Switzerland: protocol for a prospective multicentre observational cohort study, *Addict. Sci. Clin. Pract.* 18 (1) (2023) 15.
- [30] K.E. Kolaczynska, M.E. Liechti, U. Duthaler, Development and validation of an LC-MS/MS method for the bioanalysis of psilocybin's main metabolites, psilocin and 4-hydroxyindole-3-acetic acid, in human plasma, *J. Chromatogr. B Anal. Technol. Biomed. Life Sci.* 1164 (2021) 122486.
- [31] J. Thomann, L. Ley, A. Klaiber, M.E. Liechti, U. Duthaler, Development and validation of an LC-MS/MS method for the quantification of mescaline and major metabolites in human plasma, *J. Pharm. Biomed. Anal.* 220 (2022) 114980.
- [32] D. Luethi, K.E. Kolaczynska, S.B. Vogt, L. Ley, L. Erne, M.E. Liechti, U. Duthaler, Liquid chromatography-tandem mass spectrometry method for the bioanalysis of N, N-dimethyltryptamine (DMT) and its metabolites DMT-N-oxide and indole-3-acetic acid in human plasma, *J. Chromatogr. B Anal. Technol. Biomed. Life Sci.* 1213 (2022) 123534.
- [33] D. Luethi, S. Durmus, A.H. Schinkel, J.H. Schellens, J.H. Beijnen, R.W. Sparidans, Liquid chromatography-tandem mass spectrometry assay for the EGFR inhibitor pelitinib in plasma, *J. Chromatogr. B Anal. Technol. Biomed. Life Sci.* 934 (2013) 22–25.
- [34] D. Luethi, S. Durmus, A.H. Schinkel, J.H. Schellens, J.H. Beijnen, R.W. Sparidans, Liquid chromatography-tandem mass spectrometric assay for the multikinase inhibitor regorafenib in plasma, *Biomed. Chromatogr.* 28 (10) (2014) 1366–1370.
- [35] D.A. Barrett, A.L. Dyssegaard, P.N. Shaw, The effect of temperature and pH on the deacetylation of diamorphine in aqueous solution and in human plasma, *J. Pharm. Pharmacol.* 44 (7) (1992) 606–608.

3.3 Manuscript 3

Derivatization-free determination of chiral plasma pharmacokinetics of MDMA and its enantiomers

Dino Luethi^{a,*}, Deborah Rudin^a, Isabelle Straumann^a, **Jan Thomann^a**, Isidora Avedisian^a,
Matthias E. Liechti^{a,†}, Urs Duthaler^{a,b,c,†}

^a Division of Clinical Pharmacology and Toxicology, Department of Biomedicine, University Hospital Basel and University of Basel, Basel, Switzerland

^b Institute of Forensic Medicine, Department of Biomedical Engineering, University of Basel, Basel, Switzerland

^c Institute of Forensic Medicine, Health Department Basel-Stadt, Basel, Switzerland

* Corresponding author

† Equal contribution

J Chromatogr B. 2024 May 1:1238:124123

DOI: 10.1016/j.jchromb.2024.124123



Contents lists available at ScienceDirect

Journal of Chromatography B

journal homepage: www.elsevier.com/locate/jchromb

Derivatization-free determination of chiral plasma pharmacokinetics of MDMA and its enantiomers

Dino Luethi ^{a,*}, Deborah Rudin ^a, Isabelle Straumann ^a, Jan Thomann ^a, Isidora Avedisian ^a, Matthias E. Liechti ^{a,1}, Urs Duthaler ^{a,b,c,1}

^a Division of Clinical Pharmacology and Toxicology, Department of Biomedicine, University Hospital Basel and University of Basel, Basel, Switzerland

^b Institute of Forensic Medicine, Department of Biomedical Engineering, University of Basel, Basel, Switzerland

^c Institute of Forensic Medicine, Health Department Basel-Stadt, Basel, Switzerland

ARTICLE INFO

Keywords:

MDMA
Bioanalysis
Pharmacokinetics
Enantiomer
Enantioselective

ABSTRACT

3,4-Methylenedioxyamphetamine (MDMA) is an entactogen with therapeutic potential. The two enantiomers of MDMA differ regarding their pharmacokinetics and pharmacodynamics but the chiral pharmacology of MDMA needs further study in clinical trials. Here, an achiral and an enantioselective high performance liquid chromatography–tandem mass spectrometry method for the quantification of MDMA and its psychoactive phase I metabolite 3,4-methylenedioxyamphetamine (MDA) in human plasma were developed and validated. The analytes were detected by positive electrospray ionization followed by multiple reaction monitoring. The calibration range was 0.5–500 ng/mL for the achiral analysis of both analytes, 0.5–1,000 ng/mL for chiral MDMA analysis, and 1–1,000 ng/mL for chiral MDA analysis. Accuracy, precision, selectivity, and sensitivity of both bioanalytical methods were in accordance with regulatory guidelines. Furthermore, accuracy and precision of the enantioselective method were maintained when racemic calibrations were used to measure quality control samples containing only one of the enantiomers. Likewise, enantiomeric calibrations could be used to reliably quantify enantiomers in racemic samples. The achiral and enantioselective methods were employed to assess pharmacokinetic parameters in clinical study participants treated with racemic MDMA or one of its enantiomers. The pharmacokinetic parameters assessed with both bioanalytical methods were comparable. In conclusion, the enantioselective method is useful for the simultaneous quantification of both enantiomers in subjects treated with racemic MDMA. However, as MDMA and MDA do not undergo chiral inversion, enantioselective separation is not necessary in subjects treated with only one of the enantiomers.

1. Introduction

3,4-Methylenedioxyamphetamine (MDMA) displays promising potential as an adjunct in therapy for post-traumatic stress disorder [1,2]. MDMA is a substrate at the norepinephrine, serotonin, and dopamine transporter (NET, SERT, and DAT, respectively) and exhibits an entactogenic effect profile due to pronounced SERT vs. DAT interactions [3,4]. The two enantiomers of MDMA display a slightly different pharmacokinetic profile in humans [5–8]. Furthermore, previous research suggests more pronounced stimulant effects for S (+)-MDMA, whereas R(–)-MDMA maintains prosocial therapeutic effects with reduced side effects [9–11]. Controlled clinical studies are needed to further elucidate the effects of MDMA enantiomers in humans.

Such studies should aim to examine whether the chiral pharmacology of MDMA or its metabolites may be leveraged to improve the therapeutic benefits. Reliable bioanalytical methods are therefore essential to measure the pharmacokinetics of MDMA and its metabolites in plasma. Here, two liquid chromatography–tandem mass spectrometry (LC–MS/MS) methods for enantioselective and non-enantioselective quantification of MDMA and its psychoactive N-demethylated metabolite 3,4-methylenedioxyamphetamine (MDA) in human plasma were developed and validated. Both bioanalytical methods were used to assess the chiral pharmacokinetics of MDMA after controlled administration of 125 mg R-MDMA, 125 mg S-MDMA, or 125 mg racemic MDMA in human volunteers. Racemic as well as enantiomeric calibrations were used to measure the clinical study samples. The information provided by

* Corresponding author.

E-mail address: dino.luethi@unibas.ch (D. Luethi).

¹ Equal contribution.

<https://doi.org/10.1016/j.jchromb.2024.124123>

Received 14 February 2024; Received in revised form 6 April 2024; Accepted 8 April 2024

Available online 9 April 2024

1570-0232/© 2024 The Author(s). Published by Elsevier B.V. This is an open access article under the CC BY license (<http://creativecommons.org/licenses/by/4.0/>).

this study will assist clinical researchers in the efficient assessment of chiral MDMA pharmacokinetics.

2. Experimental section

2.1. Chemicals, reagents, and reference compounds

MDMA and the internal standards MDMA-d₅ and MDA-d₅ were purchased from Lipomed (Arlesheim, Switzerland). R-MDMA, S-MDMA, MDA, R-MDA, and S-MDA were synthesized by ReseaChem (Burgdorf, Switzerland). LC-MS grade water, methanol, acetonitrile, and isopropanol were obtained from Merck (Darmstadt, Germany). Formic acid (99–100%) was bought from VWR Chemicals (Radnor, PA, USA). Ammonium bicarbonate (LiChropur for LC-MS), ammonium hydroxide ($\geq 25\%$ solution for LC-MS), and dimethyl sulfoxide (DMSO) were ordered from Sigma-Aldrich (Buchs, Switzerland). Human blood collected in lithium heparin coated S-Monovette tubes (Sarstedt, Nümbrecht, Germany) was obtained from the blood donation centers of Basel and Bern. To obtain plasma, blood was centrifuged (Eppendorf 5810 R centrifuge; Hamburg, Germany) at $1,811 \times g$ for 10 min at 15 °C.

2.2. Calibration and quality control sample preparation

Separate stock solutions were made for the preparation of calibration and quality control (QC) samples. The analytes were weighed on a XP26 microbalance (Mettler Toledo, Columbus, USA) and dissolved in DMSO at a concentration of 10 mg/mL (achiral method) or 1 mg/mL (enantioselective method). For the achiral method, a working solution containing both analytes at a concentration of 250 $\mu\text{g/mL}$ in DMSO was prepared. The working solution was used to create a 10-point dilution series in DMSO in the range of 0.05–100 $\mu\text{g/mL}$. For the enantioselective method, three different DMSO dilution series were prepared containing either R-MDMA and R-MDA, S-MDMA and S-MDA, or all enantiomers in the range of 0.05–100 $\mu\text{g/mL}$. Calibration and QC samples were prepared by spiking a pool of blank human plasma from at least seven donors at a ratio of 1:100 (v/v) with the respective DMSO dilutions. QC samples were prepared at the lower limit of quantification (LLOQ) and at low, mid, and high concentration (LQC, MQC, and HQC, respectively). The following QC levels were prepared for racemic MDMA and MDA: 0.5 ng/mL (LLOQ), 1.0 ng/mL (LQC), 40 ng/mL (MQC), and 400 ng/mL (HQC); the following QC levels were prepared for the enantioselective method: 0.5 ng/mL (LLOQ for MDMA enantiomers), 1.0 ng/mL (LLOQ for MDA enantiomers and LQC for MDMA enantiomers), 2.5 ng/mL (LQC for MDA enantiomers), 50 ng/mL (MQC), and 500 ng/mL (HQC). Calibration levels are listed in [Supplementary Tables 1–3](#).

2.3. LC-MS/MS instrumentation and settings

2.3.1. HPLC settings for the achiral method

Analysis of racemic MDMA and MDA was performed with a modular high performance liquid chromatograph (HPLC, Shimadzu, Kyoto, Japan) coupled to an API 4000 QTRAP triple quadrupole tandem mass spectrometer (AB Sciex, Ontario, Canada). Chromatographic separation of all analytes was achieved with a Luna PFP(2) column (3 μm , 100 \AA , 50×2.0 mm; Phenomenex, Torrance, CA, USA). The modular HPLC system consisted of a system controller, four pumps (A, B, C, and D), two degasser units, an autosampler (set to 10 °C), and a column oven (set to 40 °C). Water containing 0.1% formic acid (v/v) was used as mobile phase A and C while methanol containing 0.1% formic acid (v/v) was used as mobile phase B. A binary flow was applied as pumping mode. The sample was transported to the column at a flow rate of 0.1 mL/min using pumps A (95%) and B (5%); subsequently, the sample was diluted with mobile phase C (0.4 mL/min, 0–0.5 min) in a T-union positioned ahead of the column. The total flow of pumps A and B was raised to 0.5 mL/min after 0.5 min. Between 0.5 and 2.5, min the methanol concentration was gradually elevated to 50%. From 2.5 to 2.75 min, it was

further raised to 95% to cleanse the column. Following a 1-min duration with 95% mobile phase B, the methanol concentration was reverted to 5% for 0.5 min to precondition the system. A single sample analysis had a total run time of 4.25 min. The eluent was directed into the mass spectrometer from 1.4 to 3.0 min. The injection volume was 5 μL ; before and after aspirating each sample, the injection needle was rinsed with 0.3 mL of a rinsing solution consisting of equal parts of water, methanol, acetonitrile, and isopropanol.

2.3.2. HPLC settings for the enantioselective method

Enantioselective analysis of MDMA and MDA was achieved using a modular HPLC (Shimadzu) coupled to an API 4000 QTRAP triple quadrupole tandem mass spectrometer (AB Sciex). For enantioselective separation, a Lux AMP column (3 μm , 1000 \AA , 150×3.0 mm; Phenomenex) was used. The HPLC system consisted of a system controller, four pumps (A, B, C, and D), two degasser units, an autosampler (set to 10 °C), and a column oven (set to 45 °C). Mobile phase A consisted of an aqueous ammonium bicarbonate solution (5 mM) adjusted to pH 11 with ammonia solution; acetonitrile was used as mobile phase B. The total flow of pumps A (50%) and B (50%) was set to 0.45 mL/min. Between 4.5 and 4.7 min, the concentration of mobile phase B was gradually increased to 95%, maintaining this level for 1.0 min. At 5.7 min, the mobile phase B concentration was reverted to 50% for 0.3 min to precondition the system. From 1.0 to 5.0 min, the eluent was directed into the mass spectrometer. The total run time was 6.0 min. The injection volume was 2.5 μL and the needle was rinsed with 1 mL of rinsing solution before and after aspiration of each sample.

2.3.3. Mass spectrometer settings

The analytes were ionized by positive electrospray ionization and were detected with multiple reaction monitoring (MRM). Mass transitions are listed in [Table 1](#). The mass spectrometer was operated using the following parameters: ion spray voltage, 5,500 V; temperature, 500 °C; curtain gas, 10 psi; nebulizer gas (ion source gas 1), 60 psi; heater gas (ion source gas 2), 50 psi; collision gas, 4 psi. Elemental nitrogen served as a gas supply. Analyst Instrumental Control and Data Processing Software (Version 1.6.2, AB Sciex) and MultiQuant Software (Version 3.0.3, AB Sciex) were used for system operation and data analysis.

2.4. Sample extraction

Plasma (50 μL) was transferred into 0.75 mL Matrix Blank Storage Tubes (Thermo Fisher Scientific, Waltham, MA, USA) and proteins were precipitated with 150 μL internal standard solution consisting of 2 ng/mL MDMA-d₅ and 10 ng/mL MDA-d₅ dissolved in methanol. The tubes were subsequently vortexed on a multi-tube vortexer (VX-2500, VWR, Radnor, PA, USA) for 30 s and centrifuged at $3,220 \times g$ for 30 min at 10 °C. After extraction, samples were kept in the autosampler at 10 °C until analysis.

Table 1
Mass spectrometry settings for achiral and enantioselective analyte detection.

Analyte	Method	Q1 [Da]	Q3 [Da]	DP [V]	EP [V]	CE [V]	CXP [V]
MDMA	achiral	194.1	163.0	61	10	19	12
MDA	achiral	180.1	133.0	31	10	25	10
MDMA-d ₅	achiral	199.2	165.1	41	10	19	14
MDA-d ₅	achiral	185.1	110.1	51	10	33	10
MDMA	enantioselective	194.1	163.0	61	10	17	12
MDA	enantioselective	180.1	133.0	51	10	25	8
MDMA-d ₅	enantioselective	199.1	165.0	61	10	19	12
MDA-d ₅	enantioselective	185.1	138.1	46	10	25	8

CE, collision energy; CXP, collision cell exit potential; DP, declustering potential; EP, entrance potential; Q1, quadrupole 1; Q3, quadrupole 3.

2.5. Method validation

Bioanalytical method validation was carried out according to the Bioanalytical Method Validation Guidance for Industry of the United States Food and Drug Administration (FDA) [12]. The validation encompassed evaluations for linearity, accuracy, precision, selectivity, sensitivity, extraction recovery, matrix effect, and analyte stability.

2.5.1. Linearity

Each analytical run was supported by a minimum of two calibration lines. Calibration lines for achiral MDMA and MDA quantification covered a range from 0.5 to 500 ng/mL. For the enantioselective method, calibration lines for *R*-MDMA and *S*-MDMA ranged from 0.5 to 1,000 ng/mL, while calibration lines for *R*-MDA and *S*-MDA ranged from 1 to 1,000 ng/mL. Prior to each calibration line, a blank sample extracted with internal standard solution was measured; after each calibration line, a double blank sample extracted with pure methanol was included. The analyte carry-over was assessed by measuring a double blank sample directly after the upper limit of quantification (ULOQ). A carry-over signal $\leq 20\%$ of the LLOQ peak area was considered to be acceptable. A linear regression line was generated with MultiQuant, employing a weighting factor of $1/x^2$. Only values within the range of 85–115% (80–120% for the LLOQ) accuracy of the nominal value were used to plot calibration lines. A calibration line was required to encompass a minimum of 75% of all calibration samples with a correlation coefficient (R) ≥ 0.99 .

2.5.2. Accuracy and precision

Intra- and inter-assay accuracy and precision were determined across three validation runs conducted on separate days. Each run comprised two calibration lines and seven replicates for each QC level (LLOQ, LQC, MQC, and HQC). Accuracy was calculated as the mean of each assessed QC level divided by the respective nominal value within each assay (intra-assay accuracy) and across three validation runs (inter-assay accuracy). The accuracy was required to be within the range of 85–115% (80–120% for the LLOQ). Precision was expressed for each QC level (LLOQ, LQC, MQC, and HQC) as the coefficient of variation (CV) within each run (intra-assay precision) and across three validation runs (inter-assay precision). The required CV was $\leq 15\%$ ($\leq 20\%$ for the LLOQ). In addition, each validation run included seven QC samples at concentrations higher than the ULOQ (i.e., 2,500 ng/mL), which were 1:10 diluted for the final concentration to fall within the calibration range.

2.5.3. Selectivity and sensitivity

To assess method selectivity and sensitivity, plasma samples from seven individuals were spiked at the LLOQ level. To demonstrate sufficient selectivity, the mean accuracy of these samples had to fall within the range of 80–120%. Additionally, at least 67% of these samples had to meet this requirement. Sufficient sensitivity is demonstrated when the signal intensity (peak area) in blank and double blank samples is $\leq 20\%$ of the LLOQ signal intensity.

2.5.4. Extraction recovery and matrix effect

To evaluate extraction recovery, plasma from seven individuals was spiked at the LQC, MQC, and HQC level before and after extraction. The peak areas of the samples spiked before extraction were then compared to those spiked after extraction, representing 100% recovery. To assess the matrix effect, plasma from seven individuals was spiked at the LQC, MQC, and HQC level and the analyte peak area was compared to QC samples spiked at equivalent levels in a methanol–water mixture (1:1). To assess recovery and matrix effect with the enantioselective method, racemates of the analytes were separated on the analytical column and the enantiomers were then analyzed separately.

2.5.5. Stability

To evaluate the stability of MDMA and MDA, seven QC samples at

the LQC, MQC, and HQC level were examined under several different storage conditions. Specifically, analyte stability was assessed after three freeze–thaw cycles (freeze–thaw stability), after exposure to room temperature for 8 h (benchtop stability), after reinjection of extracted samples stored at 10 °C for 24 h or at –20 °C for 1 week (reinjection stability), and after storage for 10 months at –20 °C (long-term stability). Analyte stability was determined to be sufficient if the decrease in concentration was $\leq 15\%$ when compared to a freshly prepared calibration line.

2.6. Clinical application

A subset of plasma samples from a phase 1 clinical trial assessing the effect of MDMA and its enantiomers in healthy volunteers was analyzed with the achiral and the enantioselective method. The study received approval from the Ethics Commission of Northwestern and Central Switzerland (BASEC 2021–02386) and was registered on clinicaltrials.gov (NCT05277636). The research adhered to the principles outlined in the Declaration of Helsinki and the guidelines of the International Conference on Harmonization for Good Clinical Practice. Five study participants received either 125 mg *R*-MDMA, 125 mg *S*-MDMA, or 125 mg racemic MDMA. None of the participants used illicit drugs within two months before the study or during the study period, which was confirmed by urine drug tests. Blood samples were collected before drug administration and repeatedly at the following time points after dosing: 0.25, 0.5, 0.75, 1, 1.5, 2, 2.5, 3, 3.5, 4, 5, 6, 7, 8, 9, and 24 h. Immediately after collection, blood samples were centrifuged at $1811 \times g$ for 10 min; the plasma was separated and stored at –80 °C until analysis. Each analytical run included two racemic and two enantiomeric calibration lines and four QC samples each at the LQC, MQC, and HQC level.

3. Results and discussion

3.1. Method development

An achiral and an enantioselective LC–MS/MS method for the quantification of MDMA and its phase I metabolite MDA in human plasma were developed and validated. A representative chromatogram for each method is shown in Fig. 1. Simple protein precipitation was used for sample preparation in both bioanalytical methods, which allows a convenient and rapid analysis of clinical study samples [13–18]. A run time of 4.25 min was sufficient for satisfactory separation of racemic MDMA and MDA with a Luna PFP(2) column. The retention time was 2.3 min for MDMA and MDMA- d_5 and 2.1 min for MDA and MDA- d_5 . Sufficient enantioselective separation with a Lux AMP column was achieved using an isocratic flow during 4.5 min. The retention time for *R*-MDMA and *S*-MDMA was 3.6 and 3.9 min, respectively; the retention time for *R*-MDA and *S*-MDA was 3.7 and 3.9 min, respectively. A washing step with 95% acetonitrile was included to prevent carry-over after high analyte concentrations, increasing the run time to 6.0 min. LC–MS/MS methods for the chiral analysis of MDMA and various of its metabolites have previously been reported using chiral derivatization [7] or chiral columns [8,19]. The aforementioned methods include different phase I and phase II metabolites and quantification of analytes in different matrices. Chiral derivatization requires a more elaborate sample preparation and recent focus was therefore placed on the development of rapid enantioselective methods [8,19]. In a recently reported method, a Lux i-Amylose-3 column was used for enantioselective separation of MDMA and MDA enantiomers within a short run time [8]. The method was later refined to achieve enantioselective separation of MDMA, MDA, 4-hydroxy-3-methoxymethamphetamine (HMMA), and 4-hydroxy-3-methoxyamphetamine (HMA) within six minutes using a Lux AMP column [19]. The enantioselective method presented here represents a straightforward alternative approach to assess chiral pharmacokinetics in a high number of clinical study samples.

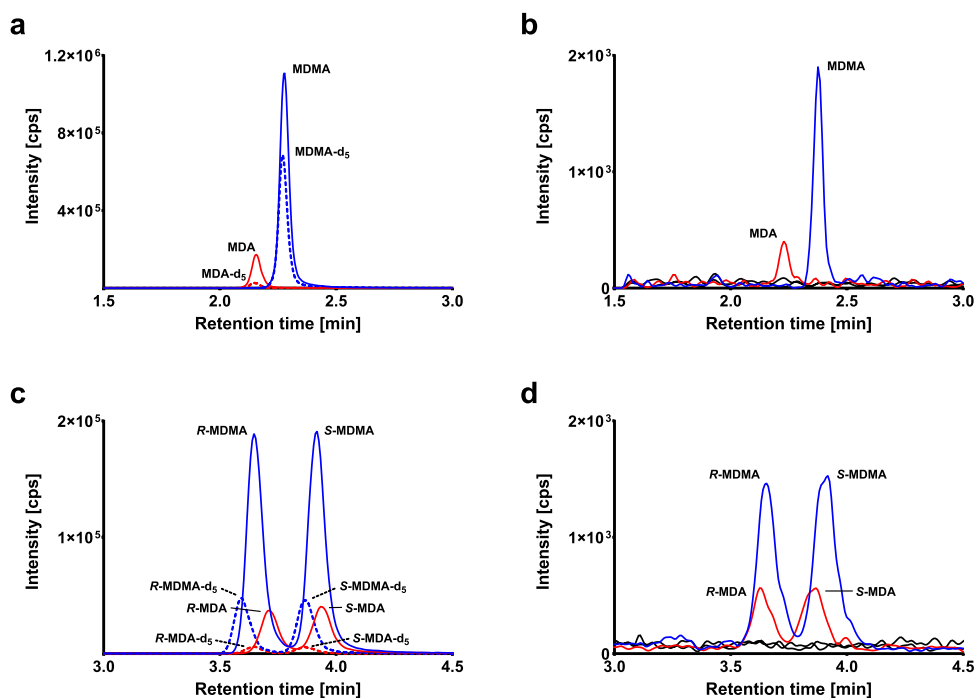


Fig. 1. a) Chromatogram of 100 ng/mL MDMA and MDA in human plasma assessed with the achiral method. b) Chromatogram of MDMA and MDA at the LLOQ (0.5 ng/mL) assessed with the achiral method. c) Chromatogram of 100 ng/mL MDMA and MDA enantiomers in human plasma assessed with the enantioselective method. d) Chromatogram of MDMA and MDA enantiomers at the LLOQ (0.5 ng/mL for MDMA enantiomers and 1 ng/mL for MDA enantiomers) assessed with the enantioselective method. Internal standards are shown as dotted lines, blank signals are shown as black lines.

3.2. Method validation

3.2.1. Linearity, accuracy, and precision

Linearity of calibration lines used to assess accuracy and precision is shown in [Supplementary Tables 1–3](#). Intra- and inter-assay accuracy and precision for achiral quantification were in line with regulatory guidelines and are shown in [Supplementary Table 4](#). For MDMA, intra-assay accuracy was 94–111% and inter-assay accuracy was 95–110%. For MDA, intra-assay accuracy was 97–110% and inter-assay accuracy was 101–106%. Intra- and inter-assay CV for MDMA were 0.5–5.8% and 1.4–4.5%, respectively. Intra- and inter-assay CV for MDA were 1.0–9.3% and 1.7–8.9%, respectively. Accuracy of QC samples at concentrations above the ULOQ (i.e., 2,500 ng/mL) was 99–100% for MDMA and 103–106% for MDA after 1:10 dilution with blank plasma. Precision (CV) for 1:10 diluted QC samples was 1.5–3.0% for MDMA and 2.1–3.8% for MDA. Accuracy and precision of enantiomeric QC samples measured with the enantioselective method using enantiomeric calibrations is shown in [Supplementary Table 5](#). Intra-day accuracy was 95–109% (1.6–5.6% CV) for R-MDMA, 94–109% (1.5–5.7% CV) for S-MDMA, 96–112% (2.5–9.7% CV) for R-MDA, and 93–107% (3.8–16.4% CV) for S-MDA. Inter-day accuracy was 97–107% (3.1–11.3% CV) for all analytes. Requirements for intra- and inter-day accuracy and precision of enantiomeric QC samples were also met when measured with the enantioselective method using racemic calibrations ([Supplementary Table 6](#)). Accuracy and precision of racemic QC samples measured with the enantioselective method using racemic calibrations is shown in [Supplementary Table 7](#). Intra-day accuracy was 86–106% (1.4–8.9% CV) for R-MDMA, 84–104% (1.4–7.3% CV) for S-MDMA, 93–111% (2.7–10.5% CV) for R-MDA, and 97–113% (1.1–11.5% CV) for S-MDA. For all analytes the inter-day accuracy ranged from 88 to 107% (3.5–10.6% CV). Intra- and inter-day accuracy and precision of racemic QC samples was also within requirements when measured with the enantioselective method using enantiomeric calibrations

([Supplementary Table 8](#)). These results indicate that regardless of the method and analytes of interest, both racemates and enantiomers can be used to plot calibration lines. However, deteriorating health of the chiral HPLC column and an associated decrease in peak separation may affect the comparability of peaks in racemic and enantiomeric mixtures.

3.2.2. Selectivity and sensitivity

No significant interferences were observed for any of the analytes in double blank and blank plasma samples of seven individuals measured with either bioanalytical method. All area counts were $\leq 7\%$ of the LLOQ ([Supplementary Table 9 and 10](#)). The accuracy of racemic MDMA and MDA in plasma derived from seven individual donors at the LLOQ was 94–99% and 89–101%, respectively ([Supplementary Table 11](#)). The accuracy of R-MDMA and S-MDMA at the LLOQ assessed with the enantioselective method was 97–117% and 93–112%, respectively; the accuracy of R-MDA and S-MDA was 82–107% and 86–119%, respectively ([Supplementary Table 12](#)). These results indicate sufficient selectivity and sensitivity for both bioanalytical methods within the validated calibration range.

3.2.3. Extraction recovery and matrix effect

Extraction recoveries and matrix effect for MDMA and MDA are listed in [Supplementary Table 13](#). Mean recoveries of racemic MDMA and MDA were 105–110% and 105–109%, respectively. The matrix effect of MDMA and MDA was 95% and 94–96%, respectively; the matrix effect of the internal standards MDMA-d₅ and MDA-d₅ was 92 and 91%, respectively. When assessed with the enantioselective method, recovery was 97–103% for R-MDMA, 96–104% for S-MDMA, 92–102% for R-MDA, and 91–102% for S-MDA. The matrix effect was 93–100% for R-MDMA, 94–101% for S-MDMA, 94–116% for R-MDA, and 94–113% for S-MDA. The matrix effect of R-MDMA-d₅ and S-MDMA-d₅ was 98 and 97%, respectively. The matrix effect of R-MDA-d₅ and S-MDA-d₅ was 97%. Simple protein precipitation used as extraction method in both

bioanalytical methods therefore yielded full extraction recovery and no significant matrix effect was observed over the whole calibration range.

3.2.4. Stability

Stability data are shown in [Supplementary Table 14](#). MDMA and MDA were stable when stored in the autosampler at 10 °C for 1 day (accuracy of 93–111% and 98–107%, respectively). Furthermore, extracted samples of MDMA and MDA were stable at –20 °C for 7 days (accuracy of 93–108% and 100–108%, respectively). After three freeze–thaw cycles, stability was maintained for MDMA (accuracy of 93–110%) as well as for MDA (accuracy of 99–104%). Both MDMA and MDA were stable when stored at ambient temperature for 8 h (accuracy of 93–110% and 99–109%, respectively). Furthermore, storage at –20 °C for 10 months did not result in significant stability loss for either MDMA (accuracy of 86–98%) or MDA (accuracy of 99–103%). Thus, analyte stability in clinical study samples is maintained under standard storage and handling conditions.

3.2.5. Clinical application

Plasma concentrations of 5 subjects each receiving 125 mg *R*-MDMA, *S*-MDMA, or racemic MDMA were assessed with the achiral and the enantioselective method including both racemic and enantiomeric calibration lines ([Fig. 2](#)). Pharmacokinetic parameters are listed in [Table 2](#) and the corresponding plasma concentration curves are shown in [Fig. 3](#). MDMA enantiomers did not undergo chiral inversion, allowing a direct comparison of concentrations measured with the achiral and the enantioselective method. For *R*-MDMA, maximal concentrations (C_{max}) of 319–378 ng/mL were reached after 3.0–3.5 h (t_{max}). The elimination half-life ($t_{1/2}$) was 10.4–10.5 h and the total AUC was 5,814–6,900 ng × h/mL. For *S*-MDMA, maximal concentrations of 242–247 ng/mL were reached after 2.8–2.9 h. The elimination half-life was 3.6 h and the total AUC was 1,849–1,912 ng × h/mL. After administration of racemic MDMA, maximal concentrations of 294–305 ng/mL were measured, which were reached after 3.0–3.2 h. The measured elimination half-life and total AUC values were 7.4 h and 4,111–4,188 ng × h/mL, respectively. For the enantioselective method, the total MDMA concentration was calculated by addition of both enantiomer concentrations. Due to the long half-life of *R*-MDA, pharmacokinetic parameters could not be reliably assessed for each subject; therefore, only parameters for *S*-MDA were compared. Maximum calculated concentrations of *S*-MDA measured after administration of 125 mg *S*-MDMA were 18.0–19.7 ng/mL, reached after 6.2–7.2 h. Elimination half-life and total AUC were 7.0–7.6 h and 276–308 ng × h/mL. These results are consistent with a longer half-life and higher plasma concentrations for *R*-MDMA vs. *S*-MDMA reported by others [6,8,20]. In the aforementioned studies, enantioselective pharmacokinetics were determined in subjects treated with racemic MDMA. To the best of the authors' knowledge, this is the first study that includes enantioselective analysis of racemic MDMA as well as both enantiomers at equal doses within the same subjects.

4. Conclusion

As MDMA and MDA do not undergo chiral inversion, enantioselective analysis is not necessary to measure clinical study samples of subjects treated with MDMA enantiomers. The main advantage of the described achiral method is the shorter run time compared to the enantioselective method. However, the enantioselective method is useful to assess chiral pharmacokinetics of MDMA and MDA in subjects dosed with racemates. For enantioselective analysis, either racemic or enantiomeric calibration lines may be included, regardless of whether the analyzed samples contain only one or both enantiomers. Both bioanalytical methods allow reliable, simple, and rapid analysis of clinical study samples. Additionally, this study offers valuable insights for researchers studying MDMA in clinical settings.

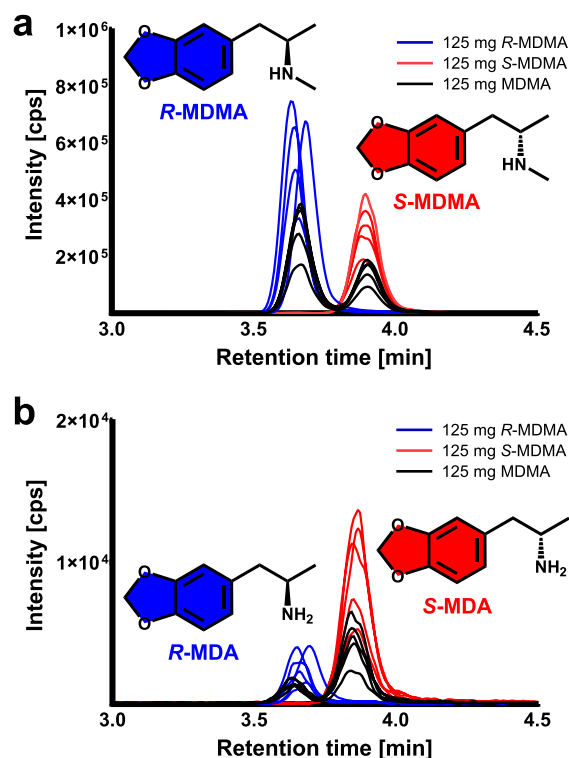


Fig. 2. Overlay of chromatograms of a) MDMA enantiomers and b) MDA enantiomers in plasma of healthy volunteers dosed with 125 mg of *R*-MDMA, *S*-MDMA, or racemic MDMA. The samples were taken 8 h after drug intake.

Funding

This work was supported by Mind Medicine Inc.

CRediT authorship contribution statement

Dino Luethi: Writing – review & editing, Writing – original draft, Visualization, Validation, Project administration, Methodology, Investigation, Formal analysis, Data curation, Conceptualization. **Deborah Rudin:** Writing – review & editing, Validation, Investigation. **Isabelle Straumann:** Writing – review & editing, Investigation, Formal analysis, Data curation. **Jan Thomann:** Methodology, Writing – original draft, Writing – review & editing. **Isidora Avedisian:** Investigation, Writing – review & editing. **Matthias E. Liechti:** Writing – review & editing, Supervision, Project administration, Funding acquisition. **Urs Duthaler:** Writing – review & editing, Validation, Methodology, Investigation, Formal analysis, Data curation, Conceptualization.

Declaration of competing interest

The authors declare the following financial interests/personal relationships which may be considered as potential competing interests: M.E.L. is a consultant for Mind Medicine, Inc. The other authors do not have any conflicts of interest to declare for this study. Knowledge and data associated with this work are owned by the University Hospital Basel and were licensed by Mind Medicine Inc. Mind Medicine Inc. had no role in planning or conducting the study and did not contribute to the manuscript.

Table 2
Pharmacokinetic parameters assessed with the achiral and the enantioselective method.

Treatment	Analyte	Method	Calibration	C _{max} [ng/mL]	t _{max} [h]	t _{1/2} [h]	Total AUC [ng × h/mL]
125 mg R-MDMA	MDMA	achiral	MDMA	368 ± 101	3.5 ± 1.5	10.5 ± 3.8	6,633 ± 2,865
	MDMA	achiral	R-MDMA	349 ± 96	3.5 ± 1.5	10.5 ± 3.8	6,280 ± 2,715
	R-MDMA	enantioselective	MDMA	378 ± 109	3.0 ± 1.7	10.4 ± 3.8	6,900 ± 2,903
	R-MDMA	enantioselective	R-MDMA	319 ± 92	3.0 ± 1.7	10.4 ± 3.8	5,814 ± 2,447
125 mg S-MDMA	MDMA	achiral	MDMA	243 ± 60	2.8 ± 0.4	3.6 ± 0.8	1,890 ± 474
	MDMA	achiral	S-MDMA	247 ± 61	2.8 ± 0.4	3.6 ± 0.8	1,912 ± 481
	S-MDMA	enantioselective	MDMA	242 ± 57	2.9 ± 0.4	3.6 ± 0.8	1,849 ± 429
	S-MDMA	enantioselective	S-MDMA	244 ± 57	2.9 ± 0.4	3.6 ± 0.8	1,863 ± 432
	MDA	achiral	MDA	19.7 ± 5.5	7.2 ± 1.8	7.4 ± 1.8	308 ± 112
	MDA	achiral	S-MDA	18.7 ± 5.1	7.2 ± 1.8	7.6 ± 1.8	299 ± 106
	S-MDA	enantioselective	MDA	18.0 ± 4.8	6.2 ± 1.3	7.2 ± 1.7	276 ± 99
	S-MDA	enantioselective	S-MDA	19.5 ± 5.3	6.2 ± 1.3	7.0 ± 1.7	294 ± 107
125 mg MDMA	MDMA	achiral	MDMA	305 ± 61	3.0 ± 0.7	7.4 ± 2.6	4,188 ± 1,528
	R-MDMA + S-MDMA	enantioselective	MDMA	294 ± 57	3.2 ± 0.9	7.4 ± 2.3	4,111 ± 1,523
	R-MDMA	enantioselective	MDMA	171 ± 40	4.5 ± 2.6	9.0 ± 3.4	2,981 ± 1,236
	S-MDMA	enantioselective	MDMA	130 ± 22	2.7 ± 0.6	4.6 ± 1.0	1,197 ± 346

The total AUC is extrapolated from time 0 to infinite time.

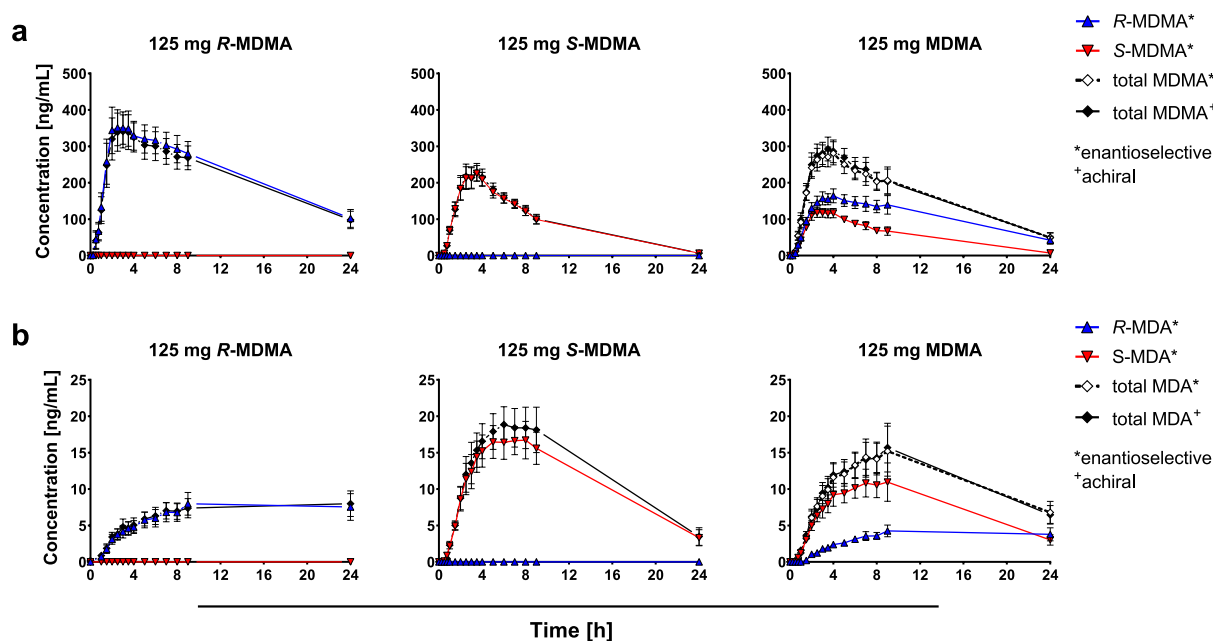


Fig. 3. Pharmacokinetic profiles of a) MDMA and its enantiomers and b) MDA and its enantiomers after administration of 125 mg R-MDMA, S-MDMA, or racemic MDMA in 5 healthy volunteers. The samples were measured with the enantioselective and the achiral method. Concentrations of both enantiomers were added to obtain the total MDMA and MDA concentrations determined with the enantioselective method. Data points represent mean ± SEM.

Data availability

Data will be made available on request.

Acknowledgements

The authors thank Beatrice Vetter for technical assistance.

Appendix A. Supplementary data

Supplementary data to this article can be found online at <https://doi.org/10.1016/j.jchromb.2024.124123>.

References

- [1] J.M. Mitchell, G.M. Ot'abora, B. van der Kolk, S. Shannon, M. Bogenschutz, Y. Gelfand, C. Paleos, C.R. Nicholas, S. Quevedo, B. Balliett, S. Hamilton, M. Mithoefer, S. Kleiman, K. Parker-Guilbert, K. Tzarfaty, C. Harrison, A. de Boer, R. Doblin, B. Yazar-Klosinski, MDMA-assisted therapy for moderate to severe PTSD: a randomized, placebo-controlled phase 3 trial, *Nat. Med* 29 (2023) 2473–2480.
- [2] J.M. Mitchell, M. Bogenschutz, A. Lilienstein, C. Harrison, S. Kleiman, K. Parker-Guilbert, G.M. Ot'abora, W. Garas, C. Paleos, I. Gorman, C. Nicholas, M. Mithoefer, S. Carlin, B. Poulter, A. Mithoefer, S. Quevedo, G. Wells, S.S. Klair, B. van der Kolk, K. Tzarfaty, R. Amiaz, R. Worthy, S. Shannon, J.D. Woolley, C. Marta, Y. Gelfand, E. Hapke, S. Amar, Y. Wallach, R. Brown, S. Hamilton, J.B. Wang, A. Coker, R. Matthews, A. de Boer, B. Yazar-Klosinski, A. Emerson, R. Doblin, MDMA-assisted therapy for severe PTSD: a randomized, double-blind, placebo-controlled phase 3 study, *Nat. Med* 27 (2021) 1025–1033.
- [3] D. Luethi, K.E. Kolaczynska, M. Walter, M. Suzuki, K.C. Rice, B.E. Blough, M. C. Hoener, M.H. Baumann, M.E. Liechti, Metabolites of the ring-substituted stimulants MDMA, methylone and MDPV differentially affect human monoaminergic systems, *J. Psychopharmacol* 33 (2019) 831–841.

- [4] L.D. Simmler, T.A. Buser, M. Donzelli, Y. Schramm, L.H. Dieu, J. Huwyler, S. Chaboz, M.C. Hoener, M.E. Liechti, Pharmacological characterization of designer cathinones in vitro, *Br. J. Pharmacol* 168 (2013) 458–470.
- [5] A.E. Steuer, C. Schmidhauser, E.H. Tingelhoff, Y. Schmid, A. Rickli, T. Kraemer, M. E. Liechti, Impact of cytochrome P450 2D6 function on the chiral blood plasma pharmacokinetics of 3,4-methylenedioxy-methamphetamine (MDMA) and its phase I and II metabolites in humans, *Plos One* 11 (2016) e0150955.
- [6] A.E. Steuer, C. Schmidhauser, Y. Schmid, A. Rickli, M.E. Liechti, T. Kraemer, Chiral plasma pharmacokinetics of 3,4-methylenedioxy-methamphetamine and its phase I and II metabolites following controlled administration to humans, *Drug. Metab. Dispos* 43 (2015) 1864–1871.
- [7] A.E. Steuer, C. Schmidhauser, M.E. Liechti, T. Kraemer, Development and validation of an LC-MS/MS method after chiral derivatization for the simultaneous stereoselective determination of methylenedioxy-methamphetamine (MDMA) and its phase I and II metabolites in human blood plasma, *Drug. Test. Anal* 7 (2015) 592–602.
- [8] A.F. Lo Faro, G. Sprega, D. Beradinelli, A. Tini, L. Poyatos, E. Papaseit, P. Berretta, A. Di Giorgi, M. Farre, N. Takaishvili, T. Farkas, F.P. Busardó, B. Chankvetadze, Development of enantioselective high-performance liquid chromatography-tandem mass spectrometry method for the quantitative determination of 3,4-methylenedioxy-methamphetamine (MDMA) and its phase-1 metabolites in human biological fluids, *J. Pharm. Biomed. Anal* 238 (2024) 115768.
- [9] K.S. Murnane, N. Murai, L.L. Howell, W.E. Fantegrossi, Discriminative stimulus effects of psychostimulants and hallucinogens in S(+)-3,4-methylenedioxy-methamphetamine (MDMA) and R(-)-MDMA trained mice, *J. Pharmacol. Exp. Ther* 331 (2009) 717–723.
- [10] W.E. Fantegrossi, N. Murai, B.O. Mathúna, N. Pizarro, R. de la Torre, Discriminative stimulus effects of 3,4-methylenedioxy-methamphetamine and its enantiomers in mice: pharmacokinetic considerations, *J. Pharmacol. Exp. Ther* 329 (2009) 1006–1015.
- [11] E.G. Pitts, D.W. Curry, K.N. Hampshire, M.B. Young, L.L. Howell, (±)-MDMA and its enantiomers: potential therapeutic advantages of R(-)-MDMA, *Psychopharmacology (berl)* 235 (2018) 377–392.
- [12] U.S. Food and Drug Administration. Bioanalytical Method Validation Guidance for Industry, 2018. <https://www.fda.gov/files/drugs/published/Bioanalytical-Method-Validation-Guidance-for-Industry.pdf> (accessed 23.01.2024).
- [13] D. Luethi, S. Durmus, A.H. Schinkel, J.H. Schellens, J.H. Beijnen, R.W. Sparidans, Liquid chromatography–tandem mass spectrometric assay for the multikinase inhibitor regorafenib in plasma, *Biomed. Chromatogr* 28 (2014) 1366–1370.
- [14] D. Luethi, S. Durmus, A.H. Schinkel, J.H. Schellens, J.H. Beijnen, R.W. Sparidans, Liquid chromatography–tandem mass spectrometry assay for the EGFR inhibitor pelitinib in plasma, *J. Chromatogr. B. Analyt. Technol. Biomed. Life. Sci* 934 (2013) 22–25.
- [15] J. Thomann, L. Ley, A. Klaiber, M.E. Liechti, U. Duthaler, Development and validation of an LC–MS/MS method for the quantification of mescaline and major metabolites in human plasma, *J. Pharm. Biomed. Anal* 220 (2022) 114980.
- [16] D. Luethi, K.E. Kolaczynska, S.B. Vogt, L. Ley, L. Erne, M.E. Liechti, U. Duthaler, Liquid chromatography–tandem mass spectrometry method for the bioanalysis of N, N-dimethyltryptamine (DMT) and its metabolites DMT-N-oxide and indole-3-acetic acid in human plasma, *J. Chromatogr. B. Analyt. Technol. Biomed. Life. Sci* 1213 (2022) 123534.
- [17] K.E. Kolaczynska, M.E. Liechti, U. Duthaler, Development and validation of an LC–MS/MS method for the bioanalysis of psilocybin’s main metabolites, psilocin and 4-hydroxyindole-3-acetic acid, in human plasma, *J. Chromatogr. B. Analyt. Technol. Biomed. Life. Sci* 1164 (2021) 122486.
- [18] J. Thomann, S.B. Vogt, A. Guessoum, M. Meyer, M. Vogel, M.E. Liechti, D. Luethi, U. Duthaler, Development and validation of an LC-MS/MS method for quantifying diamorphine and its major metabolites 6-monoacetylmorphine, morphine, morphine-3-glucuronide, and morphine-6-glucuronide in human plasma, *J. Chromatogr. B. Analyt. Technol. Biomed. Life. Sci* 1237 (2024) 124104.
- [19] G. Sprega, G. Kobidze, A.F. Lo Faro, S. Pichini, T. Farkas, A. Tini, A. Mskhiladze, F. P. Busardó, B. Chankvetadze, Optimization of enantioselective high-performance liquid chromatography-tandem mass spectrometry method for the quantitative determination of 3,4-methylenedioxy-methamphetamine (MDMA) and its phase-1 metabolites in human biological fluids, *J. Pharm. Biomed. Anal.* 243 (2024) 116076.
- [20] N. Pizarro, M. Farré, M. Pujadas, A.M. Peiró, P.N. Roset, J. Joglar, R. de la Torre, Stereochemical analysis of 3,4-methylenedioxy-methamphetamine and its main metabolites in human samples including the catechol-type metabolite (3,4-dihydroxymethamphetamine), *Drug. Metab. Dispos* 32 (2004) 1001–1007.

PART II:
METABOLIC INVESTIGATIONS

4 METABOLISM OF PSYCHEDELICS

4.1 Drug metabolism

Drug metabolism describes the chemical modification of endogenous and exogenous molecules or xenobiotics to increase their hydrophilicity for improved excretion. Often the pharmacological efficacy of a drug can be reduced, which may result in alterations to its biological properties. In general, drug metabolism can be divided into two distinct phases (Iyanagi 2007, Zhao et al. 2021).

Phase I metabolism involves the oxidation, reduction, and hydrolysis of drugs, which renders them more polar. The CYP superfamily represents the most important group of phase I enzymes. It is estimated that they are responsible for the biotransformation of approximately 60% of drugs approved by the FDA. Typically expressed in the liver, CYPs are also found extrahepatically e.g., in the intestine where they play an important role in the first-pass metabolism (Kadlubar et al. 2009, Venkatakrishnan et al. 2001, Zhao et al. 2021). Other phase I enzymes include monoamine oxidases (MAOs), flavin-containing monooxygenases (FMOs), alcohol dehydrogenases (ADHs), or aldehyde dehydrogenases (ALDHs) (Ashton et al. 2024).

Phase II metabolism involves the conjugation of the substrate with a co-substrate, which is usually carried out by transferases. The introduced co-substrate is specific to the family of phase II enzymes. The most important enzyme families in phase II metabolism are UGTs, SULTs, glutathione S-transferases (GSTs), N-acetyltransferases (NATs), thiopurine S-methyltransferases (TPMTs), and COMTs (Almazroo et al. 2017, Kadlubar et al. 2009, Zhao et al. 2021).

In the detoxification process of xenobiotics, the successive combination of the CYP system and conjugation through UGTs plays the most important role. However, the substrate specificities of different enzymes are often overlapping (Almazroo et al. 2017, Iyanagi 2007, Kadlubar et al. 2009).

4.2 Current research on the metabolism of psychedelics

Despite renewed interest in psychedelic research, the exact metabolic pathways remain a topic of ongoing investigation for most psychedelics. However, a full comprehension of the metabolic processes is important to understand the physiological mechanisms and evaluate potential risks. Downstream metabolites of psychedelics may have pharmacological activity, so awareness of their production and presence is vital (Madrid-Gambin et al. 2023). Furthermore, knowledge of the enzymes involved can help predict an individual's

susceptibility to enzymatic polymorphism. In particular, genetic variations related to the CYP superfamily may have a significant impact (Halman et al. 2024, Madrid-Gambin et al. 2023).

An example therefore is the metabolic degradation of LSD. A number of CYPs are involved in the biotransformation to its primary metabolites 2-oxo-3-hydroxy-LSD (OH-LSD) (CYP1A2, CYP2C9, CYP2E1, and CYP3A4) and 6-norlysergic acid diethylamide (nor-LSD) (CYP2E1, CYP2D6, and CYP3A4) (Libanio Osorio Marta 2019, Luethi et al. 2019a). Individuals with less functional CYP2D6 (i.e., poor metabolizer) have a slower biotransformation of LSD to nor-LSD. This results in prolonged LSD half-lives and, consequently, a prolonged subjective effect, which may have implications for personalized treatment approaches in clinical settings (Vizeli et al. 2021).

Enzymatic degradation also plays a major role in the acute subjective effects of DMT. It is rapidly metabolized in the liver by MAO-A, which catalyzes its oxidative deamination into inactive metabolites such as indole-3-acetic acid (IAA). The rapid degradation of DMT results in a brief duration of action when administered alone. However, when used in combination with monoamine oxidase inhibitors (MAOIs), such as in ayahuasca, the breakdown of DMT is inhibited which enables its psychedelic effects (Barker 2018, Egger et al. 2024, Riba et al. 2012).

The metabolic fate of mescaline, another classic psychedelic, has been the subject of investigation resulting in the proposal of several metabolic pathways. The major metabolic pathways include the formation of the inactive TMPAA or the N-acetylation to *N*-acetyl mescaline (NAM). Additionally, other minor oxidative metabolic routes have been described. However, despite existing speculation, there is a lack of comprehensive studies investigating the specific enzymes involved (Dinis-Oliveira et al. 2019, Vamvakopoulou et al. 2023). Therefore, the effect of inhibiting or inducing specific enzymes on the metabolism of mescaline remains inconclusive.

The biotransformation of psilocybin and its dephosphorylated metabolite psilocin is dominated by the inactivation through glucuronidation by several UGTs and the transformation to 4-HIAA (Dinis-Oliveira 2017, Hasler et al. 1997, Kolaczynska et al. 2021). While the general metabolic pathway of psilocybin, particularly its conversion to psilocin and subsequent glucuronidation, is well understood, significant gaps remain in the understanding of the full metabolism. Further investigation is required into the involved enzymes, alternative metabolic pathways, and the intrinsic activity of minor metabolites. Therefore, the project described in Chapter 5.1 aimed to investigate the metabolic degradation of psilocin with a particular focus on the involvement of phase I and phase II enzymes.

5 PUBLICATIONS

5.1 Manuscript 4

In vitro and in vivo metabolism of psilocybin's active metabolite psilocin

Jan Thomann^{a,b,†}, Karolina E. Kolaczynska^{a,b,†}, Oliver V. Stoeckmann^{a,b}, Deborah Rudin^{a,b}, Patrick Vizeli^{a,b}, Marius C. Hoener^c, Christopher R. Pryce^d, Franz X. Vollenweider^e, Matthias E. Liechti^{a,b,*} and Urs Duthaler^{a,b,f,g}

^a Division of Clinical Pharmacology and Toxicology, Department of Pharmaceutical Sciences, University of Basel, Basel, Switzerland

^b Division of Clinical Pharmacology and Toxicology, Department of Biomedicine, University Hospital Basel, Basel, Switzerland

^c Neuroscience Research, Pharma Research and Early Development, Roche Innovation Center Basel, F. Hoffmann-La Roche Ltd, Basel, Switzerland

^d Department of Psychiatry, Psychotherapy and Psychosomatics, Preclinical Laboratory for Translational Research Into Affective Disorders, University of Zurich, Zurich, Switzerland

^e Department of Psychiatry, Psychotherapy and Psychosomatics, Neurophenomenology and Consciousness, University of Zurich, Zurich, Switzerland

^f Institute of Forensic Medicine, Department of Biomedical Engineering, University of Basel, Basel, Switzerland

^g Institute of Forensic Medicine, Health Department Basel-Stadt, Basel, Switzerland

* Corresponding author

† Equal contribution

Front Pharmacol. 2024 Apr 29;15:1391689

DOI: 10.3389/fphar.2024.1391689



OPEN ACCESS

 EDITED BY
 Massimo Valoti,
 University of Siena, Italy

 REVIEWED BY
 Wladyslawa Anna Daniel,
 Polish Academy of Sciences, Poland
 Jesper Kristensen,
 University of Copenhagen, Denmark

 *CORRESPONDENCE
 Matthias E. Liechti,
 ✉ matthias.liechti@usb.ch

†These authors have contributed equally to this work and share first authorship

 RECEIVED 26 February 2024
 ACCEPTED 08 April 2024
 PUBLISHED 29 April 2024

 CITATION
 Thomann J, Kolaczynska KE, Stoeckmann OV,
 Rudin D, Vizeli P, Hoener MC, Pryce CR,
 Vollenweider FX, Liechti ME and Duthaler U
 (2024), *In vitro* and *in vivo* metabolism of
 psilocybin's active metabolite psilocin.
Front. Pharmacol. 15:1391689.
 doi: 10.3389/fphar.2024.1391689

 COPYRIGHT
 © 2024 Thomann, Kolaczynska, Stoeckmann,
 Rudin, Vizeli, Hoener, Pryce, Vollenweider,
 Liechti and Duthaler. This is an open-access
 article distributed under the terms of the
 Creative Commons Attribution License (CC BY).
 The use, distribution or reproduction in other
 forums is permitted, provided the original
 author(s) and the copyright owner(s) are
 credited and that the original publication in this
 journal is cited, in accordance with accepted
 academic practice. No use, distribution or
 reproduction is permitted which does not
 comply with these terms.

In vitro and *in vivo* metabolism of psilocybin's active metabolite psilocin

 Jan Thomann^{1,2†}, Karolina E. Kolaczynska^{1,2†},
 Oliver V. Stoeckmann^{1,2}, Deborah Rudin^{1,2}, Patrick Vizeli^{1,2},
 Marius C. Hoener³, Christopher R. Pryce⁴, Franz X. Vollenweider⁵,
 Matthias E. Liechti^{1,2*} and Urs Duthaler^{1,2,6,7}
¹Division of Clinical Pharmacology and Toxicology, Department of Pharmaceutical Sciences, University of Basel, Basel, Switzerland, ²Division of Clinical Pharmacology and Toxicology, Department of Biomedicine, University Hospital Basel, Basel, Switzerland, ³Neuroscience Research, Pharma Research and Early Development, Roche Innovation Center Basel, F. Hoffmann-La Roche Ltd, Basel, Switzerland, ⁴Department of Psychiatry, Psychotherapy and Psychosomatics, Preclinical Laboratory for Translational Research Into Affective Disorders, University of Zurich, Zurich, Switzerland, ⁵Department of Psychiatry, Psychotherapy and Psychosomatics, Neurophenomenology and Consciousness, University of Zurich, Zurich, Switzerland, ⁶Institute of Forensic Medicine, Department of Biomedical Engineering, University of Basel, Basel, Switzerland, ⁷Institute of Forensic Medicine, Health Department Basel-Stadt, Basel, Switzerland

In vivo, psilocybin is rapidly dephosphorylated to psilocin which induces psychedelic effects by interacting with the 5-HT_{2A} receptor. Psilocin primarily undergoes glucuronidation or conversion to 4-hydroxyindole-3-acetic acid (4-HIAA). Herein, we investigated psilocybin's metabolic pathways *in vitro* and *in vivo*, conducting a thorough analysis of the enzymes involved. Metabolism studies were performed using human liver microsomes (HLM), cytochrome P450 (CYP) enzymes, monoamine oxidase (MAO), and UDP-glucuronosyltransferase (UGT). *In vivo*, metabolism was examined using male C57BL/6J mice and human plasma samples. Approximately 29% of psilocin was metabolized by HLM, while recombinant CYP2D6 and CYP3A4 enzymes metabolized nearly 100% and 40% of psilocin, respectively. Notably, 4-HIAA and 4-hydroxytryptophol (4-HTP) were detected with HLM but not with recombinant CYPs. MAO-A transformed psilocin into minimal amounts of 4-HIAA and 4-HTP. 4-HTP was only present *in vitro*. Neither 4-HIAA nor 4-HTP showed relevant interactions at assessed 5-HT receptors. In contrast to *in vivo* data, UGT1A10 did not extensively metabolize psilocin *in vitro*. Furthermore, two putative metabolites were observed. *N*-methyl-4-hydroxytryptamine (norpsilocin) was identified *in vitro* (CYP2D6) and in mice, while an oxidized metabolite was detected *in vitro* (CYP2D6) and in humans. However, the CYP2D6 genotype did not influence psilocin plasma concentrations in the investigated study population. In conclusion, MAO-A, CYP2D6, and CYP3A4 are involved in psilocin's metabolism. The discovery of putative norpsilocin in mice and oxidized psilocin in humans further unravels psilocin's metabolism. Despite limitations in replicating phase II metabolism *in vitro*, these findings hold significance for studying drug-drug interactions and advancing research on psilocybin as a therapeutic agent.

KEYWORDS

psychedelics, psilocybin, metabolism, cytochrome P450 (CYP), pharmacokinetics, liver microsomes, recombinant enzymes, 5-HT receptor

1 Introduction

Psychedelic mushrooms (e.g., *Psilocybe azurescens* or *Psilocybe mexicana*) and their associated mind- and consciousness-altering effects have been explored for over 3,000 years (Van Court et al., 2022). Most recently, psilocybin has been investigated for its therapeutic properties in several affective disorders including anxiety, treatment-resistant major depression, and cluster headache (Moreno et al., 2006; Sewell et al., 2006; Grob et al., 2011; Griffiths et al., 2016; Ross et al., 2016; Carhart-Harris et al., 2017; Johnson et al., 2017; Bogenschutz et al., 2018; Becker et al., 2022).

As a psychoactive alkaloid, psilocybin undergoes first-pass metabolism and acts as a prodrug. Upon oral ingestion, its terminal phosphate group (PO₄) is rapidly cleaved by alkaline phosphates and non-specific esterases. This transforms psilocybin into psilocin (4-hydroxy-*N,N*-dimethyltryptamine), a more lipophilic molecule that can cross the blood-brain barrier more readily (Horita and Weber, 1961a; Horita and Weber, 1962; Eivindvik et al., 1989; Hasler et al., 1997) to produce its psychedelic effects via serotonin 5-HT_{2A} receptors (Vollenweider et al., 1998; Rickli et al., 2016). Psilocin is therefore the active agent that produces psilocybin's mind-altering effects. Psilocin concentration peaks in plasma around 2 h after oral administration and the subjective effects last for approximately 6 h (Griffiths et al., 2016; Johnson et al., 2017; Holze et al., 2022a). In humans, psilocin plasma concentrations of approximately 15–20 ng/mL and an elimination half-life (t_{1/2}) of 2–3 h were observed after a single oral dose of 25 mg psilocybin (Kolaczynska et al., 2021; Holze et al., 2022a). Psilocin is primarily excreted in urine, although only a minor fraction of administered psilocybin (1.5%) is eliminated as unconjugated psilocin in the first 24 h (Holze et al., 2022a). Psilocin is extensively glucuronidated to psilocin-O-glucuronide, a major urine metabolite. Approximately 20% of orally administered psilocybin is excreted as glucuronidated psilocin in humans within 24 h (Holze et al., 2022a). This conjugation is mainly catalyzed by UDP-glucuronosyltransferase (UGT) 1A10 and UGT1A9 which are highly expressed in the small intestine and liver, respectively (Sticht and Käferstein, 2000; Grieshaber et al., 2001; Hasler et al., 2002; Manevski et al., 2010; Kolaczynska et al., 2021). Concurrently, psilocin can undergo demethylation and oxidative deamination to form the intermediate metabolite 4-hydroxyindole-3-acetaldehyde (4-HIA), presumably catalyzed by monoamine oxidase (MAO). 4-HIA undergoes either reduction to 4-hydroxytryptophol (4-HTP) or oxidation to 4-hydroxyindole-3-acetic acid (4-HIAA) (Kalberer et al., 1962; Hasler et al., 1997; Lindenblatt et al., 1998; Kolaczynska et al., 2021). 4-HIAA is, along with psilocin-O-glucuronide, another major urine metabolite. Around 33% of a psilocybin dose is renally excreted as 4-HIAA (Holze et al., 2022a). It is suggested that similar to the metabolic pathway of serotonin (5-hydroxytryptamine, 5-HT), aldehyde (ALDH) and alcohol dehydrogenase (ADH) might play a key role in transforming 4-HIA to 4-HIAA and 4-HTP, respectively (Svensson et al., 1999; Dinis-Oliveira, 2017). A further minor metabolic route is proposed to be the hydroxylation and oxidation of the indole moiety of psilocin to form an iminoquinone or *o*-quinone structure. It is hypothesized that this reaction is exerted by oxidative enzymes such

as ceruloplasmin (copper carrying oxidase in human blood), cytochrome oxidases, or non-enzymatically by ferric oxide (Fe³⁺) but not MAO (Blaschko and Levine, 1960; Horita and Weber, 1961b; Dinis-Oliveira, 2017). However, the exact structure of the oxidized metabolite has not been experimentally elucidated. Moreover, to our best knowledge, the role of cytochrome P450 (CYP) enzymes in psilocybin's metabolism has thus far not been demonstrated. The CYP superfamily is responsible for the oxidative metabolism of several psychoactive substances and has previously been shown to be involved in the metabolism of *N,N*-dimethyltryptamine (DMT), lysergic acid diethylamide (LSD), or 3,4-methylenedioxymethamphetamine (MDMA) (Vizeli et al., 2017; Luethi et al., 2019; Eckernäs et al., 2023).

Furthermore, the pharmacological activity or relevance of psilocybin's metabolites needs to be assessed. Psilocin's 5-HT receptor binding and receptor activation potency have been determined previously with relevant activity at human 5-HT_{1A}, 5-HT_{2A}, 5-HT_{2B}, and 5-HT_{2C} receptors (Rickli et al., 2016). In addition, psilocin moderately inhibits the serotonin transporter (SERT) but not dopamine (DAT) or norepinephrine transporters (NET) (Rickli et al., 2016). However, it is not clear if any of psilocybin's remaining metabolites display relevant pharmacological activity at 5-HT receptors or the monoamine transporters.

As psilocybin transforms from a recreational substance to a potential therapeutic agent, a comprehensive understanding of its pharmacological characteristics and metabolic breakdown is necessary. In this study, we aimed to characterize the metabolic pathways of psilocin *in vitro*, focusing on the involvement of CYP enzymes. Furthermore, we compared the *in vitro* findings to *in vivo* findings in both humans and mice.

2 Material and methods

2.1 Chemicals and reagents

LC-MS grade water, methanol, acetonitrile, and isopropanol were all purchased from Merck (Darmstadt, Germany). Formic acid, dimethyl sulfoxide (DMSO), potassium phosphate dibasic (K₂HPO₄), potassium phosphate monobasic (KH₂PO₄), and bovine serum albumin (BSA) were acquired from Sigma-Aldrich (Buchs, Switzerland).

2.2 Substrates, metabolites, inhibitors, and internal standards

Psilocin was purchased from Lipomed (Arlesheim, Switzerland), while 4-HIAA and 4-HTP were synthesized by ReseaChem (Burgdorf, Switzerland). The purity of all aforementioned analytes was >98%.

CYP substrates including tizanidine hydrochloride (CYP1A2) (S)-efavirenz (CYP2B6), paclitaxel (CYP2C8), flurbiprofen (CYP2C9), omeprazole (CYP2C19), and metoprolol (CYP2D6) were obtained from Toronto Research Chemicals (TRC; Toronto, Canada). CYP3A4 substrate midazolam was acquired from Lipomed, while chlorzoxazone (CYP2E1) was purchased from Sigma-Aldrich. Metabolites including hydroxy-tizanidine (OH-tizanidine; CYP1A2),

8-hydroxy-efavirenz (OH-efavirenz; CYP2B6), 6- α -hydroxy-paclitaxel (OH-paclitaxel; CYP2C8), 4-hydroxy-flurbiprofen (OH-flurbiprofen; CYP2C9), 5-hydroxy-omeprazole (OH-omeprazole; CYP2C19), α -hydroxy-metoprolol (OH-metoprolol; CYP2D6), and 6-hydroxy-chlorzoxazone (OH-chlorzoxazone; CYP2E1) were all purchased from TRC, while α -hydroxy-midazolam (OH-midazolam; CYP3A4) was obtained from Lipomed.

CYP inhibitors ticlopidine hydrochloride (CYP2B6), sulfaphenazole (CYP2C9) (+)-*N*-3-benzylirivanol (CYP2C19), quinidine sulfate (CYP2D6), 4-methylpyrazole hydrochloride (CYP2E1), and ketoconazole (CYP3A4) were all purchased from Sigma-Aldrich. Furafylline (CYP1A2) was purchased from TRC while montelukast dicyclohexylamine (CYP2C8) was obtained from the European Directorate for the Quality of Medicines and Healthcare (Strasbourg, France).

The MAO-A and MAO-B substrate kynuramine dihydrobromide, its metabolite 4-hydroxyquinoline (4-HQ), and inhibitors clorgyline hydrochloride (MAO-A) and R-deprenyl hydrochloride (MAO-B) were all purchased from Sigma-Aldrich. *N,N*-dimethyltryptamine (DMT) and its metabolite indole-3-acetic acid (IAA) monosodium salt were acquired from Lipomed and Cayman Chemical (Ann Arbor, USA), respectively.

Internal standards (ISTD) psilocin- d_{10} and IAA- d_2 were acquired from Sigma-Aldrich, while L-tryptophan- d_5 , tizanidine- d_4 , efavirenz- d_5 , paclitaxel- d_5 , flurbiprofen- d_3 , omeprazole- d_3 , metoprolol- d_6 , chlorzoxazone- d_3 , and midazolam- d_6 were obtained from TRC. DMT- d_6 was purchased from ReseaChem.

2.3 Metabolizing enzyme systems

Corning UltraPool human liver microsomes (HLM) 150 (20 mg/mL), human intestinal microsomes (HIM) pool (10 mg/mL) as well as recombinant human CYP enzymes (with P450 oxidoreductase, OR) including CYP1A2+OR (0.5 nmol), CYP2B6+OR (0.5 nmol), CYP2C8+OR (1.0 nmol), CYP2C9*1+OR (1 nmol), CYP2C19+OR (0.5 nmol), CYP2D6*1+OR (0.5 nmol), CYP2E1+OR + cytochrome b_5 (1 nmol), CYP3A4+OR + cytochrome b_5 (0.5 nmol), MAO-A (5 mg/mL), MAO-B (5 mg/mL), and UGT1A10 (5 mg/mL) were purchased from Corning Life Sciences B.V. (Amsterdam, Netherlands). All microsomes and recombinant enzyme solutions were aliquoted and stored at -80°C until further use. Co-factors including NADPH regenerating system solution A (25 mM NADP⁺, 66 mM glucose-6-phosphate, and 66 mM MgCl₂ in water), NADPH regenerating system solution B (40 U/mL glucose-6-phosphate dehydrogenase in 5 mM sodium citrate), UGT reaction mix solution A (25 mM uridine 5'-diphosphoglucuronic acid in water), and UGT reaction mix solution B (250 mM Tris-HCl, 40 mM MgCl₂, and 0.125 mg/mL alamethicin in water) were also obtained from Corning Life Sciences B.V.

2.4 Stocks and calibration standards

For psilocin, 4-HIAA, 4-HTP, 4-HQ, DMT, and CYP metabolites, calibration working solutions were prepared by serially diluting substance working mixes in a mix of equal parts

of water and acetonitrile (for psilocin, 4-HIAA, and 4-HTP) or DMSO (for 4-HQ, DMT, and CYP metabolites). Subsequently, each calibration working solution was diluted 1:100 in the matrix of interest, namely, 0.1 M potassium phosphate buffer (pH 7.4, K₂HPO₄ and KH₂PO₄ in water, 5:1 v/v) containing 1.5% BSA, pooled mouse plasma, or pooled human plasma to cover the desired concentration range. Specific calibration ranges for each analyte are depicted in [Supplementary Table S1](#).

2.5 Enzymatic inhibition assays

2.5.1 Cytochrome P450 inhibition

The CYP inhibition assay using HLM was previously described by Luethi et al. (Luethi et al., 2019) and was adapted herein. In brief, psilocin, 4-HIAA, 4-HTP, or CYP substrate stocks were mixed (1:100 dilution) with NADPH regeneration system solution A (1:20 dilution), NADPH regenerating system solution B (1:100 dilution), and with or without CYP inhibitors (1:100 dilution) in 0.1 M PBS (pH 7.4) supplemented with 1.5% BSA. The tubes were vortexed and placed on a Thermomixer (Eppendorf, Hamburg, Germany) at 300 rpm and 37°C. Next, 50 μL of the mixture from each tube was taken out as a baseline sample and transferred to a corresponding matrix tube containing 150 μL ice cold ISTD solution. Directly after, microsomes (1:100 dilution, end concentration 0.2 mg/mL) or recombinant CYP enzymes (1:40 dilution, end concentration 0.0125 nM or 0.025 nM depending on the enzyme) were added to each reaction tube to initiate the metabolic reaction. The total volume of the reaction mixture was 500 μL . The mixture was sampled at 0, 30, 60, 120, 180, 210, and 240 min for psilocin, 4-HIAA, and 4-HTP, and 0, 30, 60, 90, 120, 150, and 180 min for CYP substrates. Afterward, the matrix tubes were vortexed and centrifuged for 30 min at 3,220 \times g (Centrifuge 5810 R, Eppendorf). Samples were either directly analyzed by liquid chromatography tandem mass spectrometry (LC-MS/MS) or briefly stored at -20°C until analysis. The ISTD solution consisted of 20 ng/mL psilocin- d_{10} and 100 ng/mL tryptophan- d_5 in methanol. A separate ISTD solution was prepared in acetonitrile for CYP substrates containing 100 ng/mL of tizanidine- d_4 , efavirenz- d_5 , flurbiprofen- d_3 , omeprazole- d_3 , metoprolol- d_6 , chlorzoxazone- d_3 , midazolam- d_6 , and 250 ng/mL paclitaxel- d_5 .

2.5.2 Monoamine oxidase inhibition

The MAO inhibition assay was based on the assay described in [section 2.5.1](#) and performed identically if not otherwise stated. Psilocin, 4-HIAA, 4-HTP, or MAO substrate kynuramine were incubated with recombinant MAO-A enzymes (1:100 dilution, end concentration 0.05 mg/mL), recombinant MAO-B enzymes (1:100 dilution, end concentration 0.05 mg/mL), or HLM (1:100 dilution, end concentration 0.2 mg/mL), and with or without MAO isoform-selective inhibitors clorgyline (MAO-A and HLM) or R-deprenyl (MAO-B). Sampling time points for psilocin, 4-HIAA, 4-HTP, and control conditions were adjusted to 0, 60, 120, 180, 240, and 300 min for MAO-A and 0, 60, 120, 180, and 240 min for MAO-B assays. DMT was incubated with recombinant MAO-A or MAO-B and sampling timepoints were 0, 60, 120, 180, and 240 min. A

methanolic solution containing 5 ng/mL DMT-d₆ and 500 ng/mL IAA-d₂ was used as ISTD.

2.5.3 Glucuronidation

In vitro, glucuronidation of psilocin was assessed using HLM, HIM, and recombinant human UGT1A10 enzymes. The assay described in section 2.5.1 was adjusted to suit the glucuronidation system. Psilocin or control substrate OH-efavirenz was diluted 1:100 in 0.1 M PBS (pH 7.4) without BSA and UGT reaction mix solution A (1:20 dilution) and B (1:100 dilution) were added as co-factors. HLM were diluted as described in section 2.5.1, while HIM or UGT1A10 enzymes were diluted 1:40 (end concentration 0.5 and 0.125 mg/mL, respectively) in the reaction mix. Sampling time points were adjusted to 0, 15, 30, 60, 90, 120, 180, and 240 min.

2.6 Human 5-HT receptor interactions

2.6.1 5-HT receptor binding

Radioligand receptor binding assays of psilocin, 4-HIAA, and 4-HTP were assessed at the 5-HT_{1A}, 5-HT_{2A}, and 5-HT_{2C} receptors as previously described in detail by Luethi et al. (Luethi et al., 2018). In general, human embryonic kidney (HEK) 293 cell line membrane preparations overexpressing either the human 5-HT_{1A}, 5-HT_{2A}, or 5-HT_{2C} receptor were incubated briefly with respective radiolabeled ligands at concentrations equivalent to the dissociation constant (K_d). Radioligands used for the receptors included [3H]8-hydroxy-2-(dipropylamino) tetralin (8-OH-DPAT; 0.90 nM) for the 5-HT_{1A} receptor [3H]ketanserin (0.40 nM) for the 5-HT_{2A} receptor, and [3H]mesulergine (1.4 nM) for the 5-HT_{2C} receptor. Thereafter, the ligand's displacement by the substance of interest was measured. Specific binding to the target site was defined by subtracting the non-specific binding (measured in the presence of the receptor's respective competitor in excess) from the total binding measured. The following competitors were used including pindolol (10 μM) for the 5-HT_{1A} receptor, spiperone (10 μM) for the 5-HT_{2A} receptor, and mianserin (10 μM) for the 5-HT_{2C} receptor.

2.6.2 5-HT activation potency

Activation of 5-HT_{1A}, 5-HT_{2A}, and 5-HT_{2B} receptors by the psilocin metabolites 4-HIAA and 4-HTP was assessed by quantifying the accumulation of inositol monophosphate 1 (IP1) utilizing the Cisbio IP-One G_q Kit (Cisbio Bioassays SAS, Codolet, France) following the manufacturer's instructions. Psilocin and 5-HT were used as comparator and control substances, respectively. NIH/3T3 cells stably expressing the human 5-HT_{1A}, 5-HT_{2A}, and 5-HT_{2B} receptors were seeded at a density of 3,000 cells (5-HT_{1A} and 5-HT_{2A}) or 4,000 cells (5-HT_{2B}) in 384-well plates using Opti-MEM medium from Gibco (ThermoFisher, Life Technologies, Zug, Switzerland). Subsequently, the test compounds were introduced, and the plates were incubated for 90 min at 37°C, followed by a 60 min incubation with Anti-IP1-Cryptate and IP1-d₂ at room temperature. The formation of stimulated IP1 was quantified by homogeneous time-resolved fluorescence (HTRF) measurements using a BioTek Synergy H1 microplate reader (Agilent Technologies, Basel, Switzerland). The obtained raw data for receptor activation were subjected to normalization, wherein the

baseline signal was set at 0%, and the maximum signal stimulated by 5-HT at the specific receptor was established as 100%.

2.7 Mouse study samples

C57BL/6J adult male mice (Janvier, Le Genest-Saint-Isle, France) were maintained in littermate pairs in standard cages (containing sawdust, a sleeping chamber, tissue paper, and a wood stick) with water and pellet food available *ad libitum*. The colony room was on a reversed light-dark cycle (dark phase 07:00 to 19:00) with temperature at 22°C and humidity at 50–60%. A total of 10 mice were dosed orally with either 3 mg/kg bodyweight psilocybin (n = 5) or saline solution (n = 5). Dosing and blood sampling were conducted between 09:00 and 13:00. The mouse was placed in a plastic restrainer with the tail protruding through a hole in the end of the tube. The tail was immersed in warm water for 1 min for vasodilation and then a small incision was made on the lateral tail surface near the distal tip. 50 μL of blood was massaged gently into an EDTA-coated capillary blood tube (Mircovette, Sarstedt, Nümbrecht, Germany). The first (baseline) blood sample was collected directly before compound administration via oral gavage and the mouse was then returned to the home cage. Further blood samples were collected at 15, 30, 60, and 120 min post-treatment. Each sample was drawn from the same incision site, with mice maintained in the home cage in the intervening periods. The blood samples were stored on ice and centrifuged for 10 min at 780 × g and 4°C. Subsequently, the plasma was transferred into cryotubes (Protein LoBind, Eppendorf) and stored at –80°C until analysis. All procedures were conducted under a permit for animal experimentation (ZH038/2022) issued by the Veterinary Office Zurich in accordance with the Animal Protection Act (1978) of Switzerland. The use of psilocybin was authorized by the Federal Office of Public Health (FOPH).

Deglucuronidation of psilocin and 4-HIAA in the plasma samples and thus determination of the conjugated metabolite fraction was performed according to a previously described method by Kolaczynska et al. (Kolaczynska et al., 2021) and adapted to the low plasma volumes available.

Pharmacokinetic parameters were calculated using Phoenix WinNonlin software (version 8.1.0, Certara, Princeton, USA). The elimination half-life ($t_{1/2}$, min) was assessed as $t_{1/2} = \ln(2)/\lambda$, while the elimination constant was calculated by linear regression in the terminal elimination phase. The maximal plasma concentration (C_{max} , ng/mL) and the time to reach this concentration (t_{max} , h) were direct read-outs of the graphical plots.

2.8 Human study samples

A subset (n = 5) of pharmacokinetic study samples from a published double-blind, placebo-controlled, crossover study by Holze et al. (Holze et al., 2022b) was reanalyzed for psilocybin metabolites. The clinical study was approved by the ethics committee of Northwestern and Central Switzerland (EKNZ) and registered at clinicaltrials.gov (ID: NCT03604744). The study was executed according to the Declaration of Helsinki and the International Conference of Harmonization for Good Clinical

Practice guidelines. Participants received an oral dose of 30 mg psilocybin and 19 blood samples were drawn in lithium heparin-coated S-Monovette tubes (Sarstedt) over a duration of 24 h post-treatment. Subsequently, blood samples were centrifuged at $1,811 \times g$ for 10 min to yield the plasma. Samples were stored at -80°C before analysis by LC-MS/MS.

2.9 Human study samples for genotyping

Human plasma samples for genotyping were obtained from two clinical studies, which were approved by the ethics committee of Northwestern and Central Switzerland (EKNZ) and registered at clinicaltrials.gov (ID: NCT03604744 and NCT04227756). The studies were published by Holze et al. (Holze et al., 2022b) and Ley et al. (Ley et al., 2023), respectively. Demographic data of the studies are displayed in Supplementary Table S4. Genomic DNA was extracted from whole blood using the QIAamp DNA Blood Mini Kit (Qiagen, Hombrechtikon, Switzerland) and an automated QIAcube system. SNP genotyping was performed using commercial TaqMan SNP genotyping assays (LuBio Science, Lucerne, Switzerland). We assayed the following SNPs and respective alleles: CYP2D6*3 (rs35742686, assay: C_32407232_50), CYP2D6*4 (rs3892097, assay: C_27102431_D0, and rs1065852, assay: C_11484460_40), CYP2D6*6 (rs5030655, assay: C_32407243_20), CYP2D6*9 (rs5030656, assay: C_32407229_60), CYP2D6*10 (rs1065852), CYP2D6*17 (rs28371706, assay: C_2222771_A0, and rs16947, assay: C_27102425_10), CYP2D6*29 (rs59421388, assay: C_3486113_20), and CYP2D6*41 (rs28371725, assay: C_34816116_20, and rs16947). CYP2D6 gene deletion (allele *5) and duplication/multiplication (allele *xN) were determined using a TaqMan Copy Number Assay (Hs04502391_cn). Activity scores for CYP2D6 were assigned according to established guidelines (Gaedigk et al., 2008; Crews et al., 2012; Hicks et al., 2013; Hicks et al., 2015; Caudle et al., 2020). The classification into different genotypes was as follows: poor metabolizer (PM, activity score = 0), intermediate metabolizer (IM, activity score = 0.5–1), extensive metabolizer (EM, activity score = 1.5–2), and ultra-rapid metabolizer (UM, activity score > 2).

2.10 LC-MS/MS instrumentation and settings

A modular high-performance liquid chromatography (HPLC) system (Shimadzu, Kyoto, Japan) with four pumps (A, B, C, and D) connected to an API 4000 QTRAP or an API 5000 tandem mass spectrometer (AB Sciex, Ontario, Canada) was used to separate and quantify the analytes of interest. Different analytical methods were applied to detect either psilocin and metabolites, CYP metabolites, UGT metabolites, or MAO metabolites. Specific parameters, mass transitions, and retention times of all analytes are summarized in Supplementary Table S1.

The method to analyze psilocin and related metabolites was previously described in detail and adapted from Kolaczynska et al. (Kolaczynska et al., 2021). Analytes were separated on a Symmetry C18 column ($3.5 \mu\text{M}$, $4.6 \times 75 \text{ mm}$, Waters, Milford, USA) using water supplemented with 0.1% formic acid and methanol

supplemented with 0.1% formic acid as mobile phases A and B, respectively. The method was expanded to also include 4-HTP, oxidized psilocin (m/z 221.0), and norpsilocin (m/z 191.0). 4-HTP and 4-HIAA eluted simultaneously but were detected in the positive and negative mode, respectively. Thus, each sample was analyzed by positive and negative ionization.

For the detection of 4-HQ, the same column and mobile phases were used as for psilocin. However, the method's flow rate and time program were adapted. In brief, the injected sample ($2.5 \mu\text{L}$) was transported using 10% mobile phase B at a 0.2 mL/min flow rate onto the analytical column. In the first, 0.5 min of each run, the sample was mixed with mobile phase A (0.6 mL/min) within a T-union positioned in front of the analytical column. The total flow rate was then increased to 0.8 mL/min and maintained at this rate until the end of the run (0.5–4.5 min). The concentration of mobile phase B was increased linearly to 95% between 0.5 and 3.0 min and held at this concentration for 1.0 min. For the last 0.5 min, the column was reconditioned with 10% mobile phase B. The HPLC was only connected to the tandem mass spectrometer from 1.0 to 3.0 min and otherwise directly to the waste. 4-HQ and tryptophan- d_5 (ISTD) were measured by multiple reaction monitoring (MRM) in the positive ionization mode. The mass transitions of tryptophan- d_5 were summed to improve sensitivity.

The CYP metabolites were quantified by the method of Luethi et al. (Luethi et al., 2019). In brief, the analytes were separated on an Atlantis T3 column ($3 \mu\text{M}$, $3.0 \times 50 \text{ mm}$, Waters). Mobile phase A consisted of water and 0.1% formic acid for positive and negative ionization modes. Mobile phase B in the positive ionization mode consisted of acetonitrile and 0.1% formic acid, while pure acetonitrile was used for analysis in the negative ionization mode.

MAO substrate DMT and its metabolite IAA were analyzed using the bioanalytical method published by Luethi et al. (Luethi et al., 2022). Analyte separation was conducted using a Luna PFP(2) analytical column ($3.0 \mu\text{M}$, $2 \times 50 \text{ mm}$, Phenomenex). Water and methanol, both supplemented with 0.1% formic acid, served as mobile phases A and B, respectively.

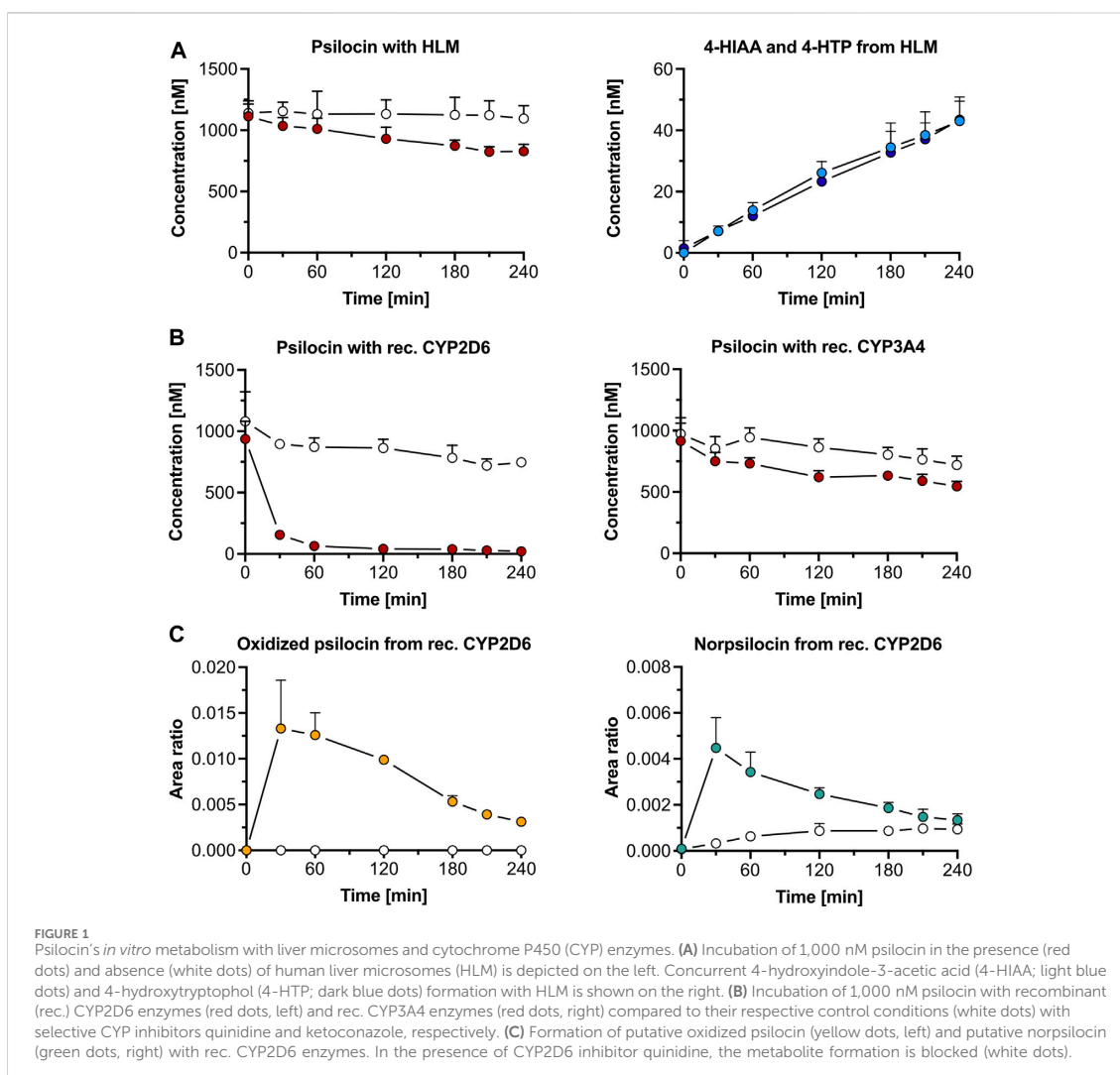
The LC-MS/MS system was operated using Analyst software (version 1.7, AB Sciex) and the data were analyzed with MultiQuant software (version 3.0.3, AB Sciex).

3 Results

3.1 *In vitro* metabolism and receptor interactions

3.1.1 Human liver microsomes

In the presence of HLM, psilocin concentration (mean \pm standard deviation, SD) decreased by 29% from $1,162 \pm 146 \text{ nM}$ to $829 \pm 32 \text{ nM}$ after 240 min incubation of $1,000 \text{ nM}$ psilocin (Figure 1A). Simultaneously, minor increases in 4-HIAA ($43.0 \pm 7.9 \text{ nM}$) and 4-HTP ($43.4 \pm 6.0 \text{ nM}$) concentrations were observed (Figure 1A). In the absence of HLM, no relevant decrease in psilocin concentration ($t = 0 \text{ min}$, $1,141 \pm 74 \text{ nM}$; $t = 240 \text{ min}$, $1,096 \pm 105 \text{ nM}$), and no metabolite formation was seen (Figure 1A). Targeted inhibition of specific CYP enzymes present in HLM did not lead to a clear inhibition of psilocin degradation (Supplementary Figure S1). However, CYP-selective substrates, employed as control



substances, were metabolized into their corresponding hydroxylated metabolites in the absence of CYP-specific inhibitors. In the presence of CYP-specific inhibitors, these reactions were inhibited (Supplementary Figure S2).

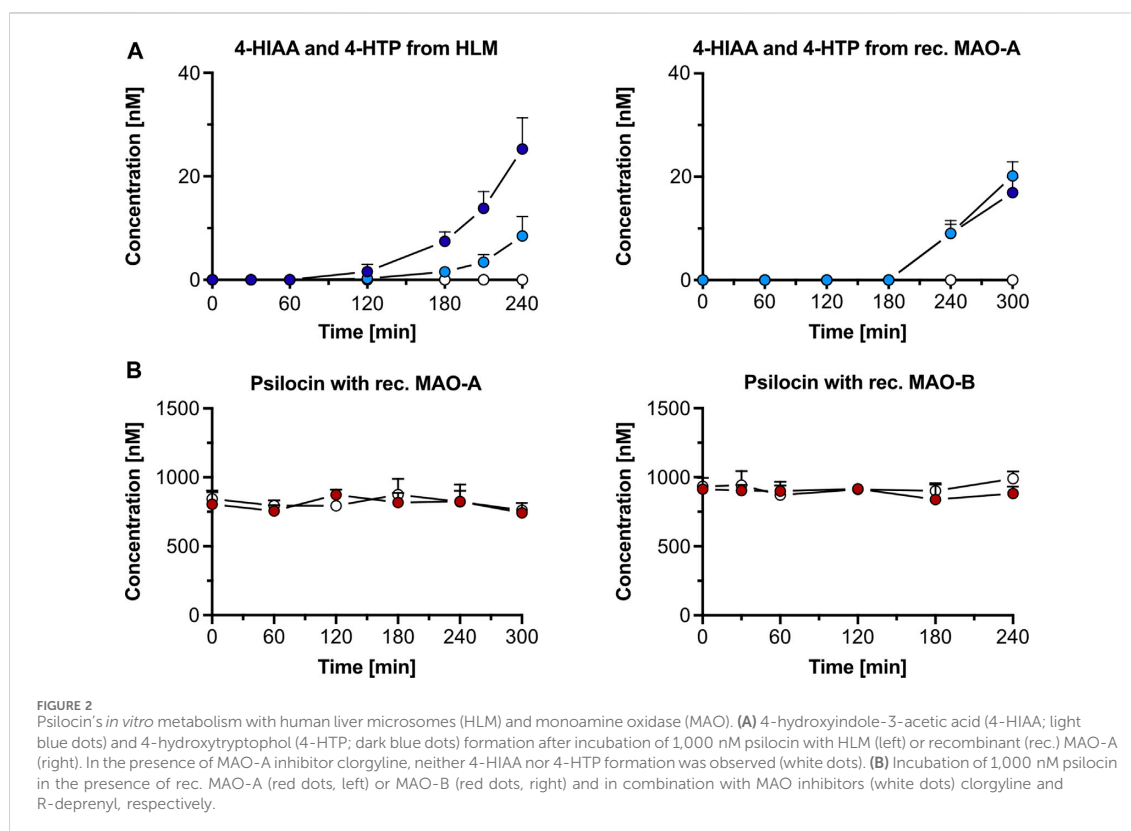
3.1.2 Recombinant cytochrome P450 enzymes

Recombinant CYP2D6 enzymes extensively metabolized 1,000 nM psilocin (mean \pm SD) over 240 min ($t = 0$ min, 937 ± 145 nM; $t = 240$ min, 21.1 ± 14.2 nM). This reaction was inhibited in the presence of quinidine, a selective CYP2D6 inhibitor ($t = 0$ min, $1,081 \pm 241$ nM; $t = 240$ min, 747 ± 30 nM) (Figure 1B). With recombinant CYP3A4 enzymes, psilocin concentration decreased by 40% ($t = 0$ min, 916 ± 145 nM; $t = 240$ min, 546 ± 41 nM). In the presence of the CYP3A4 inhibitor ketoconazole, this reaction was partially blocked as only 26% of psilocin was metabolized ($t = 0$ min, 973 ± 133 nM; $t = 240$ min, 720 ± 71 nM) (Figure 1B). Formation of

4-HIAA or 4-HTP was neither observed in the presence of recombinant CYP2D6 nor with CYP3A4 enzymes.

Two putative minor metabolites, an oxidized psilocin metabolite (m/z 221.0 \rightarrow 176.0 Da) and norpsilocin (m/z 191.0 \rightarrow 160.0 Da), were formed by CYP2D6 (Figure 1C; Supplementary Table S1). The signal intensity (area ratio) of both, oxidized psilocin ($t = 30$ min, 0.013 ± 0.005 counts; $t = 240$ min, 0.0030 ± 0.0003 counts) and norpsilocin ($t = 30$ min, 0.004 ± 0.001 counts; $t = 240$ min, 0.0010 ± 0.0003 counts), peaked after 30 min and declined again by 240 min. Co-incubation with the CYP2D6 inhibitor quinidine resulted in reduced and delayed formation of norpsilocin, whereas no oxidized psilocin metabolite was detected (Figure 1C).

Furthermore, other recombinant CYPs (1A2, 2B6, 2C8, 2C9, 2C19, and 2E1) did not metabolize psilocin and, consequently, no production of metabolites was observed (Supplementary Figure S3). In the control assays, CYP-specific substrates were metabolized to



their respective hydroxylated metabolites. These reactions were inhibited in the presence of CYP-specific inhibitors (Supplementary Figure S4).

3.1.3 Monoamine oxidases

3.1.3.1 Monoamine oxidase A inhibition in human liver microsomes

Incubation of psilocin (1,000 nM) with HLM and the MAO-A selective inhibitor clorgyline led to complete inhibition of 4-HIAA and 4-HTP formation. Minimal amounts (mean \pm SD) of 4-HIAA ($t = 240$ min, 8.5 ± 3.8 nM) and 4-HTP ($t = 240$ min, 25.3 ± 6.0 nM) were observed after incubation with HLM alone (Figure 2A). However, in this assay, psilocin concentration did not visibly decrease when incubated with HLM (Supplementary Figure S5A). Furthermore, incubation of 4-HIAA or 4-HTP with HLM did not lead to any biotransformation (Supplementary Figure S5B).

In the control condition, the non-specific MAO substrate kynuramine was readily metabolized to 4-HQ ($t = 240$ min, $1,974 \pm 302$ nM) in the presence of HLM. 4-HQ production was inhibited when incubated with the MAO inhibitor clorgyline ($t = 240$ min, 347 ± 67 nM) (Supplementary Figure S5A).

3.1.3.2 Recombinant monoamine oxidase A and B

Psilocin incubation (1,000 nM) with recombinant MAO-A and MAO-B enzymes did not visibly decrease its concentration (Figure 2B). However, a minor increase in 4-HIAA ($20.1 \pm$

2.8 nM) and 4-HTP (16.9 ± 2.9 nM) concentration was observed after incubation for 300 min with recombinant MAO-A enzymes (Figure 2A). In the presence of the MAO-A inhibitor clorgyline, the formation of both metabolites was inhibited (Figure 2A). Incubation of psilocin with MAO-B did not produce any 4-HIAA or 4-HTP (Supplementary Figure S5C).

In the control conditions, kynuramine was metabolized by MAO-A ($t = 0$ min, $135,200 \pm 23,816$ counts; $t = 300$ min, $48,503 \pm 12,251$ counts) and MAO-B ($t = 0$ min, $82,853 \pm 11,336$ counts; $t = 240$ min, $9,533 \pm 8,311$ counts). Formation of the metabolite 4-HQ was observed with MAO-A ($t = 300$ min, $2,694 \pm 264$ nM) and MAO-B ($t = 240$ min, $4,692 \pm 891$ nM) (Supplementary Figure S5D). The concentration of the MAO substrate DMT decreased when incubated with recombinant MAO-A enzymes ($t = 0$ min, 907 ± 31 nM; $t = 240$ min, 110 ± 29 nM), and its metabolite IAA was formed ($t = 240$ min, 30.3 ± 4.2 nM). The decrease in DMT concentration was almost completely inhibited by clorgyline ($t = 0$ min, 915 ± 11 nM; $t = 240$ min, 853 ± 69 nM), and no IAA was detected (Supplementary Figure S6A). DMT only marginally decreased with recombinant MAO-B ($t = 0$ min, 940 ± 47 nM; $t = 240$ min, 816 ± 56 nM), and small amounts of IAA were formed ($t = 240$ min, 11.5 ± 4.5 nM). R-deprenyl inhibited the metabolic decrease of DMT with MAO-B ($t = 0$ min, 954 ± 73 nM; $t = 240$ min, $1,008 \pm 58$ nM), and no IAA was observed (Supplementary Figure S6B).

3.1.4 Glucuronidation

3.1.4.1 Human liver microsomes and human intestinal microsomes

No glucuronidation was observed when psilocin (1,000 nM) was incubated with HLM, while incubation with HIM led to a decrease in concentration (mean \pm SD) of 37% after 240 min ($t = 0$, 1,085 \pm 157 nM; $t = 240$, 684 \pm 53 nM) through glucuronidation (Supplementary Figure S7A). In the absence of HIM, only a minor psilocin decrease was observed ($t = 0$, 980 \pm 77 nM; $t = 240$, 893 \pm 91 nM) (Supplementary Figure S7A).

In the control condition, HIM glucuronidated 99% of OH-efavirenz over 240 min ($t = 0$, 45,300 \pm 5,766 counts; $t = 240$ min, 470 \pm 394 counts) (Supplementary Figure S7B).

3.1.4.2 Recombinant UDP-glucuronosyl transferase 1A10

Psilocin concentration (1,000 nM, mean \pm SD) remained stable over 240 min in the presence of recombinant UGT1A10 enzymes ($t = 0$ min, 1,029 \pm 60 nM; $t = 240$ min, 979 \pm 95 nM) (Supplementary Figure S7A). Similar findings were observed when psilocin was incubated in the absence of UGT1A10 ($t = 0$, 980 \pm 77 nM; $t = 240$, 893 \pm 91 nM) (Supplementary Figure S7A). However, in the control condition, UGT1A10 glucuronidated 98% of OH-efavirenz over 240 min ($t = 0$, 41,700 \pm 10,936 counts; $t = 240$ min, 1,007 \pm 155 counts) (Supplementary Figure S7B).

3.1.5 5-HT receptor interactions

The interactions of psilocin, 4-HIAA, and 4-HTP with human 5-HT_{1A}, 5-HT_{2A}, 5-HT_{2B}, and 5-HT_{2C} receptors are summarized in Supplementary Table S2. Psilocin exhibited high binding affinity at the 5-HT_{1A}, 5-HT_{2A}, and 5-HT_{2C} receptors ($K_i < 136$ nM), especially at the 5-HT_{2A} receptor ($K_i = 41.1 \pm 8.9$ nM). In contrast to psilocin, the metabolites 4-HIAA and 4-HTP exhibited no relevant affinity to the examined 5-HT receptors ($K_i > 10,000$ nM). Binding at the human 5-HT_{2B} receptor was not assessed.

Psilocin showed high activation potency at the 5-HT_{1A} ($EC_{50} = 1.7 \pm 2.4$ nM), 5-HT_{2A} ($EC_{50} = 35.4 \pm 9.7$ nM), and 5-HT_{2B} ($EC_{50} = 21.5 \pm 178$ nM) receptor. 4-HIAA and 4-HTP exhibited no relevant activation at the 5-HT_{1A}, 5-HT_{2A}, and 5-HT_{2B} receptor ($EC_{50} > 10,000$ nM). The activation potency at the human 5-HT_{2C} receptor was not assessed.

3.2 *In vivo* pharmacokinetics and metabolism

3.2.1 Pharmacokinetics and metabolites in mice

The average maximal plasma concentration (C_{max} , mean \pm SD) of psilocin was 198 \pm 28 ng/mL after 0.30 \pm 0.11 h (t_{max} , mean \pm SD), while the mean C_{max} of psilocin-O-glucuronide was 2.6-fold higher (521 \pm 57 ng/mL) and peaked at 0.35 \pm 0.14 h (Figure 3A; Supplementary Table S3). 4-HIAA reached a C_{max} of 84.9 \pm 17.7 ng/mL, whilst 4-HIAA-glucuronide displayed a C_{max} of 30.0 \pm 6.7 ng/mL. The t_{max} of 4-HIAA and 4-HIAA-glucuronide was 0.30 \pm 0.11 h and 0.45 \pm 0.11 h, respectively (Figure 3B; Supplementary Table S3). The observed elimination half-life ($t_{1/2}$, mean \pm SD) of psilocin and psilocin-O-glucuronide was similar (0.91 \pm 0.11 h and 0.97 \pm 0.06 h, respectively). 4-HIAA displayed a

slightly shorter $t_{1/2}$ of 0.75 \pm 0.11 h, while $t_{1/2}$ for 4-HIAA-glucuronide was 1.38 \pm 0.27 h (Supplementary Table S3).

In addition to psilocin, 4-HIAA, and their conjugated metabolites, two minor psilocybin metabolites were observed. The oxidized psilocin metabolite had a retention time of 2.11 min and a t_{max} of approximately 0.5 h in mice (Figure 3C). On the other hand, a demethylated psilocin metabolite, likely norpsilocin, with a retention time of 2.14 min was observed (Figure 3D). The peak area of putative norpsilocin increased over time with a t_{max} at approximately 0.25 h post-treatment (Figure 3D). Neither of the aforementioned metabolites was present in blank mouse plasma. Also, psilocybin metabolite 4-HTP could not be observed in the analyzed mouse plasma samples.

3.2.2 Pharmacokinetics and metabolites in human

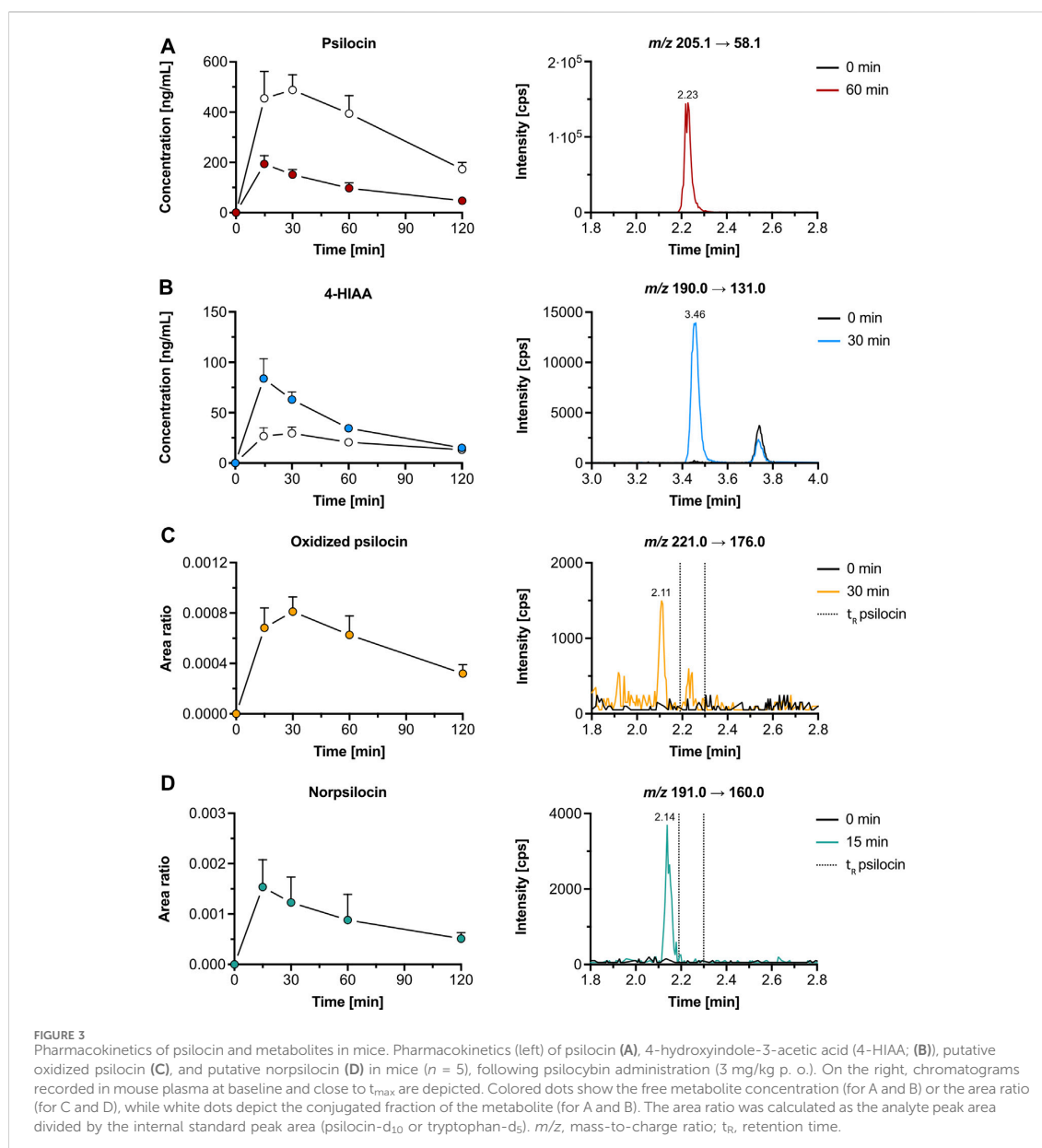
We reanalyzed psilocybin's pharmacokinetics in samples of five participants from a study by Holze et al. to assess the presence of the metabolites that we detected *in vitro* (Holze et al., 2022a). In human plasma samples, both psilocin and 4-HIAA reached t_{max} at around 2.5 h post-treatment. Their chromatographic retention was 2.26 min and 3.51 min, respectively (Figures 4A,B). Furthermore, the CYP2D6 genotype did not alter the plasma concentration of free psilocin (Supplementary Figure S8).

Additionally, we were able to detect an oxidized psilocin metabolite with a retention time of 2.11 min (Figure 4C). The metabolite reached t_{max} at 5 h and no signal was present in blank human plasma. Moreover, neither norpsilocin nor 4-HTP was detected in human samples.

4 Discussion

In the present study, we elucidated psilocybin's metabolic pathways *in vitro* by incubating psilocin with a range of human metabolic enzymes, as well as *in vivo* in mice and humans. In addition, we tested the 5-HT receptor binding affinity and activation potency of psilocin and some of its major metabolites. We observed that psilocin is metabolized by HLM and MAO-A to 4-HIAA and 4-HTP. Minor formation of psilocin-O-glucuronide was observed in HIM, but not with recombinant UGT1A10. The putative minor metabolites, norpsilocin, and oxidized psilocin, were formed by human recombinant CYP2D6. In contrast to *in vitro* observations, humans and mice showed significant psilocin glucuronidation and formation of 4-HIAA but not 4-HTP. We confirmed that putative oxidized psilocin was present in both species, while putative norpsilocin was observed solely in mice. Psilocin interacted with 5-HT_{1A}, 5-HT_{2A}, 5-HT_{2B}, and 5-HT_{2C} receptors in the nanomolar range, while the metabolites 4-HIAA and 4-HTP showed no relevant interaction.

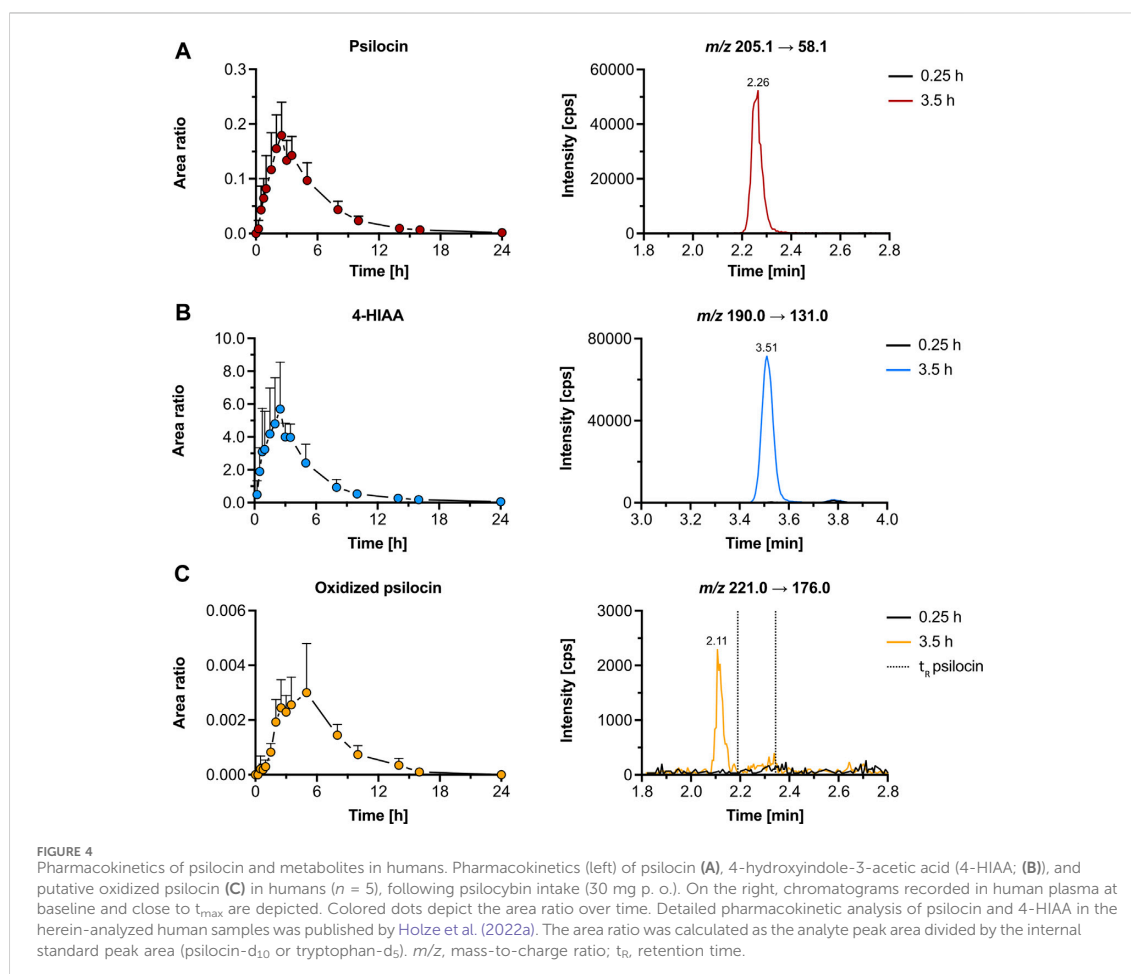
Based on our findings and the research of others, we propose a metabolic pathway for psilocybin as outlined in Figure 5. Psilocybin is rapidly dephosphorylated to psilocin by alkaline phosphatases and non-specific esterases in the intestines, kidneys, and probably also in the blood circulation (Hasler et al., 1997; Dinis-Oliveira, 2017). In mice, a competitive alkaline phosphatase substrate can occupy most of the enzyme and prevent the conversion of the prodrug psilocybin to psilocin (Horita, 1963). Studies in rats have shown that psilocybin probably undergoes a complete transformation to psilocin before



being absorbed and distributed in the blood circulation (Eivindvik et al., 1989). In accordance with these findings, we did not detect psilocybin in the plasma of humans or mice. The plasma elimination half-life of psilocin in humans is approximately 2 h, while mice metabolize psilocin at double this rate, resulting in a half-life of around 0.9 h. Therefore, psilocin is extensively metabolized and can undergo several metabolic reactions.

A major part of psilocin is glucuronidated to psilocin-O-glucuronide and is excreted via urine in the first 24 h. In clinical studies, plasma concentrations of conjugated psilocin were around 4-fold higher than concentrations of free psilocin (Holze et al.,

2022a). The half-life of psilocin-O-glucuronide in humans is around 4 h, while in mice it was approximately 4-fold lower (~1 h) (Holze et al., 2022a). Manevski et al. reported that UGT1A10 has the highest glucuronidation activity for psilocin, while UGT1A9 may also be a main contributor due to its high expression in the liver (Manevski et al., 2010). Contrary to those findings, our *in vitro* glucuronidation systems were not able to recreate the extensive *in vivo* glucuronidation of psilocin. Although the positive control OH-efavirenz was readily glucuronidated, only minor amounts of psilocin were transformed into the conjugated compound by HIM and no visible transformation was observed with

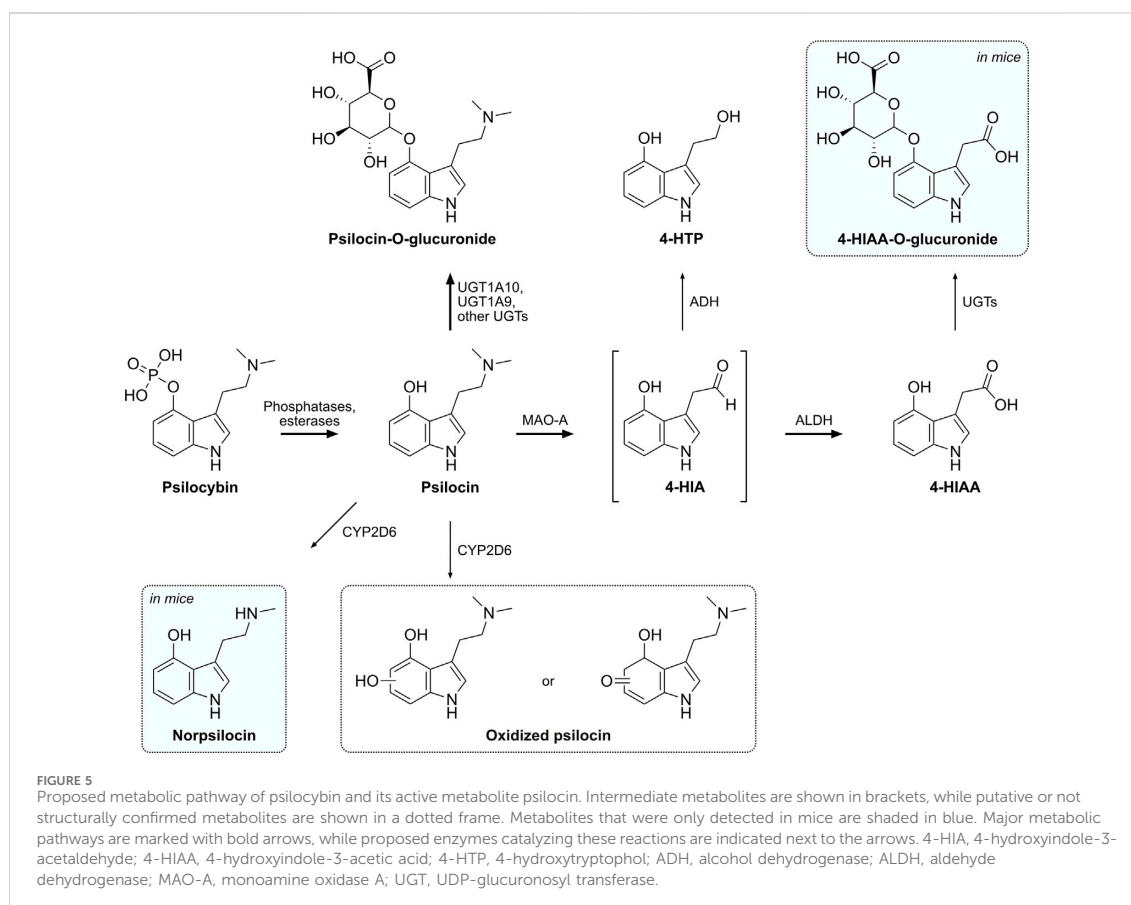


recombinant UGT1A10. Therefore, using more complex systems like primary hepatocytes or human spheroid three-dimensional models might be more suitable to investigate *in vivo* phase II metabolism of psilocybin (Ooka et al., 2020).

Psilocin undergoes another major oxidative metabolic pathway similar to the structurally related monoamine neurotransmitter 5-HT (Svensson et al., 1999). MAO enzymes metabolize the tertiary amino group of psilocin to yield the intermediate aldehyde 4-HIA (Hasler et al., 1997). 4-HIA is then rapidly metabolized to either 4-HIAA or 4-HTP (Hasler et al., 1997; Becker et al., 2022). Recombinant MAO-A enzymes as well as HLM were able to produce minor amounts of 4-HIAA and 4-HTP *in vitro*, while selective MAO-A inhibitors reduced this reaction. Neither MAO-B nor any of the assessed CYP enzymes produced 4-HIAA or 4-HTP, suggesting that only MAO-A is involved. However, since MAO-A likely only catalyzes the production of the intermediate 4-HIA, major amounts of 4-HIAA and 4-HTP might only be produced when functional ALDH or ADH enzymes are also present, similar to 5-HT's metabolism (Svensson et al., 1999; Dinis-Oliveira, 2017). Moreover, careful interpretation of the produced amounts is advised, considering that DMT, a substance well-documented to

be rapidly metabolized by MAO *in vivo*, exhibited only slow metabolism *in vitro*, thus resulting in only minor amounts of its metabolite IAA (Luethi et al., 2022; Vogt et al., 2023). Interestingly, although reported before in other studies (Horita, 1963; Hasler et al., 1997), 4-HTP was neither detected in humans nor in mice but only *in vitro* with HLM. Most likely 4-HTP is either rapidly metabolized in humans and mice or not produced at all.

Minor interspecies differences were detected when comparing the results of human with mouse samples. In humans, 4–5-fold higher maximal concentrations of 4-HIAA were found compared to psilocin (Holze et al., 2022a; Becker et al., 2022), while the concentrations in mice were 2-fold lower compared to psilocin. The elimination half-life of 4-HIAA in mice (0.75 h) was more than 2-fold shorter than in humans. Moreover, 4-HIAA is most likely glucuronidated in mice whilst in human samples there was no evidence of glucuronidated 4-HIAA. Although 4-HIAA possesses several glucuronidation sites, we suggest that it undergoes a similar metabolic reaction as 4-hydroxyindole and psilocin in humans to form the O-glucuronide (Manevski et al., 2010). The O-glucuronidation of 4-hydroxyindole in humans is mainly catalyzed by UGT1A6 and UGT1A9 which also could play an



important role in this pathway (Manevski et al., 2010). Alternatively, 4-HIAA could undergo acyl-glucuronidation, to form an unstable acyl-glucuronide, or N-glucuronidation (Regan et al., 2010; Kaivosaaari et al., 2011).

Out of the eight assessed CYP enzymes, only CYP2D6 and CYP3A4 showed a relevant metabolic activity, suggesting that CYP1A2, 2B6, 2C8, 2C9, 2C19, and 2E1 are unlikely to be involved in psilocybin's metabolism. Neither 4-HIAA nor 4-HTP formation could be observed with any of the CYP enzymes, confirming that CYPs are not involved in these metabolic pathways. Psilocin can, however, continue to follow another minor metabolic pathway that may be of relevance in the presence of MAO inhibitors (e.g., antidepressants). Several studies suggested a minor oxidative metabolite with an *o*-quinone or iminoquinone structure produced by, e.g., ceruloplasmin, cytochrome oxidases, or non-enzymatically by Fe³⁺ (Blaschko and Levine, 1960; Horita and Weber, 1961b; Horita, 1963; Kovacic, 2009). We hypothesized that CYP enzymes might be involved in this step and investigated this *in vitro*. CYP3A4 showed minor activity in metabolizing psilocin, however, no previously described metabolite could be identified. Estimating the extent of the contribution of CYP3A4 in psilocin's metabolism is challenging. Although our data implies CYP3A4 involvement, additional

investigation is necessary for a more accurate assessment. CYP2D6 was more active than CYP3A4 as it rapidly and completely metabolized psilocin. Subsequently, oxidized psilocin, potentially a quinone-type structure like psilocin iminoquinone (e.g., 4-hydroxy-5-oxo-*N,N*-dimethyltryptamine) or psilocin hydroquinone (e.g., 4,5-hydroxy-*N,N*-dimethyltryptamine) has been detected following incubation of psilocin with CYP2D6. Afterward, the compound has also been detected in human and mouse plasma. This metabolite might have been described as a psilocybin metabolite in mammalian tissue homogenates, but never before in humans (Horita and Weber, 1961b; Horita, 1963; Dinis-Oliveira, 2017). Based on the parent mass of 220.0 Da and the observed fragmentation pattern in the mass spectrometer (m/z 221.0 \rightarrow 176.0 Da), we can postulate that this metabolite possesses an additional oxygen atom on the benzene ring of the indole moiety. However, the exact position of the oxygen cannot be determined solely with tandem mass spectrometry. We can also not exclude that there are several different metabolites present with different hydroxylation or oxidation sites on the indole ring. Similar metabolic findings have been made for structurally related synthetic tryptamines (Bergh et al., 2024). An *o*-quinone structure as proposed by Dinis-Oliveira et al. can be ruled out since this metabolite would have a different molecular weight

(218.0 Da) than the metabolite observed in our experiments (Dinis-Oliveira, 2017). Further structural analysis is needed to elucidate the elemental formula and exact position of the oxygen atom.

In addition, another psilocin metabolite was identified in the CYP2D6 assay and subsequently in mouse plasma. The metabolite possesses a molecular mass of 190.0 Da and therefore most likely corresponds to norpsilocin (*N*-methyl-4-hydroxytryptamine). The fragments observed in the mass spectrometer (m/z 191.0 \rightarrow 160.0 Da) suggest that the compound arises through demethylation of the tertiary amine of psilocin. Interestingly, norpsilocin could not be detected in human plasma samples. To the best of our knowledge, this metabolite has not been observed before as a product of psilocybin's metabolism, but rather as a synthesis or metabolic product of baecocystin, a demethylated analog of psilocybin, present in hallucinogenic mushrooms of the *Psilocybe* genus (Lenz et al., 2017; Sherwood et al., 2020). Norpsilocin was previously suspected to exert psychoactive effects similar to psilocin. It is nearly a full agonist at the mouse and human 5-HT_{2A} receptor in G_q-dependent calcium flux assays (EC₅₀ < 10 nM) but interestingly did not show any psychoactive properties in head-twitch response experiments with mice (Sherwood et al., 2020). This may be due to the inability to cross the blood-brain barrier or rapid degradation of the secondary amine group (Sherwood et al., 2020; Sherwood et al., 2024). Nevertheless, further analysis with NMR or high-resolution mass spectrometry is needed to confirm the structure of this minor psilocin metabolite. Interestingly, the reduction in psilocin concentration observed with CYP2D6 can probably not be solely attributed to an oxidative metabolite or norpsilocin. This suggests the possibility of additional, unidentified metabolites being present.

Furthermore, we showed that genetically determined CYP2D6 activity did not change exposure to psilocin in humans. Thus, CYP2D6 might not be considered to be critically involved in the main metabolism of psilocin in humans and any between-individual differences in CYP2D6 activity are unlikely to influence the response to psilocin in humans. However, the significance of this data may be constrained by the limited number of samples examined. Nevertheless, these preliminary results could have direct clinical implications for psilocybin-assisted therapy and contrast with LSD and MDMA, wherein poor CYP2D6 function significantly increases exposure to these substances and enhances the acute effects (Schmid et al., 2016; Vizeli et al., 2021).

In general, there are only limited data available on the activity of psilocybin's metabolites at the human 5-HT receptors. Here, psilocin showed sub-micromolar receptor binding affinity at human 5-HT_{1A} (128 \pm 33 nM), 5-HT_{2A} (41.1 \pm 8.9 nM), and 5-HT_{2C} (136 \pm 35 nM) receptors, confirming the results of Rickli et al. (Rickli et al., 2016). Psilocin further showed sub-micromolar activation potencies at the 5-HT_{1A}, 5-HT_{2A}, and 5-HT_{2B} receptors (<74.5 \pm 6.0 nM). However, neither 4-HIAA nor 4-HTP displayed relevant binding affinity at the 5-HT_{1A}, 5-HT_{2A}, and 5-HT_{2C} receptors (K_i > 10,000 nM) and also no receptor activation potency at the 5-HT_{1A}, 5-HT_{2A}, and 5-HT_{2B} receptors (EC₅₀ > 10,000 nM). The inactivity of these metabolites at the human 5-HT receptors indicates that they are not involved in exerting the psychoactive effects in humans, which is in line with the time course of the subjective effects observed in clinical studies (Holze et al., 2022a). The herein-detected oxidative psilocin metabolite

has so far not been investigated at human 5-HT receptors due to its uncertain structure.

5 Conclusion

In conclusion, this comprehensive study explored the metabolic pathways of psilocin both *in vitro* and *in vivo* and provides new evidence of involved enzymes. In total, we were able to detect six psilocin metabolites. While confirming the glucuronidation of psilocin *in vivo*, we also detected apparent interspecies differences with the glucuronidation of 4-HIAA and the presence of putative norpsilocin in mice compared with humans. While MAO-A was identified as a key enzyme responsible for psilocin's oxidative transformation to 4-HIAA and 4-HTP, the additional roles of ALDH and ADH still have to be investigated. CYP2D6 and CYP3A4 seem to be involved to a minor extent in psilocin's metabolism. CYP2D6 produced norpsilocin and a structurally unresolved oxidized metabolite. However, no metabolite was identified with CYP3A4, requiring further investigation into the extent of its role in psilocin's metabolism. The herein-employed *in vitro* assays assisted in unraveling the metabolism of psilocin but were unable to closely reproduce phase II metabolic reactions of UGT and MAO as observed in humans and mice. Consequently, it is recommended to use and assess more complex hepatocellular assays to further investigate the metabolism of these tryptamines. The major metabolite 4-HIAA and 4-HTP were inactive at human 5-HT receptors but the activity of oxidized psilocin metabolites and norpsilocin remain to be assessed. Inhibition of psilocin inactivation by MAO could potentially augment the metabolic pathway catalyzed by CYP2D6, thereby altering the pharmacodynamics of psilocybin therapy. However, the CYP2D6 genotype did not influence psilocin concentrations in humans. Moreover, glucuronidation of psilocin would likely continue to be the predominant metabolic pathway, rendering MAO inhibition potentially less important.

Finally, our findings on psilocybin's metabolism contribute to the safety and efficacy of psilocybin therapy by indicating potential drug-drug interactions and helping advance research on psilocybin as a therapeutic agent.

Data availability statement

The raw data supporting the conclusions of this article will be made available by the authors, without undue reservation.

Ethics statement

The studies involving humans were approved by Ethics Committee of Northwestern and Central Switzerland (EKNZ), Basel, Switzerland. The studies were conducted in accordance with the local legislation and institutional requirements. The participants provided their written informed consent to participate in this study. The animal study was approved by Veterinary Office Zurich, Zurich, Switzerland. The study was

conducted in accordance with the local legislation and institutional requirements.

Author contributions

JT: Conceptualization, Formal Analysis, Investigation, Methodology, Validation, Visualization, Writing—original draft, Writing—review and editing. KEK: Conceptualization, Formal Analysis, Investigation, Methodology, Validation, Visualization, Writing—original draft, Writing—review and editing. OVS: Investigation, Writing—review and editing. DR: Investigation, Writing—review and editing. PV: Investigation, Writing—review and editing. MCH: Investigation, Resources, Writing—review and editing. CRP: Conceptualization, Investigation, Resources, Writing—review and editing. FXV: Conceptualization, Resources, Funding acquisition, Writing—review and editing. MEL: Conceptualization, Funding acquisition, Resources, Supervision, Writing—review and editing. UD: Conceptualization, Methodology, Project administration, Resources, Supervision, Validation, Writing—review and editing.

Funding

The authors declare that financial support was received for the research, authorship, and/or publication of this article. This work was co-supported by the Swiss National Science Foundation (SNF, Grant No. 32003B_185111/1) to MEL, Mind Medicine Inc., and by the Swiss Neuromatrix Foundation (Grant No. 2023-3-01) to FXV.

References

- Becker, A. M., Holze, F., Grandinetti, T., Klaiber, A., Toedtli, V. E., Kolaczynska, K. E., et al. (2022). Acute Effects of psilocybin after escitalopram or placebo pretreatment in a randomized, double-blind, placebo-controlled, crossover study in healthy subjects. *Clin. Pharmacol. Ther.* 111 (4), 886–895. doi:10.1002/cpt.2487
- Bergh, M. S., Bogen, I. L., Grafinger, K. E., Huestis, M. A., and Oiestad, Å. M. L. (2024). Metabolite markers for three synthetic tryptamines N-ethyl-N-propyltryptamine, 4-hydroxy-N-ethyl-N-propyltryptamine, and 5-methoxy-N-ethyl-N-propyltryptamine. *Drug Test. Anal.* 24, 3668. doi:10.1002/dta.3668
- Blaschko, H., and Levine, W. G. (1960). A comparative study of hydroxyindole oxidases. *Br. J. Pharmacol. Chemother.* 15 (4), 625–633. doi:10.1111/j.1476-5381.1960.tb00290.x
- Bogenschutz, M. P., Podrebarac, S. K., Duane, J. H., Amegadzie, S. S., Malone, T. C., Owens, L. T., et al. (2018). Clinical interpretations of patient experience in a trial of psilocybin-assisted psychotherapy for alcohol use disorder. *Front. Pharmacol.* 9 (100), 100. doi:10.3389/fphar.2018.00100
- Carhart-Harris, R. L., Roseman, L., Bolstridge, M., Demetriou, L., Pannekoek, J. N., Wall, M. B., et al. (2017). Psilocybin for treatment-resistant depression: fMRI-measured brain mechanisms. *Sci. Rep.* 7 (1), 13187–13211. doi:10.1038/s41598-017-13282-7
- Caudle, K. E., Sangkuhl, K., Whirl-Carrillo, M., Swen, J. J., Haidar, C. E., Klein, T. E., et al. (2020). Standardizing CYP2D6 genotype to phenotype translation: consensus recommendations from the clinical pharmacogenetics implementation consortium and Dutch pharmacogenetics working group. *Clin. Transl. Sci.* 13 (1), 116–124. doi:10.1111/cts.12692
- Crews, K. R., Gaedigk, A., Dunnenberger, H. M., Klein, T. E., Shen, D. D., Callaghan, J. T., et al. (2012). Clinical Pharmacogenetics Implementation Consortium (CPIC) guidelines for codeine therapy in the context of cytochrome P450 2D6 (CYP2D6) genotype. *Clin. Pharmacol. Ther.* 91 (2), 321–326. doi:10.1038/clpt.2011.287
- Denis-Oliveira, R. J. (2017). Metabolism of psilocybin and psilocin: clinical and forensic toxicological relevance. *Drug Metab. Rev.* 49 (1), 84–91. doi:10.1080/03602532.2016.1278228

Acknowledgments

The authors thank Beatrice Vetter for providing technical assistance.

Conflict of interest

FXV is currently on the board of directors of the Heffter Research Institute and a scientific advisor for the MIND Foundation. MCH is an employee of F. Hoffmann-La Roche. MEL is a consultant for Mind Medicine Inc.

The remaining authors declare that the research was conducted in the absence of any commercial or financial relationships that could be construed as a potential conflict of interest.

Publisher's note

All claims expressed in this article are solely those of the authors and do not necessarily represent those of their affiliated organizations, or those of the publisher, the editors and the reviewers. Any product that may be evaluated in this article, or claim that may be made by its manufacturer, is not guaranteed or endorsed by the publisher.

Supplementary material

The Supplementary Material for this article can be found online at: <https://www.frontiersin.org/articles/10.3389/fphar.2024.1391689/full#supplementary-material>

- Eckernäs, E., Macan-Schönleben, A., Andresen-Bergström, M., Birgersson, S., Hoffmann, K.-J., and Ashton, M. N. (2023). N, N-dimethyltryptamine forms oxygenated metabolites via CYP2D6 - an *in vitro* investigation. *Xenobiotica* 53 (8-9), 515–522. doi:10.1080/00498254.2023.2278488
- Eivindvik, K., Rasmussen, K. E., and Sund, R. B. (1989). Handling of psilocybin and psilocin by everted sacs of rat jejunum and colon. *Acta Pharm. Nord.* 1 (5), 295–302.
- Gaedigk, A., Simon, S. D., Pearce, R. E., Bradford, L. D., Kennedy, M. J., and Leeder, J. S. (2008). The CYP2D6 activity score: translating genotype information into a qualitative measure of phenotype. *Clin. Pharmacol. Ther.* 83 (2), 234–242. doi:10.1038/sj.cpt.6100406
- Grieshaber, A. F., Moore, K. A., and Levine, B. (2001). The detection of psilocin in human urine. *J. Forensic Sci.* 46 (3), 627–630. doi:10.1520/jfs15014j
- Griffiths, R. R., Johnson, M. W., Carducci, M. A., Umbricht, A., Richards, W. A., Richards, B. D., et al. (2016). Psilocybin produces substantial and sustained decreases in depression and anxiety in patients with life-threatening cancer: a randomized double-blind trial. *J. Psychopharmacol.* 30 (12), 1181–1197. doi:10.1177/026988116675513
- Grob, C. S., Danforth, A. L., Chopra, G. S., Hagerty, M., McKay, C. R., Halberstadt, A. L., et al. (2011). Pilot study of psilocybin treatment for anxiety in patients with advanced-stage cancer. *Archives General Psychiatry* 68 (1), 71–78. doi:10.1001/archgenpsychiatry.2010.116
- Hasler, F., Bourquin, D., Brenneisen, R., Bär, T., and Vollenweider, F. X. (1997). Determination of psilocin and 4-hydroxyindole-3-acetic acid in plasma by HPLC-ECD and pharmacokinetic profiles of oral and intravenous psilocybin in man. *Pharm. Acta Helv.* 72 (3), 175–184. doi:10.1016/s0031-6865(97)00014-9
- Hasler, F., Bourquin, D., Brenneisen, R., and Vollenweider, F. X. (2002). Renal excretion profiles of psilocin following oral administration of psilocybin: a controlled study in man. *J. Pharm. Biomed. Anal.* 30 (2), 331–339. doi:10.1016/s0731-7085(02)00278-9
- Hicks, J. K., Bishop, J. R., Sangkuhl, K., Müller, D. J., Ji, Y., Leckband, S. G., et al. (2015). Clinical pharmacogenetics implementation consortium (CPIC) guideline for

- CYP2D6 and CYP2C19 genotypes and dosing of selective serotonin reuptake inhibitors. *Clin. Pharmacol. Ther.* 98 (2), 127–134. doi:10.1002/cpt.147
- Hicks, J. K., Swen, J. J., Thorn, C. F., Sangkuhl, K., Kharasch, E. D., Ellingrod, V. L., et al. (2013). Clinical Pharmacogenetics Implementation Consortium guideline for CYP2D6 and CYP2C19 genotypes and dosing of tricyclic antidepressants. *Clin. Pharmacol. Ther.* 93 (5), 402–408. doi:10.1038/clpt.2013.2
- Holze, F., Becker, A. M., Kolaczynska, K. E., Duthaler, U., and Liechti, M. E. (2022a). Pharmacokinetics and pharmacodynamics of oral psilocybin administration in healthy participants. *Clin. Pharmacol. Ther.* 113, 822–831. doi:10.1002/cpt.2821
- Holze, F., Ley, L., Müller, F., Becker, A. M., Straumann, I., Vizeli, P., et al. (2022b). Acute dose-dependent effects of lysergic acid diethylamide in a double-blind placebo-controlled study in healthy subjects. *Neuropsychopharmacology* 47 (6), 537–544. doi:10.1038/s41386-020-00883-6
- Horita, A. (1963). Some biochemical studies on psilocybin and psilocin. *J. Neuropsychiatr.* 4, 270–273.
- Horita, A., and Weber, L. J. (1961a). Dephosphorylation of psilocybin to psilocin by alkaline phosphatase. *Proc. Soc. Exp. Biol. Med.* 106, 32–34. doi:10.3181/00379727-106-26228
- Horita, A., and Weber, L. J. (1961b). The enzymic dephosphorylation and oxidation of psilocybin and psilocin by mammalian tissue homogenates. *Biochem. Pharmacol.* 7, 47–54. doi:10.1016/0006-2952(61)90124-1
- Horita, A., and Weber, L. J. (1962). Dephosphorylation of psilocybin in the intact mouse. *Toxicol. Appl. Pharmacol.* 4 (6), 730–737. doi:10.1016/0041-008x(62)90102-3
- Johnson, M. W., Garcia-Romeu, A., and Griffiths, R. R. (2017). Long-term follow-up of psilocybin-facilitated smoking cessation. *Am. J. Drug Alcohol Abuse* 43 (1), 55–60. doi:10.3109/00952990.2016.1170135
- Kaivosaaari, S., Finel, M., and Koskinen, M. (2011). N-glucuronidation of drugs and other xenobiotics by human and animal UDP-glucuronosyltransferases. *Xenobiotica* 41 (8), 652–669. doi:10.3109/00498254.2011.563327
- Kalberer, F., Kreis, W., and Rutschmann, J. (1962). The fate of psilocin in the rat. *Biochem. Pharmacol.* 11, 261–269. doi:10.1016/0006-2952(62)90050-3
- Kolaczynska, K. E., Liechti, M. E., and Duthaler, U. (2021). Development and validation of an LC-MS/MS method for the bioanalysis of psilocybin's main metabolites, psilocin and 4-hydroxyindole-3-acetic acid, in human plasma. *J. Chromatogr. B* 1164, 122486. doi:10.1016/j.jchromb.2020.122486
- Kovacic, P. (2009). Unifying electron transfer mechanism for psilocybin and psilocin. *Med. Hypotheses* 73 (4), 626. doi:10.1016/j.mehy.2009.06.022
- Lenz, C., Wick, J., and Hoffmeister, D. (2017). Identification of ω -N-methyl-4-hydroxytryptamine (norpsilocin) as a Psilocybe natural product. *J. Nat. Prod.* 80 (10), 2835–2838. doi:10.1021/acs.jnatprod.7b00407
- Ley, L., Holze, F., Arikci, D., Becker, A. M., Straumann, I., Klaiber, A., et al. (2023). Comparative acute effects of mescaline, lysergic acid diethylamide, and psilocybin in a randomized, double-blind, placebo-controlled cross-over study in healthy participants. *Neuropsychopharmacology* 48, 1659–1667. doi:10.1038/s41386-023-01607-2
- Lindenblatt, H., Krämer, E., Holzmann-Erens, P., Gouzoulis-Mayfrank, E., and Kovar, K.-A. (1998). Quantitation of psilocin in human plasma by high-performance liquid chromatography and electrochemical detection: comparison of liquid–liquid extraction with automated on-line solid-phase extraction. *J. Chromatogr. B Biomed. Sci. Appl.* 709 (2), 255–263. doi:10.1016/s0378-4347(98)00067-x
- Luethi, D., Hoener, M. C., Krähenbühl, S., Liechti, M. E., and Duthaler, U. (2019). Cytochrome P450 enzymes contribute to the metabolism of LSD to nor-LSD and 2-oxo-3-hydroxy-LSD: implications for clinical LSD use. *Biochem. Pharmacol.* 164, 129–138. doi:10.1016/j.bcp.2019.04.013
- Luethi, D., Kolaczynska, K. E., Vogt, S. B., Ley, L., Erne, L., Liechti, M. E., et al. (2022). Liquid chromatography–tandem mass spectrometry method for the bioanalysis of N, N-dimethyltryptamine (DMT) and its metabolites DMT-N-oxide and indole-3-acetic acid in human plasma. *J. Chromatogr. B* 1213, 123534. doi:10.1016/j.jchromb.2022.123534
- Luethi, D., Trachsel, D., Hoener, M. C., and Liechti, M. E. (2018). Monoamine receptor interaction profiles of 4-thio-substituted phenethylamines (2C-T drugs). *Neuropharmacology* 134 (Pt A), 141–148. doi:10.1016/j.neuropharm.2017.07.012
- Manevski, N., Kurkela, M., Höglund, C., Mauriala, T., Court, M. H., Yli-Kauhaluoma, J., et al. (2010). Glucuronidation of psilocin and 4-hydroxyindole by the human UDP-glucuronosyltransferases. *Drug Metab. Dispos.* 38 (3), 386–395. doi:10.1124/dmd.109.031138
- Moreno, F. A., Wiegand, C. B., Taitano, E. K., and Delgado, P. L. (2006). Safety, tolerability, and efficacy of psilocybin in 9 patients with obsessive-compulsive disorder. *J. Clin. Psychiatry* 67 (11), 1735–1740. doi:10.4088/jcp.v67n1110
- Ooka, M., Lynch, C., and Xia, M. (2020). Application of *in vitro* metabolism activation in high-throughput screening. *Int. J. Mol. Sci.* 21 (21), 8182. doi:10.3390/ijms21218182
- Regan, S. L., Maggs, J. L., Hammond, T. G., Lambert, C., Williams, D. P., and Park, B. K. (2010). Acyl glucuronides: the good, the bad and the ugly. *Biopharm. Drug Dispos.* 31 (7), 367–395. doi:10.1002/bdd.720
- Rickli, A., Moning, O. D., Hoener, M. C., and Liechti, M. E. (2016). Receptor interaction profiles of novel psychoactive tryptamines compared with classic hallucinogens. *Eur. Neuropsychopharmacol.* 26 (8), 1327–1337. doi:10.1016/j.euroneuro.2016.05.001
- Ross, S., Bossis, A., Guss, J., Agin-Lieb, G., Malone, T., Cohen, B., et al. (2016). Rapid and sustained symptom reduction following psilocybin treatment for anxiety and depression in patients with life-threatening cancer: a randomized controlled trial. *J. Psychopharmacol.* 30 (12), 1165–1180. doi:10.1177/0269881116675512
- Schmid, Y., Vizeli, P., Hysek, C. M., Prestin, K., Meyer Zu Schwabedissen, H. E., and Liechti, M. E. (2016). CYP2D6 function moderates the pharmacokinetics and pharmacodynamics of 3,4-methylene-dioxymethamphetamine in a controlled study in healthy individuals. *Pharmacogenet Genomics* 26 (8), 397–401. doi:10.1097/FPC.0000000000000231
- Sewell, R. A., Halpern, J. H., and Pope, H. G. (2006). Response of cluster headache to psilocybin and LSD. *Neurology* 66 (12), 1920–1922. doi:10.1212/01.wnl.0000219761.05466.43
- Sherwood, A. M., Burkhartzmeyer, E. K., Williamson, S. E., Baumann, M. H., and Glattfelter, G. C. (2024). Psychedelic-like activity of norpsilocin analogues. *ACS Chem. Neurosci.* 15, 315–327. doi:10.1021/acschemneuro.3c00610
- Sherwood, A. M., Halberstadt, A. L., Klein, A. K., McCorvy, J. D., Kaylo, K. W., Kargbo, R. B., et al. (2020). Synthesis and biological evaluation of tryptamines found in hallucinogenic mushrooms: norbaeocystin, baeocystin, norpsilocin, and aeruginascin. *J. Nat. Prod.* 83 (2), 461–467. doi:10.1021/acs.jnatprod.9b01061
- Sticht, G., and Käferstein, H. (2000). Detection of psilocin in body fluids. *Forensic Sci. Int.* 113 (1–3), 403–407. doi:10.1016/s0379-0738(00)00213-9
- Svensson, S., Some, M., Lundsjö, A., Helander, A., Cronholm, T., and Höög, J. O. (1999). Activities of human alcohol dehydrogenases in the metabolic pathways of ethanol and serotonin. *Eur. J. Biochem.* 262 (2), 324–329. doi:10.1046/j.1432-1327.1999.00351.x
- Van Court, R. C., Wiseman, M. S., Meyer, K. W., Ballhorn, D. J., Amses, K. R., Slot, J. C., et al. (2022). Diversity, biology, and history of psilocybin-containing fungi: suggestions for research and technological development. *Fungal Biol.* 126 (4), 308–319. doi:10.1016/j.funbio.2022.01.003
- Vizeli, P., Schmid, Y., Prestin, K., Zu Schwabedissen, H. E. M., and Liechti, M. E. (2017). Pharmacogenetics of ecstasy: CYP1A2, CYP2C19, and CYP2B6 polymorphisms moderate pharmacokinetics of MDMA in healthy subjects. *Eur. Neuropsychopharmacol.* 27 (3), 232–238. doi:10.1016/j.euroneuro.2017.01.008
- Vizeli, P., Straumann, I., Holze, F., Schmid, Y., Dolder, P. C., and Liechti, M. E. (2021). Genetic influence of CYP2D6 on pharmacokinetics and acute subjective effects of LSD in a pooled analysis. *Sci. Rep.* 11 (1), 10851. doi:10.1038/s41598-021-90343-y
- Vogt, S. B., Ley, L., Erne, L., Straumann, I., Becker, A. M., Klaiber, A., et al. (2023). Acute effects of intravenous DMT in a randomized placebo-controlled study in healthy participants. *Transl. Psychiatry* 13 (1), 172. doi:10.1038/s41398-023-02477-4
- Vollenweider, F. X., Vollenweider-Scherpenhuyzen, M. F., Bäbler, A., Vogel, H., and Hell, D. (1998). Psilocybin induces schizophrenia-like psychosis in humans via a serotonin-2 agonist action. *Neuroreport* 9 (17), 3897–3902. doi:10.1097/00001756-199812010-00024

PART III:
DISCUSSION, CONCLUSION, AND OUTLOOK

6 DISCUSSION

This thesis is composed of two main sections, each of which presents a distinct investigation into the subject of psychoactive substances. Part I consists of the development and validation of LC–MS/MS methods for the rapid and robust quantification of psychoactive substances and their metabolites. The projects involved the psychedelic mescaline, the semi-synthetic opioid diamorphine, and the entactogen MDMA. The validated methods were subsequently employed for the pharmacokinetic analysis of clinical studies involving the aforementioned substances. Part II of this thesis examines the metabolic degradation of psilocybin *in vitro*, in mice, and in humans, with a particular emphasis on the involved enzymes. The following sections briefly discuss all projects, followed by a conclusion and an exploration of future perspectives.

The LC–MS/MS method described in the first project (Chapter 3.1) was developed and validated as a tool for the analysis of two clinical studies investigating mescaline. The initial study examined the comparative acute effects of LSD, psilocybin, and mescaline in healthy participants (NCT04227756) (Ley et al. 2023). The study found no qualitative differences in altered states of consciousness when equivalent doses of the different psychedelics were administered. However, differences in pharmacokinetics and duration of action were observed (Ley et al. 2023). The second study focused on the function of the 5-HT_{2A} receptor in mescaline-induced altered states of consciousness (NCT04849013) (Klaiber et al. 2024b). Participants received escalating doses of mescaline and a combination of the highest dose with the 5-HT_{2A} receptor antagonist ketanserin to block the psychedelic effects. Dose-dependent psychedelic effects were observed while ketanserin was able to reduce the acute effects (Klaiber et al. 2024b). Otherwise, contemporary mescaline research is relatively limited in comparison to other psychedelic substances (Vamvakopoulou et al. 2023). The aforementioned studies sought to address this gap, providing data on the acute psychedelic effects, tolerability, pharmacokinetics, and dose equivalence of mescaline compared to other psychedelics.

The method developed herein enables and facilitates the modern pharmacokinetic analysis of mescaline, providing a bioanalytical tool for such studies. In comparison to the existing methodology (Beyer et al. 2007, Björnstad et al. 2008, da Cunha et al. 2020, Pichini et al. 2014, Sergi et al. 2010, Yang et al. 2022), our approach exhibits a significantly reduced runtime, thereby facilitating the rapid examination of a large number of study samples. Secondly, only minimal volumes of plasma are required to analyze a sample. Moreover, to the best of our

knowledge, no previous method included the metabolites TMPAA, NAM, and 4-desmethyl mescaline. This offers valuable insights into the metabolic fate of these compounds.

A limitation of the method is that 4-desmethyl mescaline could not be analyzed in clinical study samples due to an unexpected interference with its structural isomer 3-desmethyl mescaline, which is also abundant in human plasma samples after mescaline ingestion. As a result, reliable quantification was not possible. In order to achieve a successful simultaneous analysis of the two demethylated metabolites, it would be necessary to refine the chromatographic separation.

The second project (Chapter 3.2) focused on the development and validation of an LC–MS/MS method for the analysis of the pharmacokinetics of intranasal diamorphine. The investigation is part of a multicenter observational study examining the acceptability and feasibility of intranasal diamorphine administration in diamorphine-assisted treatment for opioid-dependent patients (BASEC ID: 2020-00354, manuscript in preparation).

The straightforward sample preparation and short analytical run time allow for the efficient analysis of samples. The rapid and robust analysis is of particular importance given that diamorphine is relatively unstable in human plasma under certain storage conditions (Barrett et al. 1992, Jones et al. 2013, Karinen et al. 2009). The analytical method and the gained knowledge about pharmacokinetics help advance treatment strategies for opioid-dependent patients. Intranasal application of diamorphine-assisted treatment may result in a less stigmatized form of therapy compared to intravenous application, enhance medication adherence, and improve the overall safety profile of the treatment (Biancarelli et al. 2019, Cama et al. 2016, Vogel et al. 2023).

With the current opioid crisis in North America, improving treatment strategies is of specific interest. The main drivers of the opioid crisis are synthetic opioids such as fentanyl or nitazenes. In contrast, the opioid situation in Europe is less severe. Nevertheless, diamorphine remains a leading cause of drug-related mortality in the European Union (EU). This underlines the importance of continued research on diamorphine. However, the prevalence of synthetic opioids in Europe should not be overlooked, as they are also widespread. For example, shortages of diamorphine could potentially increase the prevalence of synthetic alternatives which could in turn lead to a synthetic opioid crisis in Europe (Griffiths et al. 2024, Seyler et al. 2021, The Lancet Regional Health - Americas 2023).

In the third project (Chapter 3.3), two LC–MS/MS methods were developed and validated for the achiral and chiral analysis of MDMA and MDA. The techniques were employed to analyze several clinical studies involving MDMA and derivatives.

One study investigated the acute effects of MDMA and LSD co-administration (NCT04516902) and found that the co-administration of MDMA did not influence the psychedelic effects of LSD (Straumann et al. 2023). However, MDMA inhibited the LSD metabolism and thus prolonged its acute effects. A potential benefit of using co-administration in psychotherapy was not observed (Straumann et al. 2023). Another study examined the acute effects of *R*-MDMA and *S*-MDMA in comparison to racemic MDMA (NCT05277636) (Straumann et al. 2024a). Differences in the stimulant properties of the enantiomers (*S*-MDMA > *R*-MDMA) and in the potency to inhibit CYP2D6 (*R*-MDMA > *S*-MDMA) were suggested. Nevertheless, the subjective and adverse effects may be comparable for the two enantiomers when dosed equivalently. Furthermore, no beneficial effects of the enantiomers were identified in comparison to racemic MDMA. Finally, the method was used to analyze a study comparing the effects of lysine-MDMA and lysine-MDA with those of racemic MDMA and MDA (NCT04847206, manuscript in preparation).

Overall, the achiral method provides the advantage of rapid sample analysis for both MDMA and MDA. Since MDMA and MDA do not undergo chiral inversion, the enantiomers *S*-MDMA, *R*-MDMA, *S*-MDA, and *R*-MDA can also be accurately analyzed using this method, provided that only one enantiomer was administered. Meanwhile, the chiral method effectively and reliably separates the enantiomers of MDMA and MDA in racemic mixtures, making it a valuable tool for analyzing the distinct pharmacokinetic properties of *R*- and *S*-MDMA after racemate treatment. Given the current relevance and significance of research on MDMA and its enantiomers as a therapeutic agent, having robust bioanalytical methods to analyze both the racemate and individual enantiomers of MDMA and MDA is crucial. This will improve clinical studies and facilitate further research on MDMA's therapeutic potential by improving the understanding of its pharmacokinetics and metabolism.

The project in Part II (Chapter 5.1) investigated the metabolic degradation of psilocybin's active metabolite psilocin. In consideration of the recent interest in psychedelics and the development of novel treatment strategies, it is crucial to understand their metabolism in detail. Although psilocybin is one of the most researched psychedelics with significant medical potential, metabolic and metabolomic studies are still limited (Lowe et al. 2021, Madrid-Gambin et al. 2023). By revealing psilocybin's metabolism and elucidating the enzymes

involved in these processes, key questions about the safety and toxicology of metabolic byproducts and drug-drug interactions might be addressed (Madrid-Gambin et al. 2023). The role of the CYP system, which is involved in the metabolism of other psychedelics (Halman et al. 2024, Luethi et al. 2019a), has not been extensively studied for psilocybin. Furthermore, studies trying to identify unknown metabolites that may be pharmacologically active are currently lacking. Consequently, the objective of this project was to address this research gap.

The involvement of the highly polymorphic enzyme CYP2D6 in psilocin's metabolism suggests potential individual differences in psilocin degradation. An enhanced or diminished production of the proposed oxidative metabolite could have an impact on the safety and efficacy of psilocybin-assisted treatment. Nevertheless, the investigation into the influence of the CYP2D6 genotype on psilocin levels did not reveal a significant difference between poor, intermediate, extensive, and ultra-rapid metabolizers. However, the sample size of poor ($n = 3$) and ultra-rapid metabolizers ($n = 2$) was limited, which reduced the power of the investigation. Moreover, the findings indicate that CYP3A4 may also play a role in psilocin metabolism. Nevertheless, no metabolite generated by CYP3A4 was identified. In general, the metabolic pathways involving CYP2D6, but also CYP3A4, are likely of minor importance, as the primary routes leading to 4-HIAA and psilocin-*O*-glucuronide are highly dominant.

The activity of the proposed oxidative metabolite in humans remains unclear. Given the multiple positions on psilocin's indole ring that could be hydroxylated, it is plausible that various constitutional isomers of this metabolite exist. Each could have distinct intrinsic activities and receptor affinities. The elucidation of the exact chemical structures and investigation of their pharmacological activity requires further investigation. In this regard, the application of advanced techniques such as high-resolution mass spectrometry (HRMS) or nuclear magnetic resonance (NMR) may prove useful.

Moreover, MAO-A has been identified as an enzyme involved in the transformation of psilocin to 4-HIAA and 4-HTP. This suggests that MAOIs, such as those used in ayahuasca (Egger et al. 2024, Riba et al. 2003), may influence the degradation of psilocybin. However, in the case of MAO inhibition, alternative metabolic pathways, such as glucuronidation to the inactive *O*-glucuronide, could compensate for this enzymatic inhibition. Nevertheless, this hypothesis has yet to be thoroughly investigated in humans. Notably, β -carbolines, which are potent reversible MAOIs, have been identified as natural components in *Psilocybe* mushrooms. Therefore MAOI may already contribute to a synergistic effect when consuming psilocybin-containing mushrooms (Blei et al. 2020).

Overall, the present project is characterized by three distinct approaches to investigate psilocybin's metabolism. The combination of *in vitro* and *in vivo* results in two different species offers a comprehensive insight into the metabolic processes. Nevertheless, the study has some limitations. It is limited by the relatively small sample sizes in both the mouse ($n = 5$) and the human study cohort ($n = 5$). Larger sample sizes in future studies would enhance the robustness of the findings. Furthermore, as previously stated, the importance of the genotyping results would be enhanced by a larger sample size of poor and ultra-rapid metabolizers. This would enable a more profound understanding of individual variations in psilocybin metabolism. Moreover, the *in vitro* and *in vivo* data are not always congruent, which demonstrates the limitations of these straightforward yet efficacious enzymatic assays. Extending these assays with more advanced methods, such as enzymatic assays in primary hepatocytes, could help to address the observed discrepancies.

7 CONCLUSION AND OUTLOOK

Concluding Part I, four LC–MS/MS methods for the robust and reliable quantitative analysis of three psychoactive substances and metabolites have been developed and validated in accordance with industry standards. The methods all stand out through non-laborious sample preparation and a simple setup, yet they facilitate rapid and robust bioanalysis. The methods were successfully implemented in routine pharmacokinetic analysis of plasma samples from clinical studies. These techniques facilitate the advancement of research on promising psychoactive substances for the treatment of various mental health issues. In the case of diamorphine, the method supports the development of novel treatment options, which may consequently enhance medication adherence and provide a less stigmatized and safer route of treatment.

The project in Part II provides valuable insight into the metabolic degradation of psilocybin, highlighting the contributing role of CYP2D, CYP3A4, and MAO-A. The identification of minor metabolites in mice and humans further elucidates the metabolic pathways involved. Future studies with larger sample sizes and advanced assays or analytical techniques will be critical to fully understand the pharmacological implications of psilocybin's metabolites. This will be essential to optimize the therapeutic outcomes of psilocybin-assisted psychotherapy while minimizing potential adverse effects.

8 REFERENCES

- AB Sciex (2008). QJet Ion Guide Technology in the API 5000 LC/MS/MS System.
- AB Sciex (2010). Hardware Guide API 5000 System.
- Akash M. S. H. and Rehman K. (2020). Essentials of Pharmaceutical Analysis. *Springer*. DOI: 10.1007/978-981-15-1547-7.
- Almazroo O. A., Miah M. K., and Venkataramanan R. (2017). Drug Metabolism in the Liver. *Clin Liver Dis*. 21(1): 1-20. DOI: 10.1016/j.cld.2016.08.001.
- Ashri N. Y. and Abdel-Rehim M. (2011). Sample Treatment Based on Extraction Techniques in Biological Matrices. *Bioanalysis*. 3(17): 2003-2018. DOI: 10.4155/bio.11.201.
- Ashton M., Groundwater P. W., Stocker S., and Todd A. (2024). Chapter 2 - Oxidative Phase I Metabolic Transformations. An Integrated Guide to Human Drug Metabolism. Wolff A. *Academic Press*. 31-84. DOI: 10.1016/B978-0-323-99133-9.00007-3.
- Atila C., Holze F., Murugesu R., Rommers N., Hutter N., Varghese N., Sailer C. O., Eckert A., Heinrichs M., Liechti M. E., and Christ-Crain M. (2023). Oxytocin in Response to MDMA Provocation Test in Patients with Arginine Vasopressin Deficiency (Central Diabetes Insipidus): A Single-Centre, Case-Control Study with Nested, Randomised, Double-Blind, Placebo-Controlled Crossover Trial. *Lancet Diabetes Endocrinol*. 11(7): 454-464. DOI: 10.1016/S2213-8587(23)00120-1.
- Baggott M. J., Garrison K. J., Coyle J. R., Galloway G. P., Barnes A. J., Huestis M. A., and Mendelson J. E. (2019). Effects of the Psychedelic Amphetamine MDA (3,4-Methylenedioxyamphetamine) in Healthy Volunteers. *J Psychoact Drugs*. 51(2): 108-117. DOI: 10.1080/02791072.2019.1593560.
- Barker S. A. (2018). N,N-dimethyltryptamine (DMT), an Endogenous Hallucinogen: Past, Present, and Future Research to Determine Its Role and Function. *Front Neurosci*. 12: 536. DOI: 10.3389/fnins.2018.00536.
- Barrett D. A., Dyssegaard A. L. P., and Shaw P. N. (1992). The Effect of Temperature and pH on the Deacetylation of Diamorphine in Aqueous Solution and in Human Plasma. *J Pharm Pharmacol*. 44(7): 606-608
- Barrett F. S., Bradstreet M. P., Leoutsakos J. S., Johnson M. W., and Griffiths R. R. (2016). The Challenging Experience Questionnaire: Characterization of Challenging Experiences with Psilocybin Mushrooms. *J Psychopharmacol*. 30(12): 1279-1295. DOI: 10.1177/0269881116678781.
- Becker A. M., Holze F., Grandinetti T., Klaiber A., Toedtli V. E., Kolaczynska K. E., Duthaler U., Varghese N., Eckert A., Grunblatt E., and Liechti M. E. (2022). Acute Effects of Psilocybin After Escitalopram or Placebo Pretreatment in a Randomized, Double-Blind, Placebo-Controlled, Crossover Study in Healthy Subjects. *Clin Pharmacol Ther*. 111(4): 886-895. DOI: 10.1002/cpt.2487.
- Beyer J., Peters F. T., Kraemer T., and Maurer H. H. (2007). Detection and Validated Quantification of Nine Herbal Phenalkylamines and Methcathinone in Human Blood

-
- Plasma by LC-MS/MS with Electrospray Ionization. *J Mass Spectrom.* 42(2): 150-160. DOI: 10.1002/jms.1132.
- Biancarelli D. L., Biello K. B., Childs E., Drainoni M., Salhaney P., Edeza A., Mimiaga M. J., Saitz R., and Bazzi A. R. (2019). Strategies Used by People Who Inject Drugs to Avoid Stigma in Healthcare Settings. *Drug Alcohol Depend.* 198: 80-86. DOI: 10.1016/j.drugalcdep.2019.01.037.
- Björnstad K., Helander A., and Beck O. (2008). Development and Clinical Application of an LC-MS-MS Method for Mescaline in Urine. *J Anal Toxicol.* 32(3): 227-231. DOI: 10.1093/jat/32.3.227.
- Blei F., Dörner S., Fricke J., Baldeweg F., Trottmann F., Komor A., Meyer F., Hertweck C., and Hoffmeister D. (2020). Simultaneous Production of Psilocybin and a Cocktail of β -Carboline Monoamine Oxidase Inhibitors in "Magic" Mushrooms. *Chem Eur J.* 26(3): 729-734. DOI: 10.1002/chem.201904363.
- Blum F. (2014). High Performance Liquid Chromatography. *Br J Hosp Med (Lond).* 75(2): C18-21. DOI: 10.12968/hmed.2014.75.Sup2.C18.
- Bogenschutz M. P., Podrebarac S. K., Duane J. H., Amegadzie S. S., Malone T. C., Owens L. T., Ross S., and Mennenga S. E. (2018). Clinical Interpretations of Patient Experience in a Trial of Psilocybin-Assisted Psychotherapy for Alcohol Use Disorder. *Front Pharmacol.* 9: 100. DOI: 10.3389/fphar.2018.00100.
- Bolser D. C. and Davenport P. W. (2007). Codeine and Cough: An Ineffective Gold Standard. *Curr Opin Allergy Clin Immunol.* 7(1): 32-36. DOI: 10.1097/ACI.0b013e3280115145.
- Boyes B. and Dong M. (2018). Modern Trends and Best Practices in Mobile-Phase Selection in Reversed-Phase Chromatography. *LC GC N Am.* 36(10): 752-768
- Boysen P. G., Patel J. H., and King A. N. (2023). Brief History of Opioids in Perioperative and Periprocedural Medicine to Inform the Future. *Ochsner J.* 23(1): 43-49. DOI: 10.31486/toj.22.0065.
- Britch S. C. and Walsh S. L. (2022). Treatment of Opioid Overdose: Current Approaches and Recent Advances. *Psychopharmacology (Berl).* 239(7): 2063-2081. DOI: 10.1007/s00213-022-06125-5.
- Cama E., Brener L., Wilson H., and von Hippel C. (2016). Internalized Stigma Among People Who Inject Drugs. *Subst Use Misuse.* 51(12): 1664-1668. DOI: 10.1080/10826084.2016.1188951.
- Carhart-Harris R., Giribaldi B., Watts R., Baker-Jones M., Murphy-Beiner A., Murphy R., Martell J., Blemings A., Erritzoe D., and Nutt D. J. (2021). Trial of Psilocybin Versus Escitalopram for Depression. *N Engl J Med.* 384(15): 1402-1411. DOI: 10.1056/NEJMoa2032994.
- Carhart-Harris R. L., Roseman L., Bolstridge M., Demetriou L., Pannekoek J. N., Wall M. B., Tanner M., Kaelen M., McGonigle J., Murphy K., Leech R., Curran H. V., and Nutt D. J. (2017). Psilocybin for Treatment-Resistant Depression: fMRI-Measured Brain Mechanisms. *Sci Rep.* 7(1): 13187. DOI: 10.1038/s41598-017-13282-7.
-

-
- Cassels B. K. and Saez-Briones P. (2018). Dark Classics in Chemical Neuroscience: Mescaline. *ACS Chem Neurosci.* 9(10): 2448-2458. DOI: 10.1021/acscchemneuro.8b00215.
- da Cunha K. F., Oliveira K. D., Huestis M. A., and Costa J. L. (2020). Screening of 104 New Psychoactive Substances (NPS) and Other Drugs of Abuse in Oral Fluid by LC–MS–MS. *J Anal Toxicol.* 44(7): 697-707. DOI: 10.1093/jat/bkaa089.
- Darke S., Hall W., Weatherburn D., and Lind B. (1999). Fluctuations in Heroin Purity and the Incidence of Fatal Heroin Overdose. *Drug Alcohol Depend.* 54(2): 155-161. DOI: 10.1016/s0376-8716(98)00159-8.
- Davenport W. J. (2016). Psychedelic and Nonpsychedelic LSD and Psilocybin for Cluster Headache. *CMAJ.* 188(3): 217. DOI: 10.1503/cmaj.1150082.
- Davis A. K., Barrett F. S., May D. G., Cosimano M. P., Sepeda N. D., Johnson M. W., Finan P. H., and Griffiths R. R. (2021). Effects of Psilocybin-Assisted Therapy on Major Depressive Disorder: A Randomized Clinical Trial. *JAMA Psychiatry.* 78(5): 481-489. DOI: 10.1001/jamapsychiatry.2020.3285.
- De Hoffmann E. and Stroobant V. (2007). Mass Spectrometry: Principles and Applications. *John Wiley & Sons.*
- de la Torre R., Farre M., Roset P. N., Pizarro N., Abanades S., Segura M., Segura J., and Cami J. (2004). Human Pharmacology of MDMA: Pharmacokinetics, Metabolism, and Disposition. *Ther Drug Monit.* 26(2): 137-144. DOI: 10.1097/00007691-200404000-00009.
- de Vos C. M. H., Mason N. L., and Kuypers K. P. C. (2021). Psychedelics and Neuroplasticity: A Systematic Review Unraveling the Biological Underpinnings of Psychedelics. *Front Psychiatry.* 12: 724606. DOI: 10.3389/fpsy.2021.724606.
- Dhaliwal A. and Gupta M. (2023). Physiology, Opioid Receptor. *StatPearls Publishing, Treasure Island (FL).*
- Dietrich A. (2009). Psychoactive Drugs and Alterations to Consciousness. Encyclopedia of Consciousness. Banks W. P. *Academic Press.* 217-229. DOI: 10.1016/B978-012373873-8.00064-5.
- Dinis-Oliveira R. J. (2017). Metabolism of Psilocybin and Psilocin: Clinical and Forensic Toxicological Relevance. *Drug Metab Rev.* 49(1): 84-91. DOI: 10.1080/03602532.2016.1278228.
- Dinis-Oliveira R. J., Pereira C. L., and da Silva D. D. (2019). Pharmacokinetic and Pharmacodynamic Aspects of Peyote and Mescaline: Clinical and Forensic Repercussions. *Curr Mol Pharmacol.* 12(3): 184-194. DOI: 10.2174/1874467211666181010154139.
- Domon B. and Aebersold R. (2006). Mass Spectrometry and Protein Analysis. *Science.* 312(5771): 212-217. DOI: 10.1126/science.1124619.
- Dos Santos R. G., Osorio F. L., Crippa J. A., Riba J., Zuardi A. W., and Hallak J. E. (2016). Antidepressive, Anxiolytic, and Antiaddictive Effects of Ayahuasca, Psilocybin and
-

-
- Lysergic Acid Diethylamide (LSD): A Systematic Review of Clinical Trials Published in the Last 25 Years. *Ther Adv Psychopharmacol.* 6(3): 193-213. DOI: 10.1177/2045125316638008.
- Egger K., Aicher H. D., Cumming P., and Scheidegger M. (2024). Neurobiological Research on N,N-Dimethyltryptamine (DMT) and its Potentiation by Monoamine Oxidase (MAO) Inhibition: From Ayahuasca to Synthetic Combinations of DMT and MAO Inhibitors. *Cell Mol Life Sci.* 81(1): 395. DOI: 10.1007/s00018-024-05353-6.
- European Medicines Agency. (2022). ICH Guideline M10 on Bioanalytical Method Validation and Study Sample Analysis. Retrieved 03.09.2024, from www.ema.europa.eu/en/documents/scientific-guideline/ich-guideline-m10-bioanalytical-method-validation-step-5_en.pdf
- Freestone C. and Eccles R. (1997). Assessment of the Antitussive Efficacy of Codeine in Cough Associated with Common Cold. *J Pharm Pharmacol.* 49(10): 1045-1049. DOI: 10.1111/j.2042-7158.1997.tb06039.x.
- Ganesh V., Poorna Basuri P., Sahini K., and Nalini C. N. (2023). Retention Behaviour of Analytes in Reversed-Phase High-Performance Liquid Chromatography - A review. *Biomed Chromatogr.* 37(7): e5482. DOI: 10.1002/bmc.5482.
- Gasser P., Holstein D., Michel Y., Doblin R., Yazar-Klosinski B., Passie T., and Brenneisen R. (2014). Safety and Efficacy of Lysergic Acid Diethylamide-Assisted Psychotherapy for Anxiety Associated with Life-Threatening Diseases. *J Nerv Ment Dis.* 202(7): 513-520. DOI: 10.1097/NMD.000000000000113.
- Geyer M. A. (2024). A Brief Historical Overview of Psychedelic Research. *Biol Psychiatry Cogn Neurosci Neuroimaging.* 9(5): 464-471. DOI: 10.1016/j.bpsc.2023.11.003.
- Griffiths P. N., Seyler T., De Moraes J. M., Mounteney J. E., and Sedefov R. S. (2024). Opioid Problems Are Changing in Europe with Worrying Signals That Synthetic Opioids May Play a More Significant Role in the Future. *Addiction.* 119(8): 1334-1336. DOI: 10.1111/add.16420.
- Griffiths R. R., Johnson M. W., Carducci M. A., Umbricht A., Richards W. A., Richards B. D., Cosimano M. P., and Klinedinst M. A. (2016). Psilocybin Produces Substantial and Sustained Decreases in Depression and Anxiety in Patients with Life-Threatening Cancer: A Randomized Double-Blind Trial. *J Psychopharmacol.* 30(12): 1181-1197. DOI: 10.1177/0269881116675513.
- Gross J. H. (2006). Mass Spectrometry: A Textbook. *Springer.* DOI: 10.1007/978-3-319-54398-7.
- Guttman E. (1936). Artificial Psychoses Produced by Mescaline. *J Ment Sci.* 82(338): 203-221. DOI: 10.1192/bjp.82.338.203.
- Guttman E. and Maclay W. S. (1936). Mescaline and Depersonalization: Therapeutic Experiments. *J Neurol Psychopathol.* 16(63): 193. DOI: 10.1136/jnnp.s1-16.63.193.
-

-
- Haag A. M. (2016). Mass Analyzers and Mass Spectrometers. Modern Proteomics—Sample Preparation, Analysis and Practical Applications. *Springer*. 157-169. DOI: 10.1007/978-3-319-41448-5_7.
- Häbel T. and Gutwinski S. (2018). Opioide. Handbuch Psychoaktive Substanzen. von Heyden M., Jungaberle H., and Majić T. *Springer Berlin Heidelberg*. 643-657. DOI: 10.1007/978-3-642-55125-3_33.
- Halman A., Conyers R., Moore C., Khatri D., Sarris J., and Perkins D. (2024). Harnessing Pharmacogenomics in Clinical Research on Psychedelic-Assisted Therapy. *Clin Pharmacol Ther*. DOI: 10.1002/cpt.3459.
- Hasler F., Bourquin D., Brenneisen R., Bar T., and Vollenweider F. X. (1997). Determination of Psilocin and 4-Hydroxyindole-3-Acetic Acid in Plasma by HPLC-ECD and Pharmacokinetic Profiles of Oral and Intravenous Psilocybin in Man. *Pharm Acta Helv*. 72(3): 175-184. DOI: 10.1016/s0031-6865(97)00014-9.
- Hermle L., Funfgeld M., Oepen G., Botsch H., Borchardt D., Gouzoulis E., Fehrenbach R. A., and Spitzer M. (1992). Mescaline-Induced Psychopathological, Neuropsychological, and Neurometabolic Effects in Normal Subjects: Experimental Psychosis as a Tool for Psychiatric Research. *Biol Psychiatry*. 32(11): 976-991. DOI: 10.1016/0006-3223(92)90059-9.
- Ho C. S., Lam C. W., Chan M. H., Cheung R. C., Law L. K., Lit L. C., Ng K. F., Suen M. W., and Tai H. L. (2003). Electrospray Ionisation Mass Spectrometry: Principles and Clinical Applications. *Clin Biochem Rev*. 24(1): 3-12
- Holka-Pokorska J. (2023). Can Research on Entactogens Contribute to a Deeper Understanding of Human Sexuality? *Pharmacol Rep*. 75(6): 1381-1397. DOI: 10.1007/s43440-023-00552-7.
- Holze F., Becker A. M., Kolaczynska K. E., Duthaler U., and Liechti M. E. (2022a). Pharmacokinetics and Pharmacodynamics of Oral Psilocybin Administration in Healthy Participants. *Clin Pharmacol Ther*. DOI: 10.1002/cpt.2821.
- Holze F., Caluori T. V., Vizeli P., and Liechti M. E. (2022b). Safety Pharmacology of Acute LSD Administration in Healthy Subjects. *Psychopharmacology (Berl)*. 239(6): 1893-1905. DOI: 10.1007/s00213-021-05978-6.
- Holze F., Liechti M. E., and Müller F. (2024a). Pharmacological Properties of Psychedelics with a Special Focus on Potential Harms. Current Topics in Behavioral Neurosciences. *Springer Berlin Heidelberg*. 1-18. DOI: 10.1007/7854_2024_510.
- Holze F., Singh N., Liechti M. E., and D'Souza D. C. (2024b). Serotonergic Psychedelics: A Comparative Review of Efficacy, Safety, Pharmacokinetics, and Binding Profile. *Biol Psychiatry Cogn Neurosci Neuroimaging*. 9(5): 472-489. DOI: 10.1016/j.bpsc.2024.01.007.
- Iyanagi T. (2007). Molecular Mechanism of Phase I and Phase II Drug-Metabolizing Enzymes: Implications for Detoxification. *Int Rev Cytol*. 260: 35-112. DOI: 10.1016/S0074-7696(06)60002-8.
-

-
- Jaiswal D. and Wangikar P. P. (2020). SWATH: A Data-Independent Tandem Mass Spectrometry Method to Quantify ¹³C Enrichment in Cellular Metabolites and Fragments. *Metabolic Flux Analysis in Eukaryotic Cells: Methods and Protocols*. Nagrath D. *Springer US*. 189-204. DOI: 10.1007/978-1-0716-0159-4_9.
- Jia M., Li L., Xiong B., Feng L., Cheng W., and Dong W. F. (2023). Multi-Parameter Auto-Tuning Algorithm for Mass Spectrometer Based on Improved Particle Swarm Optimization. *Bioengineering (Basel)*. 10(9). DOI: 10.3390/bioengineering10091079.
- Johnson M. W., Garcia-Romeu A., and Griffiths R. R. (2017). Long-Term Follow-Up of Psilocybin-Facilitated Smoking Cessation. *Am J Drug Alcohol Abuse*. 43(1): 55-60. DOI: 10.3109/00952990.2016.1170135.
- Johnson M. W., Richards W. A., and Griffiths R. R. (2008). Human Hallucinogen Research: Guidelines for Safety. *J Psychopharmacol*. 22(6): 603-620. DOI: 10.1177/0269881108093587.
- Jones J. M., Raleigh M. D., Pentel P. R., Harmon T. M., Keyler D. E., Rimmel R. P., and Birnbaum A. K. (2013). Stability of Heroin, 6-Monoacetylmorphine, and Morphine in Biological Samples and Validation of an LC-MS Assay for Delayed Analyses of Pharmacokinetic Samples in Rats. *J Pharm Biomed Anal*. 74: 291-297. DOI: 10.1016/j.jpba.2012.10.033.
- Kadlubar S. and Kadlubar F. F. (2009). Enzymatic Basis of Phase I and Phase II Drug Metabolism. *Enzyme- and Transporter-Based Drug-Drug Interactions: Progress and Future Challenges*. *Springer*. 3-25. DOI: 10.1007/978-1-4419-0840-7_1.
- Karinen R., Andersen J. M., Ripel Å., Hasvold I., Hopen A. B., Mørland J., and Christophersen A. S. (2009). Determination of Heroin and its Main Metabolites in Small Sample Volumes of Whole Blood and Brain Tissue by Reversed-Phase Liquid Chromatography-Tandem Mass Spectrometry. *J Anal Toxicol*. 33(7): 345-350. DOI: 10.1093/jat/33.7.345.
- Kaza M., Karazniewicz-Lada M., Kosicka K., Siemiatkowska A., and Rudzki P. J. (2019). Bioanalytical Method Validation: New FDA Guidance Vs. EMA Guideline. Better or Worse? *J Pharm Biomed Anal*. 165: 381-385. DOI: 10.1016/j.jpba.2018.12.030.
- Klaiber A., Humbert-Droz M., Ley L., Schmid Y., and Liechti M. E. (2024a). Safety Pharmacology of Acute Mescaline Administration in Healthy Participants. *Br J Clin Pharmacol*. DOI: 10.1111/bcp.16349.
- Klaiber A., Schmid Y., Becker A. M., Straumann I., Erne L., Jelusic A., Thomann J., Luethi D., and Liechti M. E. (2024b). Acute Dose-Dependent Effects of Mescaline in a Double-Blind Placebo-Controlled Study in Healthy Subjects. *Transl Psychiatry*. 14(1): 395. DOI: 10.1038/s41398-024-03116-2.
- Knopf A. (2024). Back to the Drawing Board for Lykos' MDMA Therapy. *Brown Univ Child Adolesc Psychopharm Update*. 26(10): 7-8. DOI: 10.1002/cpu30905.
- Kolaczynska K. E., Liechti M. E., and Duthaler U. (2021). Development and Validation of an LC-MS/MS Method for the Bioanalysis of Psilocybin's Main Metabolites, Psilocin and 4-Hydroxyindole-3-Acetic Acid, in Human Plasma. *J Chromatogr B*. 1164: 122486. DOI: 10.1016/j.jchromb.2020.122486.
-

- Kumar A. and Sharma C. (2023). Fine and Targeted Tuning of a Single Quadrupole MS Hyphenated with Gas Chromatography Using Taguchi Method. *Microchem J.* 195: 109491. DOI: 10.1016/j.microc.2023.109491.
- Kupferschmidt K. (2017). All Clear for the Decisive Trial of Ecstasy in PTSD Patients. Retrieved 30.08.2024, from www.science.org/content/article/all-clear-decisive-trial-ecstasy-ptsd-patients. DOI: 10.1126/science.aap7739.
- Ley L., Holze F., Arikci D., Becker A. M., Straumann I., Klaiber A., Coviello F., Dierbach S., Thomann J., Duthaler U., Luethi D., Varghese N., Eckert A., and Liechti M. E. (2023). Comparative Acute Effects of Mescaline, Lysergic Acid Diethylamide, and Psilocybin in a Randomized, Double-Blind, Placebo-Controlled Cross-Over Study in Healthy Participants. *Neuropsychopharmacology*. 48(11): 1659-1667. DOI: 10.1038/s41386-023-01607-2.
- Libanio Osorio Marta R. F. (2019). Metabolism of Lysergic Acid Diethylamide (LSD): An Update. *Drug Metab Rev.* 51(3): 378-387. DOI: 10.1080/03602532.2019.1638931.
- Liechti M. E. (2017). Modern Clinical Research on LSD. *Neuropsychopharmacology*. 42(11): 2114-2127. DOI: 10.1038/npp.2017.86.
- Liechti M. E. and Vollenweider F. X. (2000). The Serotonin Uptake Inhibitor Citalopram Reduces Acute Cardiovascular and Vegetative Effects of 3,4-Methylenedioxymethamphetamine ('Ecstasy') in Healthy Volunteers. *J Psychopharmacol.* 14(3): 269-274. DOI: 10.1177/026988110001400313.
- Lowe H., Toyang N., Steele B., Valentine H., Grant J., Ali A., Ngwa W., and Gordon L. (2021). The Therapeutic Potential of Psilocybin. *Molecules*. 26(10). DOI: 10.3390/molecules26102948.
- Luethi D., Hoener M. C., Krahenbuhl S., Liechti M. E., and Duthaler U. (2019a). Cytochrome P450 Enzymes Contribute to the Metabolism of LSD to Nor-LSD and 2-Oxo-3-Hydroxy-LSD: Implications for Clinical LSD Use. *Biochem Pharmacol.* 164: 129-138. DOI: 10.1016/j.bcp.2019.04.013.
- Luethi D., Kolaczynska K. E., Walter M., Suzuki M., Rice K. C., Blough B. E., Hoener M. C., Baumann M. H., and Liechti M. E. (2019b). Metabolites of the Ring-Substituted Stimulants MDMA, Methylone and MDPV Differentially Affect Human Monoaminergic Systems. *J Psychopharmacol.* 33(7): 831-841. DOI: 10.1177/0269881119844185.
- Luethi D. and Liechti M. E. (2020). Designer Drugs: Mechanism of Action and Adverse Effects. *Arch Toxicol.* 94(4): 1085-1133. DOI: 10.1007/s00204-020-02693-7.
- Madden K., Flood B., Young Shing D., Ade-Conde M., Kashir I., Mark M., MacKillop J., Bhandari M., and Adili A. (2024). Psilocybin for Clinical Indications: A Scoping Review. *J Psychopharmacol.* 2698811241269751. DOI: 10.1177/02698811241269751.
- Madrid-Gambin F., Fabregat-Safont D., Gomez-Gomez A., Olesti E., Mason N. L., Ramaekers J. G., and Pozo O. J. (2023). Present and Future of Metabolic and Metabolomics Studies Focused on Classical Psychedelics in Humans. *Biomed Pharmacother.* 169: 115775. DOI: 10.1016/j.biopha.2023.115775.

- Martins M. L. F., Wilthagen E. A., Oviedo-Joekes E., Beijnen J. H., de Grave N., Uchtenhagen A., Beck T., Van den Brink W., and Schinkel A. H. (2021). The Suitability of Oral Diacetylmorphine in Treatment-Refractory Patients with Heroin Dependence: A Scoping Review. *Drug Alcohol Depend.* 227: 108984. DOI: 10.1016/j.drugalcdep.2021.108984.
- Maurer H. H., Sauer C., and Theobald D. S. (2006). Toxicokinetics of Drugs of Abuse: Current Knowledge of the Isoenzymes Involved in the Human Metabolism of Tetrahydrocannabinol, Cocaine, Heroin, Morphine, and Codeine. *Ther Drug Monit.* 28(3): 447-453. DOI: 10.1097/01.ftd.0000211812.27558.6e.
- Mitchell J. M., Ot'alora G. M., van der Kolk B., Shannon S., Bogenschutz M., Gelfand Y., Paleos C., Nicholas C. R., Quevedo S., Balliett B., Hamilton S., Mithoefer M., Kleiman S., Parker-Guilbert K., Tzarfaty K., Harrison C., de Boer A., Doblin R., Yazar-Klosinski B., and Group M. S. C. (2023). MDMA-Assisted Therapy for Moderate to Severe PTSD: A Randomized, Placebo-Controlled Phase 3 Trial. *Nat Med.* 29(10): 2473-2480. DOI: 10.1038/s41591-023-02565-4.
- Mithoefer M. C., Wagner M. T., Mithoefer A. T., Jerome L., and Doblin R. (2011). The Safety and Efficacy of +/-3,4-Methylenedioxymethamphetamine-Assisted Psychotherapy in Subjects with Chronic, Treatment-Resistant Posttraumatic Stress Disorder: The First Randomized Controlled Pilot Study. *J Psychopharmacol.* 25(4): 439-452. DOI: 10.1177/02698811110378371.
- Moein M. M., El Beqqali A., and Abdel-Rehim M. (2017). Bioanalytical Method Development and Validation: Critical Concepts and Strategies. *J Chromatogr B.* 1043: 3-11. DOI: 10.1016/j.jchromb.2016.09.028.
- Moldoveanu S. C. and David V. (2022). Essentials in Modern HPLC Separations. *Elsevier.* DOI: 10.1016/C2010-0-65748-8.
- Moreno F. A., Wiegand C. B., Taitano E. K., and Delgado P. L. (2006). Safety, Tolerability, and Efficacy of Psilocybin in 9 Patients with Obsessive-Compulsive Disorder. *J Clin Psychiatry.* 67(11): 1735-1740. DOI: 10.4088/jcp.v67n1110.
- Morris C. (2022). Diamorphine for Pain and Distress in Young Patients: Case Examples and Discussion of Mechanisms. *BMJ Support Palliat Care.* 12(1): 53-57. DOI: 10.1136/bmjspcare-2021-003295.
- Muller C. P. and Homberg J. R. (2015). The Role of Serotonin in Drug Use and Addiction. *Behav Brain Res.* 277: 146-192. DOI: 10.1016/j.bbr.2014.04.007.
- Nagy K. and Vékey K. (2008). Chapter 5 - Separation Methods. Medical Applications of Mass Spectrometry. *Elsevier.* 61-92. DOI: 10.1016/B978-044451980-1.50007-0.
- Nash J. F., Roth B. L., Brodtkin J. D., Nichols D. E., and Gudelsky G. A. (1994). Effect of the R(-) and S(+) Isomers of MDA and MDMA on Phosphatidyl Inositol Turnover in Cultured Cells Expressing 5-HT_{2A} or 5-HT_{2C} Receptors. *Neurosci Lett.* 177(1-2): 111-115. DOI: 10.1016/0304-3940(94)90057-4.
- National Academies of Sciences (2022). The National Academies Collection: Reports Funded by National Institutes of Health. Exploring Psychedelics and Entactogens as Treatments

- for Psychiatric Disorders: Proceedings of a Workshop. Stroud C., Posey Norris S. M., Matney C., and Bain L. *National Academies Press (US)*. DOI: 10.17226/26648.
- Nichols D. E. (2004). Hallucinogens. *Pharmacol Ther.* 101(2): 131-181. DOI: 10.1016/j.pharmthera.2003.11.002.
- Nichols D. E. (2016). Psychedelics. *Pharmacol Rev.* 68(2): 264-355. DOI: 10.1124/pr.115.011478.
- Nichols D. E. (2020). Psilocybin: From Ancient Magic to Modern Medicine. *J Antibiot (Tokyo)*. 73(10): 679-686. DOI: 10.1038/s41429-020-0311-8.
- Nichols D. E. (2022). Entactogens: How the Name for a Novel Class of Psychoactive Agents Originated. *Front Psychiatry*. 13: 863088. DOI: 10.3389/fpsy.2022.863088.
- Nichols D. E. and Nichols C. D. (2008). Serotonin Receptors. *Chem Rev.* 108(5): 1614-1641. DOI: 10.1021/cr078224o.
- Olejniskova-Ladislavova L., Fujakova-Lipski M., Sichova K., Danda H., Syrova K., Horacek J., and Palenicek T. (2024). Mescaline-Induced Behavioral Alterations Are Mediated by 5-HT_{2A} and 5-HT_{2C} Receptors in Rats. *Pharmacol Biochem Behav.* 245: 173903. DOI: 10.1016/j.pbb.2024.173903.
- Papaseit E., Perez-Mana C., Torrens M., Farre A., Poyatos L., Hladun O., Sanvisens A., Muga R., and Farre M. (2020). MDMA Interactions with Pharmaceuticals and Drugs of Abuse. *Expert Opin Drug Metab Toxicol.* 16(5): 357-369. DOI: 10.1080/17425255.2020.1749262.
- Pergolizzi J. V., Jr., Raffa R. B., and Rosenblatt M. H. (2020). Opioid Withdrawal Symptoms, a Consequence of Chronic Opioid Use and Opioid Use Disorder: Current Understanding and Approaches to Management. *J Clin Pharm Ther.* 45(5): 892-903. DOI: 10.1111/jcpt.13114.
- Pichini S., Marchei E., Garcia-Algar O., Gomez A., Di Giovannandrea R., and Pacifici R. (2014). Ultra-High-Pressure Liquid Chromatography Tandem Mass Spectrometry Determination of Hallucinogenic Drugs in Hair of Psychedelic Plants and Mushrooms Consumers. *J Pharm Biomed Anal.* 100: 284-289. DOI: 10.1016/j.jpba.2014.08.006.
- Pitts E. G., Curry D. W., Hampshire K. N., Young M. B., and Howell L. L. (2018). (±)-MDMA and Its Enantiomers: Potential Therapeutic Advantages of R(-)-MDMA. *Psychopharmacology (Berl)*. 235(2): 377-392. DOI: 10.1007/s00213-017-4812-5.
- Reardon S. (2024a). FDA Rejects Ecstasy as a Therapy: What's Next for Psychedelics? *Nature*. Retrieved 03.09.2024, from www.nature.com/articles/d41586-024-02597-x. DOI: 10.1038/d41586-024-02597-x.
- Reardon S. (2024b). MDMA Therapy for PTSD Rejected by FDA Panel. *Nature*. Retrieved 03.09.2024, from www.nature.com/articles/d41586-024-01622-3. DOI: 10.1038/d41586-024-01622-3.
- Riba J., McIlhenny E. H., Valle M., Bouso J. C., and Barker S. A. (2012). Metabolism and Disposition of N,N-Dimethyltryptamine and Harmala Alkaloids After Oral Administration of Ayahuasca. *Drug Test Anal.* 4(7-8): 610-616. DOI: 10.1002/dta.1344.

- Riba J., Valle M., Urbano G., Yritia M., Morte A., and Barbanoj M. J. (2003). Human Pharmacology of Ayahuasca: Subjective and Cardiovascular Effects, Monoamine Metabolite Excretion, and Pharmacokinetics. *J Pharmacol Exp Ther.* 306(1): 73-83. DOI: 10.1124/jpet.103.049882.
- Rickli A., Hoener M. C., and Liechti M. E. (2015a). Monoamine Transporter and Receptor Interaction Profiles of Novel Psychoactive Substances: Para-Halogenated Amphetamines and Pyrovalerone Cathinones. *Eur Neuropsychopharmacol.* 25(3): 365-376. DOI: 10.1016/j.euroneuro.2014.12.012.
- Rickli A., Kopf S., Hoener M. C., and Liechti M. E. (2015b). Pharmacological Profile of Novel Psychoactive Benzofurans. *Br J Pharmacol.* 172(13): 3412-3425. DOI: 10.1111/bph.13128.
- Rickli A., Luethi D., Reinisch J., Buchy D., Hoener M. C., and Liechti M. E. (2015c). Receptor Interaction Profiles of Novel N-2-Methoxybenzyl (NBOMe) Derivatives of 2,5-Dimethoxy-Substituted Phenethylamines (2C Drugs). *Neuropharmacology.* 99: 546-553. DOI: 10.1016/j.neuropharm.2015.08.034.
- Rickli A., Moning O. D., Hoener M. C., and Liechti M. E. (2016). Receptor Interaction Profiles of Novel Psychoactive Tryptamines Compared with Classic Hallucinogens. *Eur Neuropsychopharmacol.* 26(8): 1327-1337. DOI: 10.1016/j.euroneuro.2016.05.001.
- Rook E. J., Huitema A. D., van den Brink W., van Ree J. M., and Beijnen J. H. (2006). Pharmacokinetics and Pharmacokinetic Variability of Heroin and Its Metabolites: Review of the Literature. *Curr Clin Pharmacol.* 1(1): 109-118. DOI: 10.2174/157488406775268219.
- Ross S., Bossis A., Guss J., Agin-Liebes G., Malone T., Cohen B., Mennenga S. E., Belser A., Kalliontzis K., Babb J., Su Z., Corby P., and Schmidt B. L. (2016). Rapid and Sustained Symptom Reduction Following Psilocybin Treatment for Anxiety and Depression in Patients with Life-Threatening Cancer: A Randomized Controlled Trial. *J Psychopharmacol.* 30(12): 1165-1180. DOI: 10.1177/0269881116675512.
- Rudin D., McCorvy J. D., Glatfelter G. C., Luethi D., Szollosi D., Ljubisic T., Kavanagh P. V., Dowling G., Holy M., Jaentsch K., Walther D., Brandt S. D., Stockner T., Baumann M. H., Halberstadt A. L., and Sitte H. H. (2022). (2-Aminopropyl)benzo[*beta*]thiophenes (APBTs) Are Novel Monoamine Transporter Ligands That Lack Stimulant Effects but Display Psychedelic-Like Activity in Mice. *Neuropsychopharmacol.* 47(4): 914-923. DOI: 10.1038/s41386-021-01221-0.
- Sargent M. (2013). Guide to Achieving Reliable Quantitative LC-MS Measurements. *RSC Analytical Methods Committee.*
- Schindler E. A. D., Sewell R. A., Gottschalk C. H., Luddy C., Flynn L. T., Lindsey H., Pittman B. P., Cozzi N. V., and D'Souza D. C. (2021). Exploratory Controlled Study of the Migraine-Suppressing Effects of Psilocybin. *Neurotherapeutics.* 18(1): 534-543. DOI: 10.1007/s13311-020-00962-y.
- Schlüter H. (1999). Chapter 3 - Reversed-Phase Chromatography. Protein Liquid Chromatography. Kastner M. *Elsevier.* 147-234. DOI: 10.1016/S0301-4770(08)60531-X.

- Schmitt-Koopmann C., Baud C. A., Junod V., and Simon O. (2022). Switzerland's Dependence on a Diamorphine Monopoly. *Front Psychiatry*. 13: 882299. DOI: 10.3389/fpsy.2022.882299.
- Sergi M., Compagnone D., Curini R., D'Ascenzo G., Del Carlo M., Napoletano S., and Risoluti R. (2010). Micro-Solid Phase Extraction Coupled with High-Performance Liquid Chromatography-Tandem Mass Spectrometry for the Determination of Stimulants, Hallucinogens, Ketamine and Phencyclidine in Oral Fluids. *Anal Chim Acta*. 675(2): 132-137. DOI: 10.1016/j.aca.2010.07.011.
- Seyler T., Giraudon I., Noor A., Mounteney J., and Griffiths P. (2021). Is Europe Facing an Opioid Epidemic: What Does European Monitoring Data Tell Us? *Eur J Pain*. 25(5): 1072-1080. DOI: 10.1002/ejp.1728.
- Simmler L. D., Rickli A., Schramm Y., Hoener M. C., and Liechti M. E. (2014). Pharmacological Profiles of Aminoindanes, Piperazines, and Pipradrol Derivatives. *Biochem Pharmacol*. 88(2): 237-244. DOI: 10.1016/j.bcp.2014.01.024.
- Smith K. W., Sicignano D. J., Hernandez A. V., and White C. M. (2022). MDMA-Assisted Psychotherapy for Treatment of Posttraumatic Stress Disorder: A Systematic Review With Meta-Analysis. *J Clin Pharmacol*. 62(4): 463-471. DOI: 10.1002/jcph.1995.
- Snyder L. R., Kirkland J. J., and Dolan J. W. (2011). Introduction to Modern Liquid Chromatography. *John Wiley & Sons*. DOI: 10.1002/9780470508183.
- Steuer A. E., Schmidhauser C., Schmid Y., Rickli A., Liechti M. E., and Kraemer T. (2015). Chiral Plasma Pharmacokinetics of 3,4-Methylenedioxymethamphetamine and Its Phase I and II Metabolites Following Controlled Administration to Humans. *Drug Metab Dispos*. 43(12): 1864-1871. DOI: 10.1124/dmd.115.066340.
- Straumann I., Avedisian I., Klaiber A., Varghese N., Eckert A., Rudin D., Luethi D., and Liechti M. E. (2024a). Acute Effects of R-MDMA, S-MDMA, and Racemic MDMA in a Randomized Double-Blind Cross-Over Trial in Healthy Participants. *Neuropsychopharmacology*. DOI: 10.1038/s41386-024-01972-6.
- Straumann I., Holze F., Becker A. M., Ley L., Halter N., and Liechti M. E. (2024b). Safety Pharmacology of Acute Psilocybin Administration in Healthy Participants. *Neuroscience Applied*. 3: 104060. DOI: 10.1016/j.nsa.2024.104060.
- Straumann I., Ley L., Holze F., Becker A. M., Klaiber A., Wey K., Duthaler U., Varghese N., Eckert A., and Liechti M. E. (2023). Acute Effects of MDMA and LSD Co-Administration in a Double-Blind Placebo-Controlled Study in Healthy Participants. *Neuropsychopharmacology*. 48(13): 1840-1848. DOI: 10.1038/s41386-023-01609-0.
- Studerus E., Kometer M., Hasler F., and Vollenweider F. X. (2011). Acute, Subacute and Long-Term Subjective Effects of Psilocybin in Healthy Humans: A Pooled Analysis of Experimental Studies. *J Psychopharmacol*. 25(11): 1434-1452. DOI: 10.1177/0269881110382466.
- Takahama K. and Shirasaki T. (2007). Central and Peripheral Mechanisms of Narcotic Antitussives: Codeine-Sensitive and -Resistant Coughs. *Cough*. 3: 8. DOI: 10.1186/1745-9974-3-8.

-
- The Lancet Regional Health - Americas (2023). Opioid Crisis: Addiction, Overprescription, and Insufficient Primary Prevention. *Lancet Reg Health Am.* 23: 100557. DOI: 10.1016/j.lana.2023.100557.
- Trescot A. M., Datta S., Lee M., and Hansen H. (2008). Opioid Pharmacology. *Pain Physician.* 11(2 Suppl): S133-153
- Tyls F., Palenicek T., and Horacek J. (2014). Psilocybin – Summary of Knowledge and New Perspectives. *Eur Neuropsychopharmacol.* 24(3): 342-356. DOI: 10.1016/j.euroneuro.2013.12.006.
- Unger S. M. (1963). Mescaline, LSD, Psilocybin, and Personality Change. *Psychiatry.* 26: 111-125. DOI: 10.1080/00332747.1963.11023344.
- United States Food and Drug Administration. (2018). Bioanalytical Method Validation Guidance for Industry. Retrieved 27.09.2024, from www.fda.gov/files/drugs/published/Bioanalytical-Method-Validation-Guidance-for-Industry.pdf
- Vamvakopoulou I. A., Narine K. A. D., Campbell I., Dyck J. R. B., and Nutt D. J. (2023). Mescaline: The Forgotten Psychedelic. *Neuropharmacology.* 222: 109294. DOI: 10.1016/j.neuropharm.2022.109294.
- Venkatakrishnan K., Von Moltke L. L., and Greenblatt D. J. (2001). Human Drug Metabolism and the Cytochromes P450: Application and Relevance of In Vitro Models. *J Clin Pharmacol.* 41(11): 1149-1179. DOI: 10.1177/00912700122012724.
- Verrico C. D., Miller G. M., and Madras B. K. (2007). MDMA (Ecstasy) and Human Dopamine, Norepinephrine, and Serotonin Transporters: Implications for MDMA-Induced Neurotoxicity and Treatment. *Psychopharmacology (Berl).* 189(4): 489-503. DOI: 10.1007/s00213-005-0174-5.
- Vizeli P. and Liechti M. E. (2017). Safety Pharmacology of Acute MDMA Administration in Healthy Subjects. *J Psychopharmacol.* 31(5): 576-588. DOI: 10.1177/0269881117691569.
- Vizeli P., Straumann I., Holze F., Schmid Y., Dolder P. C., and Liechti M. E. (2021). Genetic Influence of CYP2D6 on Pharmacokinetics and Acute Subjective Effects of LSD in a Pooled Analysis. *Sci Rep.* 11(1): 10851. DOI: 10.1038/s41598-021-90343-y.
- Vogel M., Meyer M., Westenberg J. N., Kormann A., Simon O., Salim Hassan Fadlelseed R., Kurmann M., Broer R., Devaud N., Sanwald U., Baumgartner S., Binder H., Strasser J., Krausz R. M., Beck T., Dursteler K. M., and Falcato L. (2023). Safety and Feasibility of Intranasal Heroin-Assisted Treatment: 4-Week Preliminary Findings from a Swiss Multicentre Observational Study. *Harm Reduct J.* 20(1): 2. DOI: 10.1186/s12954-023-00731-y.
- von Rotz R., Schindowski E. M., Jungwirth J., Schuldt A., Rieser N. M., Zahoranzky K., Seifritz E., Nowak A., Nowak P., Jancke L., Preller K. H., and Vollenweider F. X. (2023). Single-Dose Psilocybin-Assisted Therapy in Major Depressive Disorder: A Placebo-Controlled, Double-Blind, Randomised Clinical Trial. *EClinicalMedicine.* 56: 101809. DOI: 10.1016/j.eclinm.2022.101809.
-

- Wadley G. (2016). How Psychoactive Drugs Shape Human Culture: A Multi-Disciplinary Perspective. *Brain Res Bull.* 126(Pt 1): 138-151. DOI: 10.1016/j.brainresbull.2016.04.008.
- Yang S., Shi Y., Chen Z., Chen M., Liu X., Liu W., Su M., and Di B. (2022). Detection of Mescaline in Human Hair Samples by UPLC-MS/MS: Application to 19 Authentic Forensic Cases. *J Chromatogr B.* 1195: 123202. DOI: 10.1016/j.jchromb.2022.123202.
- Zhao M., Ma J., Li M., Zhang Y., Jiang B., Zhao X., Huai C., Shen L., Zhang N., He L., and Qin S. (2021). Cytochrome P450 Enzymes and Drug Metabolism in Humans. *Int J Mol Sci.* 22(23). DOI: 10.3390/ijms222312808.
- Zuvela P., Skoczylas M., Jay Liu J., Ba Czek T., Kaliszan R., Wong M. W., Buszewski B., and Heberger K. (2019). Column Characterization and Selection Systems in Reversed-Phase High-Performance Liquid Chromatography. *Chem Rev.* 119(6): 3674-3729. DOI: 10.1021/acs.chemrev.8b00246.

APPENDIX

9 CURRICULUM VITAE

Jan Thomann

Personal information

Birth date: 21st of Mai 1995
Nationality: Swiss
OrcidID: orcid.org/0000-0003-3820-2671

Education

07/2021 – 12/2024 **PhD in Pharmaceutical Sciences at the University of Basel**

08/2019 – 06/2021 **MSc in Drug Sciences at the University of Basel**
120 ETCS

08/2016 – 07/2019 **BSc in Pharmaceutical Sciences at the University of Basel**
180 ETCS

08/2010 – 07/2014 **Matura at the Gymnasium St. Klemens Ebikon**
Focus subject 'biochemistry'

Research history

07/2021 – 12/2024 **PhD at the University of Basel and University Hospital Basel**
Clinical Pharmacology and Toxicology Research Group
Project: Bioanalysis and Metabolic Investigation of Psychoactive Substances, supervised by Prof. Dr. Matthias E. Liechti and PD Dr. Urs Duthaler

09/2020 – 06/2021 **Master's Thesis at the University of Basel and University Hospital Basel**
Clinical Pharmacology and Toxicology Research Group
Project: Pharmacological characterization of synthetic cathinones related to MDPV at the monoamine transporters and receptors in vitro, supervised by Prof. Dr. Matthias E. Liechti and Dr. Karolina E. Kolaczynska

Institutional responsibilities

- 2021 – 2023 Organization of the seminar ‘Klinische Pharmakologie’ for the Clinical Pharmacology and Toxicology Research Group at the University of Basel
- 2021 – 2024 Representative of the PhD Association of Pharmaceutical Sciences at the University of Basel

Supervision junior researchers

- 08/2022 – 05/2023 Master’s Thesis in Drug Sciences (University of Basel)

Teaching activities

- 2021 – 2024 Practical Course ‘Laboratory Methods in Drug Sciences’ at the University of Basel
Topic: Drug metabolism and detection of metabolites

Presentations at conferences

Kolaczynska, K. E., Becker, A. M., **Thomann, J.**, Liechti, M. E., Duthaler, U. Drug Metabolism and Pharmacokinetics of Psilocin In Vitro and In Humans. 5th Interdisciplinary Conference on Psychedelic Research (ICPR), 22–24 September 2022, Haarlem.

Thomann J., Stoeckmann O. V., Rudin D., Liechti M. E., and Duthaler U. In Vitro and In Vivo Metabolism of Psilocybin’s Active Metabolite Psilocin. Department of Biomedicine (DBM) Summer Symposium 2024, 22 August 2024, Basel.

Poster contributions at conferences

Thomann, J., Klaiber, A., Schmid, Y., Luethi, D., Liechti, M. E. Clinical and Molecular Metabolism of Mescaline. 6th Interdisciplinary Conference on Psychedelic Research (ICPR), 06–08 June 2024, Haarlem.

Thomann, J., Kolaczynska, K. E., Stoeckmann, O. V., Becker, A. M., Liechti, M. E., Duthaler, U. In Vitro and In Vivo Metabolism of Psilocybin’s Active Metabolite Psilocin. World Congress of Basic & Clinical Pharmacology 2023 (WCP), 02–07 July 2023, Glasgow.

Thomann, J., Ley, L., Holze, F., Liechti, M. E., Duthaler, U. Development of a Bioanalytical Method for Quantifying Mescaline and its Metabolites in Human Plasma and Urine. 5th Interdisciplinary Conference on Psychedelic Research (ICPR), 22–24 September 2022, Haarlem.

10 PUBLICATION LIST

- Klaiber A., Schmid Y., Becker A. M., Straumann I., Erne L., Jelusic A., **Thomann J.**, Luethi D., and Liechti M. E. (2024). Acute Dose-Dependent Effects of Mescaline in a Double-Blind Placebo-Controlled Study in Healthy Subjects. *Transl Psychiatry*. 14(1): 395. DOI: 10.1038/s41398-024-03116-2.
- Thomann J.**, Kolaczynska K. E., Stoeckmann O. V., Rudin D., Vizeli P., Hoener M. C., Pryce C. R., Vollenweider F. X., Liechti M. E., and Duthaler U. (2024a). In Vitro and In Vivo Metabolism of Psilocybin's Active Metabolite Psilocin. *Front Pharmacol*. 15: 1391689. DOI: 10.3389/fphar.2024.1391689.
- Luethi D., Rudin D., Straumann I., **Thomann J.**, Avedisian I., Liechti M. E., and Duthaler U. (2024). Derivatization-Free Determination of Chiral Plasma Pharmacokinetics of MDMA and Its Enantiomers. *J Chromatogr B*. 1238: 124123. DOI: 10.1016/j.jchromb.2024.124123.
- Thomann J.**, Vogt S. B., Guessoum A., Meyer M., Vogel M., Liechti M. E., Luethi D., and Duthaler U. (2024b). Development and Validation of an LC-MS/MS Method for Quantifying Diamorphine and Its Major Metabolites 6-Monoacetylmorphine, Morphine, Morphine-3-glucuronide, and Morphine-6-glucuronide in Human Plasma. *J Chromatogr B*. 1237: 124104. DOI: 10.1016/j.jchromb.2024.124104.
- Ley L., Holze F., Arikci D., Becker A. M., Straumann I., Klaiber A., Coviello F., Dierbach S., **Thomann J.**, Duthaler U., Luethi D., Varghese N., Eckert A., and Liechti M. E. (2023). Comparative Acute Effects of Mescaline, Lysergic Acid Diethylamide, and Psilocybin in a Randomized, Double-Blind, Placebo-Controlled Cross-Over Study in Healthy Participants. *Neuropsychopharmacology*. 48(11): 1659-1667. DOI: 10.1038/s41386-023-01607-2.
- Thomann J.**, Ley L., Klaiber A., Liechti M. E., and Duthaler U. (2022). Development and Validation of an LC-MS/MS Method for the Quantification of Mescaline and Major Metabolites in Human Plasma. *J Pharm Biomed Anal*. 220: 114980. DOI: 10.1016/j.jpba.2022.114980.
- Kolaczynska K. E., **Thomann J.**, Hoener M. C., and Liechti M. E. (2021). The Pharmacological Profile of Second Generation Pyrovalerone Cathinones and Related Cathinone Derivative. *Int J Mol Sci*. 22(15). DOI: 10.3390/ijms22158277.